IL
NUOVO CIMENTO
ORGANO DELLA SOCIETÀ ITALIANA DI FISICA
SOTTO GLI AUSPICI DEL CONSIGLIO NAZIONALE DELLE RICERCHE

VOL. XII, N. 3 *Serie decima* 1° Maggio 1959

Diagonalization of Hamiltonian.

L. M. GARRIDO and P. PASCUAL
Junta de Energia Nuclear - Madrid

(ricevuto il 26 Luglio 1958)

Summary. — We present a general method to diagonalize the hamiltonian of particles of arbitrary spin. In particular we study the cases of spin 0, $\frac{1}{2}$, 1 and see that for spin $\frac{1}{2}$ our transformation agrees with Foldy's and obtain the expression for different observables for particles of spin 0 and 1 in the new representation.

1. – Introduction.

FOLDY [1] gave a transformation that diagonalizes the Dirac particle hamiltonian. In general, this diagonalization clarifies the physical interpretation of the mathematical formalism [2], as it has been shown by H. FESHBACH and F. VILLARS. CASE [3] extended this transformation to particles of spin 0 and 1 using a hamiltonian formulation, whose covariance is not well manifested.

We intend to present a transformation that does just that from a general viewpoint, and so, we start from the equations for particles of arbitrary spin as presented by UMEZAWA's book *Quantum Field Theory*. Our transformation is valid for all spins and includes the precedent formulations.

---

[1] L. L. FOLDY and S. A. WOUTHUYSEN: *Phys. Rev.*, **78**, 29 (1950).
[2] H. FESHBACH and F. VILLARS: *Rev. Mod. Phys.*, **30**, 24 (1958).
[3] K. M. CASE: *Phys. Rev.*, **95**, 1323 (1954).

2. – Unitary transformation.

In the cases when the relativistic wave equation for particles of arbitrary spin

$$(\beta_\mu \partial_\mu + m)\psi = 0$$

may be written in the hamiltonian form

$$p_0\psi = (\alpha_k p_k + m\beta)\psi \qquad (k = 1, 2, 3)$$

where

$$p_0 = -\partial_4\,, \quad p_k = -i\partial_k\,, \quad \alpha_k = -\frac{i}{g} S_{k4}\,, \quad \beta = \beta_4\,,$$

and $S_{\mu\nu}$ are the generators of infinitesimal Lorentz transformations defined as

$$S_{\mu\nu} = g^2(\beta_\mu\beta_\nu - \beta_\nu\beta_\mu)\,,$$

where g is a peculiar constant for each spin ([4]), we can find a general unitary transformation that diagonalizes the hamiltonian,

$$H = \alpha_k p_k + m\beta\,.$$

Such an expression for H has been studied by CASE ([5]).

HEPNER ([4]) shows that there exists a unitary transformation

$$S = \exp\left[\tfrac{1}{2} i\pi g\beta\right]$$

such that

$$S^{-1}\alpha S_k = \beta_k$$

$$S^{-1}\beta\, S = \beta_4$$

under which H becomes

$$H' = S^{-1}HS = \beta_k p_k + m\beta_4\,.$$

Our problem will be solved if we evaluate the transformation R that makes

$$R^{-1}H'R = E\beta_4\,,$$

where E the total energy

$$E = \sqrt{p_k^2 + m^2}\,.$$

([4]) W. A. HEPNER: *Phys. Rev.*, **84**, 744 (1951).
([5]) K. M. CASE: *Phys. Rev.*, **100**, 1513 (1955).

To start with we will consider the simpler case when $p_2 = p_3 = 0$; we call R_1 the corresponding transformation.

The transformation R_1 is a rotation in the plane (1, 4) whose infinitesimal expression is

$$\delta R_1 = 1 + S_{14}\,\delta\omega$$

and, therefore

$$R_1 = \exp\left[S_{14}\omega\right],$$

where ω is the angle through which we have rotated

$$\omega = \mathrm{tg}^{-1}\frac{m}{p_1}.$$

The infinitesimal rotation in the plane determined by the axis β_4 and an arbitrary unit vector n_k is

$$\delta R_n = 1 + S_{k4} n_k\,\delta\omega$$

and, therefore, the finite rotation that we look for is

$$R = \exp\left[S_{k4}\,\frac{p}{p_k}\,\mathrm{tg}^{-1}\frac{p}{m}\right],$$

where

$$p = \sqrt{p_k^2}\,.$$

Reversing the transformation S the hamiltonian will be diagonalized by

$$\Lambda = SRS^{-1} = \exp\left[-ig\,\frac{\beta_k p_k}{p}\,\mathrm{tg}^{-1}\frac{p}{m}\right],$$

that in the case of a Dirac particle $g = \frac{1}{2}$ yields Foldy's transformation [1]

$$\Lambda_{\frac{1}{2}} = \exp\left[-\frac{1}{2}\beta\,\frac{\alpha_k p_k}{p}\,\mathrm{tg}^{-1}\frac{p}{m}\right].$$

3. – Spin 0 and 1.

Spins zero and one correspond to $g = 1$. For a Duffin-Hemmer particle represented by the equation of motion

$$(\beta_\mu \partial_\mu + m)\psi = 0\,,$$

$$\beta_\mu\beta_\nu\beta_\lambda + \beta_\lambda\beta_\nu\beta_\mu = \beta_\mu\,\delta_{\nu\lambda} + \beta_\lambda\,\delta_{\nu\mu}\,.$$

there exists ([5,6]) a hamiltonian formulation as follows

$$H = \boldsymbol{\alpha p} + m\beta_4 , \qquad H\psi = i\frac{\partial \psi}{\partial t} ,$$

and the initial condition is

$$(H\beta_4 - m)\psi = 0 ,$$

where

$$\alpha_k = -iS_{k4} , \qquad S_{\mu\nu} = \beta_\mu\beta_\nu - \beta_\nu\beta_\mu ,$$

$$p_k = -i\partial_k , \qquad \sigma_k = -iS_{lm} \qquad (k, l, m \text{ cyclic}).$$

The hamiltonian is diagonalized by

$$\Lambda = \exp\left[-i\frac{\boldsymbol{\beta p}}{p}\,\mathrm{tg}^{-1}\frac{p}{m}\right],$$

so that

(I) $$\Lambda^{-1}H\Lambda = E\beta_4 , \qquad E = \sqrt{p^2 + m^2} ,$$

and the initial condition becomes

$$\{\beta_4(\boldsymbol{\alpha}\cdot\boldsymbol{p}) - m\beta_4^2 + m\}\psi' = 0 ,$$

where $\psi' = \Lambda^{-1}\psi$. It is quite easy to see that it eliminates the zero energy states.

Expression (I) may be expanded

$$\Lambda = I - \frac{1}{E(E+m)}(\boldsymbol{\beta}\cdot\boldsymbol{p})^2 - \frac{i}{E}(\boldsymbol{\beta}\cdot\boldsymbol{p}) ,$$

according to the formulae (A.1).

4. – Dynamical variables.

We call in the new representation O' the operators corresponding to O in the old one

$$O' = \Lambda^{-1}O\Lambda$$

and so, with the help of the formulae of the Appendix, we find Table I.

As it has been shown by FOLDY ([1]) for the Dirac particle the mean spin operator and mean orbital angular momentum are also in these case separately constants of motion.

([6]) N. KEMMER: *Proc. Roy. Soc.*, A **173**, 91 (1939).

TABLE I.

	Operator in the old representation	Operator in the new representation
Position	$\boldsymbol{x}$	$\boldsymbol{x}' = \boldsymbol{x} + \frac{i(\boldsymbol{\beta}\cdot\boldsymbol{p})+(E+m)}{E^2(E+m)^2}(\boldsymbol{\beta}\boldsymbol{p})\boldsymbol{p} + \frac{1}{E(E+m)}(\boldsymbol{p}\times\boldsymbol{\sigma}) + \frac{1}{E}\boldsymbol{\beta}$
Momentum	$\boldsymbol{p} \equiv -i\nabla$	$\boldsymbol{p}' = \boldsymbol{p}$
Hamiltonian	$H = \boldsymbol{\alpha}\cdot\boldsymbol{p} + m\beta_4$	$H' = E\beta_4$
Velocity	$\dot{\boldsymbol{x}} = \boldsymbol{\alpha}$	$\boldsymbol{\alpha}' = \boldsymbol{\alpha} + \frac{\boldsymbol{p}}{E}\beta_4 - \frac{\boldsymbol{p}}{E(E+m)}(\boldsymbol{\alpha}\boldsymbol{p})$
Orbital angular momentum	$(\boldsymbol{x}\times\boldsymbol{p})$	$(\boldsymbol{x}'\times\boldsymbol{p}) = (\boldsymbol{x}\times\boldsymbol{p}) + \frac{1}{E(E+m)}(\boldsymbol{p}\times\boldsymbol{\sigma})\times\boldsymbol{p} + \frac{1}{E}(\boldsymbol{\beta}\times\boldsymbol{p})$
Spin	$\boldsymbol{\sigma}$	$\boldsymbol{\sigma}' = \frac{m}{E}\boldsymbol{\sigma} + \frac{1}{E(E+m)}(\boldsymbol{\sigma}\boldsymbol{p})\boldsymbol{p} - \frac{1}{E}(\boldsymbol{\beta}\times\boldsymbol{p})$
Projection operator	$\Lambda_p = \frac{\boldsymbol{\alpha}\boldsymbol{p}+m\beta_4}{E}$	$\Lambda_p' = \beta_4$
Mean position	$\boldsymbol{X} = \boldsymbol{x} + \frac{i(\boldsymbol{\beta}\boldsymbol{p})-(E+m)}{E^2(E+m)^2}(\boldsymbol{\beta}\cdot\boldsymbol{p})\boldsymbol{p} + \frac{1}{E(E+m)}(\boldsymbol{p}\times\boldsymbol{\sigma}) - \frac{\boldsymbol{\beta}}{E}$	$\boldsymbol{X}' = \boldsymbol{x}$
Mean velocity	$\dot{\boldsymbol{X}} = \frac{\boldsymbol{p}}{E}\frac{H}{E}$	$\dot{\boldsymbol{X}}' = \frac{\beta_4\boldsymbol{p}}{E}$
Mean orbital angular momentum	$(\boldsymbol{X}\times\boldsymbol{p}) = (\boldsymbol{x}\times\boldsymbol{p}) + \frac{1}{E(E+m)}\cdot(\boldsymbol{p}\times\boldsymbol{\sigma})\times\boldsymbol{p} - \frac{1}{E}(\boldsymbol{\beta}\times\boldsymbol{p})$	$(\boldsymbol{X}'\times\boldsymbol{p}') = (\boldsymbol{x}\times\boldsymbol{p})$
Mean spin	$\boldsymbol{\Sigma} = \frac{m}{E}\boldsymbol{\sigma} + \frac{1}{E(E+m)}\cdot(\boldsymbol{\sigma}\cdot\boldsymbol{p})\boldsymbol{p} + \frac{1}{E}(\boldsymbol{\beta}\times\boldsymbol{p})$	$\boldsymbol{\Sigma}' = \boldsymbol{\sigma}$

The eigenvalues of the velocity operator $\dot{x} = \alpha$ are $\pm c$ and 0. This last one is eliminated by the initial condition. This instantaneous velocity is due, as in the case of Dirac particles, to a rapidly oscillating motion (Zitterbewegung) since by means of $\dot{O} = i[H, O]$ we deduce

$$\ddot{\alpha} = Hp - E^2\alpha$$

and

$$\dddot{\alpha} = -E^2\dot{\alpha} ,$$

differential equation whose solution is

$$\alpha = A \exp[-iEt] + B \exp[+iEt] + \frac{H}{E^2} p,$$

where A and B are integration constants, expression whose interpretation is well known.

If we divide the spin σ' into parts parallel and perpendicular to the momentum by means of

$$\sigma_{\parallel} = \frac{(\sigma \cdot p)}{p^2} p, \qquad \sigma_{\perp} = \sigma - \sigma_{\parallel} ,$$

we get

$$\sigma' = \sigma_{\parallel} + \frac{m}{E}\sigma_{\perp} - \frac{1}{E}(\beta \times p) .$$

It is easy to see that the expected value of $(\beta \times p)$ is zero and therefore

$$\langle \sigma \rangle' = \langle \sigma_{\parallel} \rangle + \frac{m}{E} \langle \sigma_{\perp} \rangle .$$

Appendix

The formulae used for all these calculations are:

$$\text{(A.1)} \quad \left| \begin{array}{ll|ll}
(\beta\cdot p)^{2n} & = p^{2n-2}(\beta\cdot p)^2 & (\beta\cdot p)^{2n+1} & = p^{2n}(\beta\cdot p) \\
[x, (\beta\cdot p)] & = i\beta & [x, (\beta\cdot p)^2] & = i\{(\beta\cdot p)\beta + \beta(\beta\cdot p)\} \\
[\beta, (\beta\cdot p)] & = i(p\times\sigma) & [\beta, (\beta\cdot p)^2] & = i\{(\beta\cdot p)(p\times\sigma) + (p\times\sigma)(\beta\cdot p)\} \\
[(\alpha p), (\beta\cdot p)] & = i\beta_4 p^2 & [(\alpha p), (\beta\cdot p)^2] & = 2ip^2(\beta\cdot p)\beta_4 + p^2(\alpha\cdot p) \\
[\beta_4, (\beta\cdot p)] & = -i(\alpha\cdot p) & [\beta_4, (\beta\cdot p)^2] & = \beta_4 p^2 - 2(\beta\cdot p)^2\beta_4 \\
[\sigma, (\beta\cdot p)] & = -i(\beta\times p) & [\sigma, (\beta\cdot p)^2] & = -i\{(\beta\cdot p)(\beta\times p) + (\beta\times p)(\beta\cdot p)\} \\
[\sigma, (\beta\cdot p)] & = i\beta_4 p & [\alpha, (\beta\cdot p)^2] & = ip\{(\beta\cdot p)\beta_4 + \beta_4(\beta\cdot p)\} ,
\end{array} \right.$$

$$[(\beta\cdot p), (\beta\times p)] = i\{(\sigma\cdot p)\cdot p - \sigma p^2\} ,$$

$$(\beta\cdot p)\beta(\beta\cdot p) = (\beta\cdot p)p ,$$

$$(\boldsymbol{\beta}\cdot\boldsymbol{p})(\boldsymbol{\alpha}\boldsymbol{p}) = -i(\boldsymbol{\beta}\cdot\boldsymbol{p})^2\beta_4\,, \qquad (\boldsymbol{\beta}\cdot\boldsymbol{p})^2(\boldsymbol{\alpha}\boldsymbol{p}) = -ip^2(\boldsymbol{\beta}\cdot\boldsymbol{p})\beta_4\,,$$
$$(\boldsymbol{\beta}\cdot\boldsymbol{p})(\boldsymbol{\beta}\times\boldsymbol{p})(\boldsymbol{\beta}\cdot\boldsymbol{p}) = 0\,,$$
$$(\boldsymbol{\beta}\cdot\boldsymbol{p})(\boldsymbol{\alpha}\cdot\boldsymbol{p})(\boldsymbol{\beta}\cdot\boldsymbol{p}) = 0\,,$$
$$(\boldsymbol{\beta}\cdot\boldsymbol{p})\beta_4(\boldsymbol{\beta}\cdot\boldsymbol{p}) = 0\,.$$

and a representation of the Duffin-Kemmer algebra is obtained from those matrices given by UMEZAWA (7) that we will call β'_μ by means of the following unitary matrices:

Spin 0

$$U = \begin{vmatrix} \frac{1}{\sqrt{2}} & \frac{1}{\sqrt{2}} & 0 & 0 & 0 \\ 0 & 0 & 1 & 0 & 0 \\ 0 & 0 & 0 & 1 & 0 \\ 0 & 0 & 0 & 0 & 1 \\ -\frac{i}{\sqrt{2}} & -\frac{i}{\sqrt{2}} & 0 & 0 & 0 \end{vmatrix}.$$

$$\beta_\mu = U^+\beta'_\mu U$$

$$\beta_1 = \left|\begin{array}{cc:ccc} & & \frac{-i}{\sqrt{2}} & 0 & 0 \\ \multicolumn{2}{c:}{0} & \frac{+i}{\sqrt{2}} & 0 & 0 \\ \hdashline \frac{i}{\sqrt{2}} & \frac{-i}{\sqrt{2}} & \multicolumn{3}{c}{\multirow{2}{*}{0}} \\ 0 & 0 & & & \\ 0 & 0 & \multicolumn{3}{c}{} \end{array}\right|, \qquad \beta_2 = \left|\begin{array}{cc:ccc} & & 0 & \frac{-i}{\sqrt{2}} & 0 \\ \multicolumn{2}{c:}{0} & 0 & \frac{+i}{\sqrt{2}} & 0 \\ \hdashline 0 & 0 & \multicolumn{3}{c}{\multirow{2}{*}{0}} \\ \frac{i}{\sqrt{2}} & \frac{-i}{\sqrt{2}} & & & \\ 0 & 0 & \multicolumn{3}{c}{} \end{array}\right|,$$

$$\beta_3 = \left|\begin{array}{cc:ccc} & & 0 & 0 & \frac{-i}{\sqrt{2}} \\ \multicolumn{2}{c:}{0} & 0 & 0 & \frac{+i}{\sqrt{2}} \\ \hdashline 0 & 0 & \multicolumn{3}{c}{\multirow{2}{*}{0}} \\ 0 & 0 & & & \\ \frac{i}{\sqrt{2}} & \frac{-i}{\sqrt{2}} & \multicolumn{3}{c}{} \end{array}\right|, \qquad \beta_4 = \left|\begin{array}{cc:ccc} & & 1 & 0 & \\ \multicolumn{2}{c:}{0} & 0 & -1 & 0 \\ \hdashline \multicolumn{2}{c:}{\multirow{2}{*}{0}} & \multicolumn{3}{c}{\multirow{2}{*}{0}} \\ & & & & \\ \multicolumn{2}{c:}{} & \multicolumn{3}{c}{} \end{array}\right|,$$

(7) H. UMEZAWA: *Quantum Field Theory* (1956).

Spin 1

$$U = \left|\begin{array}{ccc:ccc:cc:c} \frac{1}{\sqrt{2}} & & 0 & \frac{1}{\sqrt{2}} & & 0 & & & \\ & \frac{1}{\sqrt{2}} & & & \frac{1}{\sqrt{2}} & & 0 & & 0 \\ 0 & & \frac{1}{\sqrt{2}} & 0 & & \frac{1}{\sqrt{2}} & & & \\ \hdashline & 0 & & & 0 & & 1 & 0 & \\ & & & & & & & 1 & 0 \\ & & & & & & 0 & 1 & \\ \hdashline \frac{i}{\sqrt{2}} & & & \frac{-i}{\sqrt{2}} & & 0 & & & \\ & \frac{i}{\sqrt{2}} & & & \frac{-i}{\sqrt{2}} & & 0 & & 0 \\ & & \frac{i}{\sqrt{2}} & 0 & & \frac{-i}{\sqrt{2}} & & & \\ \hdashline & 0 & & & 0 & & 0 & & 1 \end{array}\right|,$$

$$\beta_1 = \left|\begin{array}{ccc:ccc:ccc:c} & & & & & & 0 & 0 & 0 & \frac{-1}{\sqrt{2}} \\ & 0 & & & 0 & & 0 & 0 & \frac{-i}{\sqrt{2}} & 0 \\ & & & & & & 0 & \frac{i}{\sqrt{2}} & 0 & 0 \\ \hdashline & & & & & & 0 & 0 & 0 & \frac{-1}{\sqrt{2}} \\ & 0 & & & 0 & & 0 & 0 & \frac{i}{\sqrt{2}} & 0 \\ & & & & & & 0 & \frac{-i}{\sqrt{2}} & 0 & 0 \\ \hdashline 0 & 0 & 0 & 0 & 0 & 0 & & & & \\ 0 & 0 & \frac{-i}{\sqrt{2}} & 0 & 0 & \frac{+i}{\sqrt{2}} & & 0 & & 0 \\ 0 & \frac{+i}{\sqrt{2}} & 0 & 0 & \frac{-i}{\sqrt{2}} & 0 & & & & \\ \hdashline \frac{-1}{\sqrt{2}} & 0 & 0 & \frac{-1}{\sqrt{2}} & 0 & 0 & & 0 & & 0 \end{array}\right|,$$

$$\beta_2 = \left|\begin{array}{cccccc|ccc|c}
 & & & & & & 0 & 0 & \frac{i}{\sqrt{2}} & 0 \\
 & & & & & & 0 & 0 & 0 & \frac{-1}{\sqrt{2}} \\
 & 0 & & & 0 & & \frac{-i}{\sqrt{2}} & 0 & 0 & 0 \\
 & & & & & & 0 & 0 & \frac{-i}{\sqrt{2}} & 0 \\
 & & & & & & 0 & 0 & 0 & \frac{-1}{\sqrt{2}} \\
 & 0 & & & 0 & & \frac{i}{\sqrt{2}} & 0 & 0 & 0 \\
\hline
0 & 0 & \frac{i}{\sqrt{2}} & 0 & 0 & \frac{-i}{\sqrt{2}} & & & & \\
0 & 0 & 0 & 0 & 0 & 0 & & 0 & & 0 \\
\frac{-i}{\sqrt{2}} & 0 & 0 & \frac{i}{\sqrt{2}} & 0 & 0 & & & & \\
\hline
0 & \frac{-1}{\sqrt{2}} & 0 & 0 & \frac{-1}{\sqrt{2}} & 0 & & 0 & & 0
\end{array}\right|,$$

$$\beta_3 = \left|\begin{array}{cccccc|ccc|c}
 & & & & & & 0 & \frac{-i}{\sqrt{2}} & 0 & 0 \\
 & & & & & & \frac{i}{\sqrt{2}} & 0 & 0 & 0 \\
 & 0 & & & 0 & & 0 & 0 & 0 & \frac{-1}{\sqrt{2}} \\
 & & & & & & 0 & \frac{i}{\sqrt{2}} & 0 & 0 \\
 & & & & & & \frac{-i}{\sqrt{2}} & 0 & 0 & 0 \\
 & 0 & & & 0 & & 0 & 0 & 0 & \frac{-1}{\sqrt{2}} \\
\hline
0 & \frac{-i}{\sqrt{2}} & 0 & 0 & \frac{+i}{\sqrt{2}} & 0 & & & & \\
\frac{i}{\sqrt{2}} & 0 & 0 & \frac{-i}{\sqrt{2}} & 0 & 0 & & 0 & & 0 \\
0 & 0 & 0 & 0 & 0 & 0 & & & & \\
\hline
0 & 0 & \frac{-1}{\sqrt{2}} & 0 & 0 & \frac{-1}{\sqrt{2}} & & 0 & & 0
\end{array}\right|,$$

$$\beta_4 = \begin{pmatrix} 1 & & & \\ & 1 & 0 & 0 & 0 \\ & & 1 & & \\ & & & -1 & \\ 0 & & -1 & 0 & 0 \\ & & & -1 & \\ 0 & & 0 & 0 & 0 \\ 0 & & 0 & 0 & 0 \end{pmatrix}.$$

RIASSUNTO (*)

Presentiamo un metodo generale per la diagonalizzazione dell'hamiltoniana delle particelle di spin arbitrario. In particolare studiamo i casi degli spin 0, $\frac{1}{2}$, 1 e vediamo che per lo spin $\frac{1}{2}$ la nostra trasformazione si accorda con quella di Foldy ed otteniamo l'espressione, per differenti osservabili, per le particelle di spin 0 ed 1 nella nuova rappresentazione.

(*) *Traduzione a cura della Redazione.*

IL NUOVO CIMENTO Vol. XII, N. 3 1° Maggio 1959

On the Emission of Low Energy Photons from a Quantized System.

R. Ascoli

Istituto di Fisica dell'Università - Torino
Istituto Nazionale di Fisica Nucleare - Sezione di Torino

(ricevuto il 4 Agosto 1958)

Summary. — We solve here the problem of the emission of photons from a general quantized system when the reaction of the photons on the system is neglected. Till now this problem had been solved only in the case of the emission from a classical system. We deduce a general expression for the average number of photons which are emitted when a time dependent perturbation produces a transition between two arbitrary states of the system. The discussion of this expression leads to the conclusion that the average number of low energy photons emitted in any experiment which can really be done is finite: this conclusion generalizes a result previously obtained by the author in the case of a classical source to the case of quantized source. Moreover, neglecting the reaction of the photons on the charges, we show here that the average number of emitted photons is equal to the first term of the expansion in powers of e of the emission probability of one photon. The application of this conclusion to the case of a transition between two definite momentum states shows that the Bloch-Nordsieck divergence and the infrared divergence of the perturbative calculation have their origin in the divergence of the same mathematical expression, although they have an entirely different physical meaning. Finally we show that the problem studied here in general has no meaning in the case of a time independent perturbation.

1. – Introduction.

The problem of the emission of photons of sufficiently low energy may be studied independently from the perturbative expansion using an approximation method in which the reaction of the electromagnetic field on the charges is neglected.

Such an approximation was introduced firstly by BLOCH and NORDSIECK [1].

Till now, however, this method has been applied rigorously and extensively only in the case in which the photons are emitted from a classical system of charges [2]. For this classical case there are several general and elegant treatments [3]. The most simple and general of them is the one of THIRRING and TOUSCHEK [3,4], which uses Heisenberg picture.

The most known result concerns the case of a charge undergoing a transition between two states of motion of constant momentum; in this case the average number of emitted photons results infinite (Bloch-Nordsieck divergence), whereas the probability that a finite number of photons is emitted is found to be zero [1,5].

In a previous work [4] I have studied the expression of the average number of photons emitted by a general classical system of charges, and I have shown that this number is always finite, provided the charges are confined in a finite region of space. Therefore I have concluded that in every experiment which can actually be done the number of emitted photons is finite, so that the divergence found by BLOCH and NORDSIECK has its source in the fact that the particular problem in which it appears corresponds to an experiment which cannot be made, because an infinite region of space is needed.

The main purposes of the present work are:

1) To give an exact meaning to the problem of the emission of low energy photons from a « given » quantized system, when the reaction of these photons is neglected.

2) To give a general treatment of this problem, using Heisenberg picture.

3) To apply the result to the case of the transition of a charge between two definite momentum states, and to show rigorously that the result found in the classical case holds also in the quantum mechanical one, provided the duration of the transition is neglected.

4) To show that the number of photons emitted in an experiment which can really be performed is always finite, extending the result previously obtained in the classical case to the quantum mechanical case.

---

[1] F. BLOCH and A. NORDSIECK: *Phys. Rev.*, **52**, 54 (1937).

[2] Only a very particular case of emission from a quantummechanical system was treated rigorously by FIERZ and PAULI (W. PAULI and M. FIERZ: *Nuovo Cimento*, **15**, 107 (1938)). See also, J. M. JAUCH and F. ROHRLICH: *Helv. Phys. Acta*, **27**, 613 (1954).

[3] W. THIRRING and B. TOUSCHEK: *Phil. Mag.*, **42**, 244 (1951); ROJ J. GLAUBER: *Phys. Rev.*, **84**, 395 (1951); J. SCHWINGER: *Phys. Rev.*, **91**, 728 (1953).

[4] See also: R. ASCOLI: *Nuovo Cimento*, **2**, 413 (1955).

[5] See also: RES JOST: *Phys. Rev.*, **72**, 815 (1947); R. ASCOLI: *Nuovo Cimento*, **2**, 1 (1955).

5) To prove that a simple connexion exists between the results of this treatment and the result of the perturbative calculations.

6) To discuss the connexion between the Bloch-Nordsieck divergence and the infrared divergence which arises in the perturbative calculation ([6]).

2. – Considerations holding in both the cases of a classical and of a quantized source.

Let us consider the equations of motion of an arbitrary system in Heisenberg picture.

The approximation treated here consists in the following proceeding; in the equations of motion of the charges we neglect the term of interaction with the photons of energy lower than some fixed value ε in a given reference system, whereas nothing is neglected in the equation of motion of the electromagnetic field ([7]).

Let us call

— Degrees of freedom $\boldsymbol{e}$: all the degrees of freedom except those of the photons of energy lower than ε;

— Degrees of freedom $\boldsymbol{p}$: those of the photons of energy lower than ε (« low energy photons »).

Then the problem is solved in two steps:

1) The motion of the degrees of freedom $\boldsymbol{e}$ is studied as if the degrees of freedom $\boldsymbol{p}$ would not exist at all; that is the degrees of freedom $\boldsymbol{e}$ are treated as belonging to an independent system. We call it system $\boldsymbol{e}$ or « external system », because it corresponds to an external source in the classical case.

([6]) A preliminary account of some results of the present work has been published on *Nature* with a synthetic deduction. See R. Ascoli: *Nature*, **179**, 727 (1957).

([7]) A simple formulation of this approximative method from the beginning is only possible using Heisenberg picture. In fact we are using an approximation in which the influence of the low energy photons on the charges is neglected, whereas the influence of the charges on the low energy photons is taken into account.

Therefore both the Schrödinger and the interaction pictures are not appropriate to deal with such a problem, because in the interaction Hamiltonian the influence of the field on the charges and the influence of the charges on the field cannot be separated. So, using these pictures it is not possible to face the problem clearly from the beginning, and it is necessary to make the required approximations at the appropriate points during calculation.

On the contrary, in the Heisenberg equations of motion the influence of the field on the charges and the influence of the charges on the field are separated from the beginning.

In such a way an expression is obtained for the density of electric current $j(x)$ as a function of only the quantities referring to the system $\boldsymbol{e}$.

2) The density of electric current $j(x)$ so obtained is introduced in the equations of motion of the low energy photons and these equations are solved.

We suppose here that the first part of the problem has been solved in some exact or approximate way.

We observe that the expression of any operator O^e referring to the degrees of freedom $\boldsymbol{e}$ at any time will contain only the quantities referring to system $\boldsymbol{e}$, so that O^e will commute with any operator O^p and with any state vector $|\varphi\rangle$ referring only to the low energy photons

$$[O^e O^p] = 0 , \tag{1}$$

$$O^e|\varphi\rangle = |\varphi\rangle O . \tag{2}$$

The second part of the problem consists in the treatment of the equation ([8]):

$$\Box A = -j , \tag{3}$$

where j is supposed to be known and where we are interested only in the components of the field $A(x)$ of energy smaller than ε.

Let us define $A(k)$ and $j(k)$ through ([9]):

$$A(x) = \frac{1}{(2\pi)^3}\int \mathrm{d}k \exp[i(kx)]\delta(k^2)A(k) , \tag{4}$$

$$j(x) = \frac{1}{(2\pi)^4}\int \mathrm{d}k \exp[i(kx)]j(k) . \tag{5}$$

Defining in the usual way incoming and outgoing field operators $A^{\mathrm{in}}(x)$ and $A^{\mathrm{out}}(x)$, it is easy to show that the simple relation holds:

$$A^{\mathrm{out}}(k) = A^{\mathrm{in}}(k) + i\varepsilon(k)j(k) , \tag{6}$$

where $A^{\mathrm{in}}(k)$ and $A^{\mathrm{out}}(k)$ are defined analogously to $A(k)$ by (4) and $\varepsilon(k) = 1$ for $k_0 > 0$, $\varepsilon(k) = -1$ for $k_0 < 0$ ([10]).

([8]) A and j denote fourvectors; $e = 1$; $\hbar = 1$ in the following.

([9]) (kx) denotes fourdimensional scalar product.

([10]) See, for example, the work of THIRRING and TOUSCHEK ([3]) or the work of the author ([4]).

Introducing the quantization of the electromagnetic field, the observable to which we shall be mainly interested is the number N of photons, whose momentum k lies in a volume V_k of the momentum space, and whose polarization vector is $e(k)$. We have

$$N = \frac{1}{(2\pi)^3}\int_{V_k} \mathrm{d}k\, \delta(k^2) A_e(k)^* A_e(k)\,, \tag{7}$$

where $A_e(k) = (A(k)\, e(k))$.

Correspondingly we define the number N^{out} of outgoing photons using the outgoing field A^{out} instead of A.

We shall call $|0\rangle$ the vacuum state of the low energy free photons, $|1ke\rangle$ the state of one free photon of momentum k and polarization e. Then it is

$$A^{\mathrm{in}}(k)\,|0\rangle = 0\,. \tag{8}$$

3. – Precisation of the problem for the case of a quantized source.

As it was remembered in the Introduction, till now only the case in which the external system is classical had been treated in general.

Let us now suppose that the external system $\boldsymbol{e}$ is quantized. In this case it is necessary to specify what a kind of quantum-theoretical problem for the external system is considered. We shall first consider the case of a transition caused in the external system by a time-dependent perturbation of finite duration between two eigenstates of an unperturbed energy. In this way an unperturbed and a perturbed external system are defined.

— *Unperturbed external system.* – We call α a complete set of observables referring to the external system commuting with each other and with the unperturbed energy, α_r $(r = 1, 2, \ldots)$ a set of eigenvalues of these observables, $|\alpha_r\rangle$ the corresponding eigenstates in Heisenberg picture, E_r the energies of such eigenstates. We shall also introduce the corresponding eigenstates in Schrödinger picture $|\alpha_r(x_0)\rangle$. Then it is:

$$|\alpha_r(x_0)\rangle = |\alpha_r\rangle \exp[-iE_r x_0]\,, \qquad \langle\alpha_r(x_0)| = \exp[iE_r x_0]\langle\alpha_r|\,. \tag{9}$$

— *Perturbed external system.* – We suppose that the origin of the time x_0 has been fixed so that the time-dependent perturbation acts during the finite time interval $0 < x_0 < T$.

We define in the usual way the incoming and outgoing eigenstates $|\alpha_r^{\mathrm{in}}\rangle$, $|\alpha_r^{\mathrm{out}}\rangle$ of the total energy in Heisenberg picture. Then we introduce the cor-

responding eigenstates in Schrödinger picture $|\alpha_r^{\text{in}}(x_0)\rangle$, $|\alpha_r^{\text{out}}(x_0)\rangle$ and the unitary transformation operators in interaction picture $U^e(x_0)$ and $U^e_-(x_0)$ (11) referring to the external system, so that:

$$|\alpha_r^{\text{in}}(x_0)\rangle = U^e(x_0)|\alpha_r(x_0)\rangle = \sum_i U^e_{ir}(x_0)|\alpha_i(x_0)\rangle , \tag{10}$$

$$|\alpha_r^{\text{out}}(x_0)\rangle = U^e_-(x_0)|\alpha_r(x_0)\rangle = \sum_i U^e_{-ir}(x_0)|\alpha_i(x_0)\rangle . \tag{11}$$

The S-matrix for the external system is then defined by

$$S^e_{sr} = \langle \alpha_s^{\text{out}} | \alpha_r^{\text{in}} \rangle \tag{12}$$

and it is

$$U^e_-(x_0) = U^e(x_0)(S^e)^{-1} . \tag{13}$$

Let us choose the different pictures so that they coincide for $T = -\infty$. Then for a perturbation acting only from the time 0 to the time T we have

$$S^e = U^e(T) = U^e_-(0); \tag{14}$$

for $x_0 < 0$

$$U^e(x_0) = 1 , \quad U^e_{ir}(x_0) = \delta_{ir} , \quad U^e_-(x_0) = (U^e)^{-1}(T) , \quad U^e_{-ir}(x_0) = U^{e*}_{ri}(T), \tag{15}$$

for $x_0 > T$

$$U^e_-(x_0) = 1 , \quad U^e_{-ir}(x_0) = \delta_{ir} ; \quad U^e(x_0) = U^e(T) , \quad U^e_{ir}(x_0) = U^e_{ir}(T) . \tag{16}$$

Finally we define incoming and outgoing states for the total system. We call $|\alpha_r O^{\text{in}}\rangle$ the state of the total system in which for $x_0 \to -\infty$ the external system is in the state $|\alpha_r\rangle$, while there is no low energy photon present. Analogously we define $|\alpha_r O^{\text{out}}\rangle$, $|\alpha_r 1\, k c^{\text{out}}\rangle$.

4. – Calculation of the average number of emitted photons. First part.

The most interesting quantity is the average number $\overline{N}_{rs}$ of photons emitted with a given polarization in a given volume of the k space when the external system has undergone a transition between a state $|\alpha_r\rangle$ and a state $|\alpha_s\rangle$, supposing that initially no low energy photon is present (12).

Then the state of the experiment is $|\alpha_r O^{\text{in}}\rangle$.

An expression for $\overline{N}_{rs}$ may be found as follows.

(11) See for instance, B. A. Lippmann and J. Schwinger: *Phys. Rev.*, **79**, 469 (1950).

(12) In Appendix I is shown that the corresponding probability W_{Nrs} for the emission of N photons may be immediately calculated, when $\overline{N}_{rs}$ is known.

Let us introduce the observable $\delta_{\alpha^{\text{out}}\alpha_s}$ having the value 1, when a measurement of the observables α at the end of the experiment gives the value α_0 (that is when at the end of the experiment the external system is in the state $|\alpha_s\rangle$), the value 0 when the external system is in an eigenstate of the unperturbed system different from $|\alpha_s\rangle$.

Let us consider the expression

$$\langle \alpha_r O^{\text{in}} | N^{\text{out}} \delta_{\alpha^{\text{out}}\alpha_s} | \alpha_r O^{\text{in}} \rangle . \tag{17}$$

This is the expectation value of the observable $N^{\text{out}}\delta_{\alpha^{\text{out}}\alpha_s}$ in the state $|\alpha_r O^{\text{in}}\rangle$ of the experiment. Let us now measure N and α at the end of the experiment. Then the observable $N^{\text{out}}\delta_{\alpha^{\text{out}}\alpha_s}$ has the value of N when the final state of the external system is $|\alpha_s\rangle$, O when it is another state of the set $|\alpha_i\rangle$. Thus its expectation value (17) gives the average number of photons emitted in the transition $r \to s$, multiplied by the probability that such a transition occurs.

So $\overline{N}_{rs}$ is obtained dividing the expression (17) by $|S^e_{sr}|^2$:

$$\overline{N}_{rs} = \frac{\langle \alpha_r O^{\text{in}} | N^{\text{out}} \delta_{\alpha^{\text{out}}\alpha_s} | \alpha_r O^{\text{in}} \rangle}{|S^e_{sr}|^2} . \tag{18}$$

This expression now may be transformed in such manner as to eliminate from it all the quantities referring to the field of the low energy photons.

Using (7) we obtain from (18):

$$\overline{N}_{rs} = \frac{1}{|S^e_{sr}|^2} \frac{1}{(2\pi)^3} \int \mathrm{d}k \delta(k^2) \langle \alpha_r O^{\text{in}} | A_s^{\text{out}*}(k) A_e^{\text{out}}(k) \delta_{\alpha^{\text{out}}\alpha_s} | \alpha_r O^{\text{in}} \rangle . \tag{19}$$

Using (1) with $O^e = \delta_{\alpha^{\text{out}}\alpha_s}$, $O^p = A_e^{\text{out}}(k)$ and (6) we may transform the expectation value E in (19) as it follows:

$$E = \langle \alpha_r O^{\text{in}} | A_s^{\text{out}*}(k) A_e^{\text{out}}(k) \delta_{\alpha^{\text{out}}\alpha_s} | \alpha_r O^{\text{in}} \rangle = \tag{20}$$

$$= \langle \alpha_r O^{\text{in}} | \left(A_e^{\text{in}*}(k) - i j_e^*(k) \right) \delta_{\alpha^{\text{out}}\alpha_s} \left(A_e^{\text{in}}(k) + i j_e(k) \right) | \alpha_r O^{\text{in}} \rangle .$$

At this point we suppose to use the special Heisenberg picture which coincides with the Schrödinger picture as $x_0 \to -\infty$.

Then $|\alpha_r O^{\text{in}}\rangle = |\alpha_r\rangle |O\rangle$.

Using (8) and (2) we obtain

$$E = \langle O | O \rangle \langle \alpha_r | j_e^*(k) \delta_{\alpha^{\text{out}}\alpha_s} j_e(k) | \alpha_r \rangle = \langle \alpha_r^{\text{in}} | j_e^*(k) \delta_{\alpha^{\text{out}}\alpha_s} j_e(k) | \alpha_r^{\text{in}} \rangle , \tag{21}$$

where we may return to a general Heisenberg picture in the last expression.

So we have obtained an expression containing only quantities referring to the external system.

We have further:

$$(22) \qquad E = \sum_i \langle \alpha_r^{in} | j_e^*(k) \delta_{\alpha^{out}\alpha_s} | o_i^{out} \rangle \langle \alpha_i^{out} | j_e(k) | \alpha_r^{in} \rangle =$$

$$= \langle \alpha_r^{in} | j_e^*(k) | \alpha_s^{out} \rangle \langle \alpha_s^{out} | j_e(k) | \alpha_r^{in} \rangle = | \langle \alpha_s^{out} | j_e(k) | \alpha_r^{in} \rangle |^2$$

and, finally, substituting into (19),

$$(23) \qquad \bar{N}_r = \frac{1}{|S_{sr}^e|^2} \frac{1}{(2\pi)^3} \int \mathrm{d}k \, \delta(k^2) | \langle \alpha_s^{out} | j(k) | \alpha_r^{in} \rangle |^2 .$$

This is a general expression which permits to calculate $\bar{N}_{rs}$ whenever the quantities referring to the external system are known.

An important feature of this expression is that it is proportional to e, e being the coupling constant of the charges with the low energy photons ([13]).

5. - Comparison with the result of the first order perturbative calculation of the probability of emission of one photon.

The expression (23) may be used to calculate or to discuss directly the average number $\bar{N}_{rs}$ of emitted photons.

However we prefer firstly to compare it with the expression of the probability W_{1rs} of emission of one photon, when the transition $r \to s$ occurs.

This quantity is given by

$$(24) \qquad W_{1rs} = \frac{1}{|S_{sr}^e|^2} \frac{1}{(2\pi)^3} \int \mathrm{d}k \, \delta(k^2) | \langle \alpha_s 1 k e^{out} | \alpha_r O^{in} \rangle |^2 .$$

The matrix element M in the expression (24) can be transformed as it follows:

$$(25) \qquad M = \langle \alpha_s 1 \, k e^{out} | \alpha_r O^{in} \rangle = \langle \alpha_s O^{out} | A_e^{out}(k) | \alpha_r O^{in} \rangle = i \langle \alpha_s O^{out} | j_e(k) | \alpha_r O^{in} \rangle ,$$

where $j_e(k) = (j(k) e(k))$ and we have used (6) and (8).

Now let us call e the coupling constant of the charges with the low energy photons. Then let us suppose to calculate W_{1rs} with the perturbative method, using e as expansion parameter, and to retain only the first term $W_{1rs}^{(1)}$ of the

([13]) This property has been already pointed out and used in my paper ([6]).

expansion. The result of such a calculation will be obtained expanding the matrix element M which appears in (24) in powers of e, and retaining only the first term $M^{(1)}$ of the expansion.

Let us first expand $|\alpha_r O^{\text{in}}\rangle$ in powers of e. The first term of the expansion is obtained putting $e = 0$, that is eliminating the interaction. Now without interaction the field of the low energy photons at any time is still in the vacuum state, while the external system is in the state $|\alpha_r^{\text{in}}\rangle$ in any case, so that we obtain:

$$|\alpha_r O^{\text{in}}\rangle = |\alpha_r^{\text{in}}\rangle |O\rangle + \text{terms of higher order in } e .$$

Then we use the Heisenberg picture which coincides with the Schrödinger picture at the end of the experiment. Then $\langle \alpha_s O^{\text{out}}| = \langle \alpha_s^{\text{out}}| \langle O|$. Now observing that $\langle \alpha_s^{\text{out}}| \langle O|$ does not depend on e, and that $j_e(k)$ is simply proportional to e, we have, using (2):

$$M^{(1)} = i \langle \alpha_s^{\text{out}}| \langle O| j_e(k) |\alpha_r^{\text{in}}\rangle |O\rangle = i \langle \alpha_s^{\text{out}}| j_e(k) |\alpha_r^{\text{in}}\rangle . \tag{26}$$

At this point we may return to a general Heisenberg picture, since the last expression is invariant for transformation of picture.

Substituting into (24) we obtain:

$$W_{1rs}^{(1)} = \frac{1}{|S_{sr}^e|^2} \frac{1}{(2\pi)^3} \int \mathrm{d}k \, \delta(k^2) |\langle \alpha_s^{\text{out}}| j_e(k) |\alpha_r^{\text{in}}\rangle|^2 . \tag{27}$$

The comparison of this expression with (20) leads to the important result [14]:

$$\overline{N}_{rs} = W_{1rs}^{(1)} , \tag{28}$$

that is, when the reaction of the photons is neglected, the average number of photons emitted in a transition is equal to the first term of the expansion in powers of e of the emission probability of one photon in the same transition.

The consequences of this result will be discussed later. Here I observe only that this result reduces the calculation of $\overline{N}_{rs}$ to a perturbation problem. However such a perturbation problem till now has been treated only in particular cases, neglecting the duration of the transition.

Here a general rigorous method of calculating expression (23) will be given, with the purpose of discussing the result in the most interesting cases.

---

[14] This result has been reported in [6] where it was deduced without direct calculations, using a different synthetical argument.

6. – Calculation of the average number of emitted photons. Second part.

Let us now derive an explicit expression for the matrix element appearing in (23).

Inverting (5) we have:

$$j(k) = \int \mathrm{d}x \exp[-i(kx)] j(x) \,. \tag{29}$$

So we obtain

$$\langle \alpha_s^{\mathrm{out}} | j(k) | \alpha_r^{\mathrm{in}} \rangle = \int \mathrm{d}x \exp[-i(kx)] \langle \alpha_s^{\mathrm{out}} | j(x) | \alpha_r^{\mathrm{in}} \rangle \,. \tag{30}$$

Here, to introduce more explicitly the known behaviour of the external system, we pass to the Schrödinger picture coinciding with the Heisenberg picture at $t = -\infty$. Then using (10) and (11) we have

$$\begin{aligned} \langle \alpha_s^{\mathrm{out}} | j(k) | \alpha_r^{\mathrm{in}} \rangle &= \int \mathrm{d}x \exp[-i(kx)] \langle \alpha_s^{\mathrm{out}}(x_0) | j(\boldsymbol{x}) | \alpha_r^{\mathrm{in}}(x_0) \rangle = \\ &= \sum_{ij} \int \mathrm{d}x \exp[-i(kx)] U_{js}^{e*}(x_0) U_{ir}^{e}(x_0) \langle \alpha_j(x_0) | j(\boldsymbol{x}) | \alpha_i(x_0) \rangle \,, \end{aligned} \tag{31}$$

where the operator $j(\boldsymbol{x})$ is constant with time.

Now, using (9), we have

$$\int \mathrm{d}^3 x \exp[-i(kx)] \langle \alpha_j(x_0) | j(\boldsymbol{x}) | \alpha_i(x_0) \rangle = A_{ji}(\boldsymbol{k}) \exp[-i(E_i - E_j - k_0) x_0] \,, \tag{32}$$

where we have introduced the quantities

$$A_{ji}(\boldsymbol{k}) = \int \mathrm{d}^3 x \exp[-i\boldsymbol{k}\cdot\boldsymbol{x}] \langle \alpha_j | j(\boldsymbol{x}) | \alpha_i \rangle \,. \tag{33}$$

Substituting (32) into (31) we obtain

$$\langle \alpha_s^{\mathrm{out}} | j(k) | \alpha_r^{\mathrm{in}} \rangle = i \sum_{ij} A_{ji}(\boldsymbol{k}) \int \mathrm{d}x_0 U_{js}^{e*}(x_0) U_{ir}^{e}(x_0) \exp[-i(E_i - E_j - k_0) x_0] \,. \tag{34}$$

Here we remember that we have assumed that the perturbation causing transitions between the states $|\alpha_i\rangle$ is different from zero only during the time interval between 0 and T.

Then (15) and (16) hold, and subdividing the integration over the time

in eq. (34) in three parts: from $-\infty$ to 0, from T to $+\infty$, from 0 to T, we obtain

$$(35)\qquad \langle \alpha_s^{\text{out}} | j(k) | \alpha_r^{\text{in}} \rangle = i \left(\sum_j A_{jr}(\boldsymbol{k})\, U^e_{sj}(T) \int_{-\infty}^{0} \mathrm{d}x_0 \exp\left[-i(E_r - E_j - k_0)x_0 \right] + \right.$$

$$+ \sum_i A_{si}(\boldsymbol{k})\, U^e_{ir}(T) \int_{T}^{\infty} \mathrm{d}x_0 \exp\left[-i(E_i - E_s - k_0)x_0 \right] +$$

$$\left. + \sum_{ij} A_{ji}(\boldsymbol{k}) \int_0^T \mathrm{d}x_0\, U^{e*}_{-js}(x_0)\, U^e_{ir}(x_0) \exp\left[-i(E_i - E_j - k_0)x_0 \right] \right) =$$

$$= i \left(\sum_j A_{jr}(\boldsymbol{k})\, U^e_{sj}(T) \left(\pi\delta(E_r - E_j - k_0) + \frac{i}{E_r - E_j - k_0} \right) + \right.$$

$$+ \sum_i A_{si}(\boldsymbol{k})\, U^e_{is}(T) \exp\left[-i(E_i - E_s - k_0)T \right] \left(\pi\delta(E_i - E_s - k_0) - \frac{i}{E_i - E_s - k_0} \right) +$$

$$\left. + \sum_{ji} A_{ji}(\boldsymbol{k}) \int_0^T \mathrm{d}x_0\, U^{e*}_{-js}(x_0)\, U^e_{ir}(x_0) \exp\left[-i(E_i - E_j - k_0)x_0 \right] \right).$$

Substituting this result in (23), a general expression for $\bar{N}_{rs}$ is obtained, which may be calculated when we know the eigenstates of the unperturbed external system (energies E_i and matrix elements $A_{ji}(\boldsymbol{k})$, formula (32)) and the transformation matrix $U^e(x_0)$ of the interaction picture as a function of time.

If the external system is constituted of electrons and positrons treated with second quantization, then we have:

$$(36)\qquad j(x) = ie\bar{\psi}(x)\gamma\psi(x)$$

and (33) becomes:

$$(37)\qquad A_{ji}(\boldsymbol{k}) = ie \int \mathrm{d}^3 x \exp\left[-i\boldsymbol{k}\cdot\boldsymbol{x} \right] \langle \alpha_j | \bar{\psi}(\boldsymbol{x})\gamma\psi(\boldsymbol{x}) | \alpha_i \rangle .$$

Let us consider the case in which the external system is constituted of one electron in an external field. Calling $|\beta_i\rangle$ its eigenstates in the configuration space, and $\psi_i(\boldsymbol{x}') = \langle \boldsymbol{x}' | \beta_i \rangle$ its time independent unperturbed eigenfunctions, we have in this case from (37) [15]:

$$(38)\quad A_{ji}(\boldsymbol{k}) = ie \int \mathrm{d}^3 x' \exp\left[-i\boldsymbol{k}\cdot\boldsymbol{x}' \right] \bar{\psi}_j(\boldsymbol{x}')\gamma\psi_i(\boldsymbol{x}') = ie \langle \beta_j | \gamma_4 \exp\left[-i\boldsymbol{k}\cdot\boldsymbol{x} \right] \gamma | \beta_i \rangle ,$$

where here $\boldsymbol{x}$ is an operator.

[15] Or putting $j(x) = \gamma\,\delta(\boldsymbol{x} - \boldsymbol{x}')$ into (32).

7. – Proof of the finiteness of the average number of photons emitted in a transition between two bound states.

Let us now discuss the conditions for the finiteness of $\bar{N}_{rs}$.

Calling $d\Omega_k$ the element of solid angle in the $\boldsymbol{k}$ space, the expression (23) may be written more explicitly

$$\bar{N}_{rs} = \frac{1}{|S^e_{sr}|^2} \frac{1}{2(2\pi)^3} \int d\Omega_k \int dk_0 k_0 |\langle \alpha_s^{\text{out}} | j_0(k) | \alpha_r^{\text{in}} \rangle|^2 . \tag{39}$$

Now we remember that we are treating the case of emission of photons the energy of which is sufficiently low to allow this kind of approximate treatment. So the integrals in (23) or in (39) are extended only to a finite region V_k of the $\boldsymbol{k}$ space. If this region does not contain the point $\boldsymbol{k} = 0$, $\bar{N}_{rs}$ is certainly finite, otherwise an infinite amount of energy would be emitted: in fact an infinite number of photons of finite energy would be emitted.

Therefore a divergence of the integrals appearing in (23) or (39) may only occur in the neighbourhood of $\boldsymbol{k} = 0$.

So $\bar{N}_{rs}$ is finite when the integral over $(\boldsymbol{k})$ in (39) does not diverge in the neighbourhood of $\boldsymbol{k} = 0$.

A sufficient condition to be in this case is that the matrix element $\langle \alpha_s^{\text{out}} | j(k) | \alpha_r^{\text{in}} \rangle$ be a steady finite function of k_0 at $k_0 = 0$, for all the directions of $\boldsymbol{k}$.

A more general sufficient condition is that

$$\langle \alpha_s^{\text{out}} | j(k) | \alpha_r^{\text{in}} \rangle = f(\boldsymbol{k}) + g(\boldsymbol{k}) \delta(k_0) , \tag{40}$$

with $f(\boldsymbol{k})$ and $g(\boldsymbol{k})$ steady finite functions of k_0 at $k_0 = 0$, for all the directions of $\boldsymbol{k}$. In fact such an expression gives rise in (39) to integrals of the form

$$\int dk_0 k_0 \delta(k_0) \qquad \text{and} \qquad \int dk_0 k_0 \delta^2(k_0) ,$$

which are finite ([16]).

Now we shall prove that $\bar{N}_{rs}$ is finite when the photons are emitted in a transition between two unperturbed energy eigenstates $|\alpha_r\rangle$ and $|\alpha_s\rangle$ belonging to a discrete spectrum. We firstly suppose that no other unperturbed energy eigenstate with the same energy of the states $|\alpha_r\rangle$ or $|\alpha_s\rangle$ occurs.

([16]) For the meaning and the value of the second integral see footnote ([5]) of reference ([4]).

Then we may write again formula (35) in the form:

$$(41)\qquad \langle \alpha_s^{\mathrm{out}} | j(k) | \alpha_r^{\mathrm{in}} \rangle = \frac{1}{k_0} U_{sr}^e(T) \left(A_{rr}(\boldsymbol{k}) - A_{ss}(\boldsymbol{k}) \exp[ik_0 T]\right) +$$

$$+ i\pi\delta(k_0) U_{sr}^e(T) \left(A_{rr}(\boldsymbol{k}) + A_{ss}(\boldsymbol{k}) \exp[ik_0 T]\right) -$$

$$- \left(\sum_{j \neq r} A_{jr}(\boldsymbol{k}) U_{sj}^e(T) \frac{1}{E_r - E_j - k_0} - \sum_{i \neq s} A_{si}(\boldsymbol{k}) U_{ir}^e(T) \cdot \right.$$

$$\left. \cdot \exp[-i(E_i - E_s - k_0)T] \frac{1}{E_i - E_s - k_0} \right) + i\pi \Big(\sum_{j \neq r} A_{jr}(\boldsymbol{k}) U_s^e(T) \delta(E_r - E_j - k_0) +$$

$$+ \sum_{i \neq s} A_{si}(\boldsymbol{k}) U_{ir}^e(T) \exp[-i(E_i - E_s - k_0)T] \delta(E_i - E_s - k_0) \Big) +$$

$$+ \int_0^T \mathrm{d}x \exp[-i(kx)] \langle \alpha_s^{\mathrm{out}}(x_0) | j(\boldsymbol{x}) | \alpha_r^{\mathrm{in}}(x_0) \rangle ,$$

where the last term has been written in its original form (31). Now we show that (41) has the form (40) in the neighbourhood of $k_0 = 0$.

We observe firstly that, owing to the assumption of the discrete spectrum, the fourth term of (41) is 0 in the neighbourhood of $k_0 = 0$.

For the same reason the factors $1/(E_r - E_j - k_0)$ and $1/(E_i - E_s - k_0)$ in the third term of the right hand side of (41) are always finite in the neighbourhood of $k_0 = 0$. Therefore each term of the sums over j and i is finite and it is easy to show that even the result is finite for the same values of k_0. A rigorous proof is given in the Appendix II.

The last term in (41) is certainly finite because the integration over the time is extended to a finite interval, and the integrand is finite owing to the supposition of bound states ([17]).

At first sight the first term of (41) could give rise to an infinity of the form $1/k_0$. But this does not happen because the last factor of this term is 0 for $k_0 = 0$.

In fact we have from (33):

$$(42)\qquad \boldsymbol{A}_{rr}(0) = \int \mathrm{d}^3 x \langle \alpha_r | \boldsymbol{j}(\boldsymbol{x}) | \alpha_r \rangle .$$

Now $\langle \alpha_r | \boldsymbol{j}(\boldsymbol{x}) | \alpha_r \rangle$ is the average value of the density of current in a statio-

([1]) A direct proof may be given starting from the explicit expression (35). Then the finiteness of this expression may be proved using formula (II.3) of Appendix II and arguments analogous to those used in Appendix II to prove the finiteness of the third term of (41).

nary state, so that ([18]),

$$\operatorname{div} \langle \alpha_r | \boldsymbol{j}(\boldsymbol{x}) | \alpha_r \rangle = 0 \,. \tag{43}$$

Therefore a vector field $\boldsymbol{I}(x)$ exists, for which

$$\langle \alpha_r | \boldsymbol{j}(\boldsymbol{x}) | \alpha_r \rangle = \operatorname{rot} \boldsymbol{I}(\boldsymbol{x}) \,. \tag{44}$$

Then we have

$$\boldsymbol{A}_{rr}(0) = \int \mathrm{d}^3 x \operatorname{rot} \boldsymbol{I}(\boldsymbol{x}) \,. \tag{45}$$

The vector field $\boldsymbol{I}(\boldsymbol{x})$ may be chosen so that it tends to zero as $|\boldsymbol{x}|$ tends to infinity. In fact $\langle \alpha_r | \boldsymbol{j}(\boldsymbol{x}) | \alpha_r \rangle$ decreases exponentially as $|\boldsymbol{x}|$ tends to infinity, owing to the assumption of $|\alpha_r\rangle$ being a bound state, so that (44) becomes rot $\boldsymbol{I}(\boldsymbol{x}) \simeq 0$ in the neighbourhood of the infinity of $|\boldsymbol{x}|$, and a solution of it is $\boldsymbol{I}(\boldsymbol{x}) = 0$ in the same region.

Now let us consider a component of the vector $\boldsymbol{A}_{rr}(0)$, for instance the third one $A_{rr3}(0)$. It is:

$$A_{rr3}(0) = \int \mathrm{d}\boldsymbol{x} \left(\frac{\partial I_3(\boldsymbol{x})}{\partial x_2} - \frac{\partial I_2(\boldsymbol{x})}{\partial x_3} \right) = \int_\sigma \mathrm{d}\sigma \left(n_2(\boldsymbol{x}) I_3(\boldsymbol{x}) - n_3(\boldsymbol{x}) I_2(\boldsymbol{x}) \right) \,, \tag{46}$$

where we have transformed the integration over the volume into an integration

---

([18]) Indeed let us consider the unperturbed problem for the external system. The electric current in Heisenberg picture $j^0(x)$ in this problem satisfies the continuity equation:

$$\operatorname{div} \boldsymbol{j}^0(x) = - \frac{\partial j_0^0(x)}{\partial x_0} \,.$$

So we have:

$$\operatorname{div} \langle \alpha_r | \boldsymbol{j}^0(x) | \alpha_r \rangle = - \frac{\partial}{\partial x_0} \langle \alpha_r | j_0^0(x) | \alpha_r \rangle \,.$$

Then, passing to the Schrödinger picture, which coincides with the Heisenberg picture at $t = -\infty$, and using (9), we have

$$\operatorname{div} \langle \alpha_r | \boldsymbol{j}^0(\boldsymbol{x}) | \alpha_r \rangle = - \frac{\partial}{\partial x_0} \langle \alpha_r(x_0) | j_0^0(\boldsymbol{x}) | \alpha_r(x_0) \rangle = - \frac{\partial}{\partial x_0} \langle \alpha_r | j_0^0(\boldsymbol{x}) | \alpha_r \rangle = 0 \,.$$

Now at $t = -\infty$ the perturbed external system coincides with the unperturbed external system, so that the result holds also for the perturbed external system and it may be written in the form (43).

over a surface at the infinity, $\boldsymbol{n}(\boldsymbol{x})$ being the unit vector normal to the surface element.

Then we see that the result is certainly zero because $\boldsymbol{I}(\boldsymbol{x})$ goes to zero exponentially as $|\boldsymbol{x}|$ tends to infinity.

Therefore it is $\boldsymbol{A}_{rr}(0) = 0$.

So the first term of (41) has the form 0/0, as k_0 tends to zero, and it is easy to see that it tends to a finite value, as k_0 tends to zero ([19]).

The factor which multiplies the $\delta(k_0)$ function in the second term of (41) is certainly finite for $k_0 = 0$ (we have shown that it is zero), so that (41) has the form (40).

In this manner we have proved that the number of photons $\bar{N}_{rs}$ emitted in a transition between two discrete unperturbed energy eigenstates $|\alpha_r\rangle$ and $|\alpha_s\rangle$ is finite in the case in which no other unperturbed energy eigenstate with the same energy as the states $|\alpha_r\rangle$ or $|\alpha_s\rangle$ exists.

It is easy to extend the proof to the case in which there are other discrete unperturbed energy eigenstates with the same energy as the states $|\alpha_r\rangle$ or $|\alpha_s\rangle$. This is done in Appendix III.

The case in which the unperturbed energy of the external system has a continuum spectrum containing also the energy of the state $|\alpha_r\rangle$ or $|\alpha_s\rangle$ is more complicated. The extension of the proof to this case is treated in Appendix IV ([20]).

8. – Average number of photons emitted in a transition between two states belonging to a continuum spectrum.

It is easy to modify the formula (35) for the case in which the initial and final states of the external system belong to a continuum spectrum. Let p be a set of parameters labelling the unperturbed eigenstates $|\alpha_p\rangle$, of energies E_p, which belong to the continuum spectrum.

Let $\varrho(p)$ be the weight function of such a representation. Then, instead of (35), we have, for a transition between the states $|\alpha_r\rangle$ and $|\alpha_s\rangle$ of the

---

([19]) In fact from De l'Hospital's rule we have:

$$\lim_{k_0 \to 0} \frac{\boldsymbol{A}_{rr}(\boldsymbol{k})}{k_0} = \lim_{k_0 \to 0} \frac{\mathrm{d}\boldsymbol{A}_{rr}(\boldsymbol{k})}{\mathrm{d}k_0} .$$

Now this limit exists certainly and it is finite because $\boldsymbol{A}_{rr}(\boldsymbol{k})$ is the Fourier transform of a function of $\boldsymbol{x}$ which falls to zero exponentially as $|\boldsymbol{x}|$ tends to infinity.

([20]) The notation used in Appendix IV is explained in the next Section 8.

continuum:

$$(47)\quad \langle \alpha_s^{\text{out}} | j(k) | \alpha_r^{\text{in}} \rangle =$$

$$= i\Bigg(\int \mathrm{d}p\, \varrho(p) A_{rp}(\boldsymbol{k})\, U^e_{sp}(T) \Big(\pi\, \delta(E_r - E_p - k_0) + \frac{i}{E_r - E_p - k_0} \Big) + \sum_j \ldots +$$

$$+ \int \mathrm{d}p\, \varrho(p) A_{sp}(\boldsymbol{k})\, U^e_{pr}(T) \exp[-i(E_p - E_s - k_0)T] \cdot$$

$$\cdot \Big(\pi\, \delta(E_p - E_s - k_0) - \frac{i}{E_p - E_s - k_0} \Big) + \sum_i \ldots + \int \mathrm{d}p\, \mathrm{d}p'\, \varrho(p)\, \varrho(p') A_{p'p}(\boldsymbol{k}) \cdot$$

$$\cdot \int_0^T \mathrm{d}x_0\, U^{e*}_{-p's}(x_0)\, U^e_{pr}(x_0) \exp[-i(E_p - E_{p'} - k_0)x_0] + \sum_{ij} \ldots \Bigg),$$

where the terms $\sum_j \ldots$, $\sum_i \ldots$, $\sum_{ij} \ldots$ have the same form as in (35), and the summations must be extended over the eventually existing discrete unperturbed eigenstates.

We see from this formula that the arguments used to prove the finiteness of $\overline{N}_{rs}$ in the case of a transition between two bound states do no more hold. This fact is due to the terms containing the factors $i/(E_r - E_p - k_0)$ and $i/(E_p - E_s - k_0)$, which increase arbitrarily for $k_0 = 0$ when p has values in the neighbourhood of r and s respectively.

Therefore the most important contributions to (47) come from these two terms for values of the variables of integration p near r and s respectively.

Hence assuming that $U^e_{sp}(T)$ is continuous for $p = r$ and $U^e_{pr}(T)$ is continuous for $p = s$, we have, neglecting the terms of (47) which remain finite as k_0 tends to zero:

$$(48)\quad \langle \alpha_s^{\text{out}} | j(k) | \alpha^{\text{in}} \rangle \simeq -S^e_{sr} \int \mathrm{d}p\, \varrho(p) \Big(A_{pr}(\boldsymbol{k}) \frac{1}{E_r - E_p - k_0} - A_{sp}(\boldsymbol{k}) \frac{1}{E_p - E_s - k_0} \Big).$$

The approximations used to derive this simplified formula are the same used by Res Jost (5) and by Jauch and Rohrlich (2) in the calculation of $W^{(1)}_{1rs}$ in the particular case of the transition between two plane waves of one charged particle.

9. – Case of the transition of one electron between two definite momentum states.

The expression (48) may be easily calculated in the particular case of a transition between two plane wave states of one electron. The explicit calculation is given in Appendix V.

The same result may be derived also using the general property (28). Indeed the first order perturbative calculation of the probability amplitude of emission of one electron in this particular case has been made by RES JOST ([5]) and by JAUCH and ROHRLICH ([2]) with the same approximations; from the result it may be deduced:

$$W^{(1)}_{1rs} = \frac{e^2}{2(2\pi)^3}\int \mathrm{d}k\,\delta(k^2)\left|\frac{(p_r e)}{(p_r k)} - \frac{(p_s e)}{(p_s k)}\right|^2 . \tag{49}$$

Now, from (28) it follows that the same expression gives the average number of emitted photons $\overline{N}_{rs}$. This result is confirmed from the direct calculation of Appendix V.

The expression (49) coincides with the expression found by THIRRING and TOUSCHEK ([3]) for the average number of photons emitted in the analogous classical problem, with analogous approximations.

Therefore the number of photons emitted in the transition between two definite momentum states is the same in the classical and in the quantum-mechanical problems, provided the duration and the particularities of the transition are neglected, as it was made deriving (48) from (47) ([21]).

10. – Extension to the case of a transition between two non-stationary states.

I observe that the arguments leading to formula (18) for $\overline{N}_{rs}$ hold also when $|\alpha_r\rangle$ and $|\alpha_s\rangle$ are non-stationary states of the unperturbed external system: in this case α is a complete set of commuting observables having $|\alpha_r\rangle$ and $|\alpha_s\rangle$ as eigenstates. Moreover, all the arguments leading to formula (23) hold also in this case, so that the average number of photons emitted in the transition between two non-stationary states $|\beta_r\rangle$ and $|\beta_s\rangle$ is given by:

$$\overline{N}_{rs} = \frac{1}{|S^e_{s'}|^2}\,\frac{1}{(2\pi)^3}\int \mathrm{d}k\,\delta(k^2)\,|\langle\beta^{\mathrm{out}}_s|j_e(k)|\beta^{\mathrm{in}}_r\rangle|^2 . \tag{50}$$

Now let us express $|\beta_r\rangle$ and $|\beta_s\rangle$ as a superposition of stationary states $|\alpha_i\rangle$. Then it is

$$\langle\beta^{\mathrm{out}}_s|j(x)|\beta^{\mathrm{in}}_r\rangle = \sum_{m\,i}\langle\beta_s|\alpha_n\rangle\langle\alpha_m|\beta_r\rangle\langle\alpha^{\mathrm{out}}_n|j(k)|\alpha^{\mathrm{in}}_m\rangle . \tag{51}$$

([21]) So this rigorous proof confirms the arguments given by JAUCH and ROHRLICH ([2]) to deduce $\overline{N}_{rs}$ in this particular case.

So this problem too is reduced to the calculation of matrix elements of $j(k)$ between stationary states, and may be solved using formula (35).

Moreover from this remark we deduce easily the finiteness of the number of photons emitted from an arbitrary system in a transition between two states that are superposition of bound states.

11. – Remarks on the case of a transition caused by a constant perturbation.

Till now we have studied the problem of the emission of low energy photons in a transition between two states, caused by a perturbation of duration limited in time.

There are in general conceptual difficulties to extend the problem to the case of a transition due to a time-independent perturbation.

Let us first consider the case in which the effect of the time-independent perturbation on each particle is not limited to a finite time interval.

Then the definition of a transition probability per unit time in the case of a time-independent perturbation implies the existence of times that are long compared to the periods involved in the transition, and small compared to the average life time of the initial state ([22]).

Such a condition is certainly not satisfied in the problem of emission of photons of sufficiently low energy in a transition between two discrete states, caused by a time-independent perturbation.

Indeed for sufficiently low energy of the photons the periods of the photons, the emission of which is studied, become longer than the average life time of the initial state.

So the problem of emission of photons of arbitrarily small energy in a transition between two states caused by a constant perturbation has in this case no meaning.

The extension of these considerations to the case of a transition between states of the continuum, however, requires further examination. Indeed in this case the effect of the perturbation on each particle may have a finite duration, even when the perturbation is constant in time.

Here we make only some remarks about this problem.

Let us consider a transition between plane waves due to a time independent perturbation (usual S matrix problem).

Then we have to distinguish whether the perturbation energy is different from zero only in a finite region of space or not.

([22]) See P. A. M. Dirac: *The Principles of Quantum Mechanics* (Cambridge, 1947), page 181.

In the first case (S matrix problem with external field) the effect of the perturbation causing the transition on each particle is limited to a finite time interval. It is then possible to define the problem of emission of photons of arbitrarily low energy in a transition due to the external field, and we can apply the treatment of Sections **10** and **11**, which in particular leads to the Bloch-Nordsieck divergence.

In the second case (S matrix problem without external field, for instance: relativistic quantum-field theory) the effet of the perturbation on each particle is not limited to a finite time interval.

Therefore it seems reasonable to conclude that in this case the problem of emission of photons of arbitrarily low energy in a transition due to the interaction of the fields of the system has no meaning. Therefore the Bloch-Nordsieck divergence does not occur in an S matrix problem without external field, because the problem itself to which it refers does not exist in this case ([23]).

12. – Remarks on the finiteness of N_{rs} in real experiments.

In Sections **7** and **10** I have proved the finiteness of the number of photons emitted from an arbitrary quantized system in an arbitrary transition between two bound states or between two superpositions of them.

This result is sufficient to conclude that in all the real well determined experiments the number of photons is finite. In fact it is reasonable to assume that in all the real experiments the initial and final states are bound states or superpositions of them, otherwise an infinite region of space would be necessary to perform the experiment.

This statement seems at first sight to contradict the fact that most of the experiments are undertaken with the purpose of measuring transition probabilities between plane wave states. However a further analysis of the experiments shows that only non-stationary states are prepared, that during some time interval behave as like as possible as plane waves. But before and after this time interval the particles behave in quite a different fashion, and generally sooner or later they come to rest in some part of the laboratory. Therefore the consideration of the experiments as scattering experiments is only an ap-

([23]) Therefore, if we start from the knowledge of the S-matrix without external field, the Bloch-Nordsieck divergence is an interference effect that occurs when a superposition of plane waves is considered, so as to form ingoing and outgoing wave packets. Indeed in this case the effect on each particle of the perturbation causing the transition has a duration limited to the time interval during which the wave packets interact on each other: so the consideration of wave packets instead of plane waves has an effect similar to the effect of an external field.

proximation, which is very good when the emission of photons of sufficiently small wave length is considered, but becomes inappropriate when we consider the emission of photons the wave length of which is of the same order as the dimensions of the laboratory or greater. In this latter case the appropriate approximation is to speak of a transition between two bound states ([24]).

It is important to remark that the finiteness of the number of photons is no consequence of the fact that every detector of photons cannot reveal photons of energy lower than some limit, but it is a property of the spectrum of the photon emitted from a source of finite size in the region of long wave lengths.

Precisely it is easy to see that the finiteness of the number of emitted photons is equivalent to the property that the energy emitted per unit of frequency-range tends to zero as the frequency tends to zero.

13. – Connection with the infrared divergence of the perturbative calculation.

Let us consider the case of a transition between two definite momentum states.

Then we know that in the perturbative calculation of the probability of emission of one photon (bremsstrahlung) a divergence of this probability for photons of low energy is found. Such a divergence is called infrared divergence.

Now in this same problem even the average number of emitted photons diverges. This was well known in the classical case (Bloch-Nordsieck divergence) and I have proved it rigorously in the quantum-mechanical case, in Section **9**.

Then the application of formula (28) to this problem immediately shows that these two divergences, although they refer to quite different physical quantities, are the consequence of the divergence of the same mathematical quantity, and therefore they are intimately connected to each other ([25]).

14. – Conclusions.

The principal results of this work may be so summarized:

1) I have given a general treatment of the problem of the emission of photons from a quantized system, when the reaction of the photons on the system is neglected. Till now such a problem had been solved only in the case of emission from a classical system. The most interesting quantity is the

---

([24]) See also ([6]).
([25]) See also ([6]).

average number of emitted photons, which is given from the general formula (23) or, more explicitly from (35).

2) I have proved that the average number of photons emitted in an experiment, which can really be made and therefore need not an infinite region of space, is always finite: this is a particular property of the emission spectrum in the neighbourhood of the energy zero (Sections **7**, **10**, **12**).

3) I have proved rigorously that the emission of low energy photons in a transition between two definite momentum states of a quantum-mechanical particle is the same as in the case of a classical particle, provided the duration of the transition is neglected (Section **9**).

4) A connexion has been found between the results of the perturbative calculation and those of the exact calculation, which holds exactly when the reaction of the photons on the charges is neglected: the average number of photons emitted in a transition is equal to the first term of the expansion in powers of e of the emission probability of one photon in the same transition (Section **5**).

5) The application of this property to the case of a transition between two definite momentum states leads to the conclusion that the Bloch-Nordsieck divergence and the infrared divergence of the perturbation calculation have their origin in the divergence of the same expression, notwithstanding they are divergences of different physical quantities (Section **13**).

Appendix I

Let us call $W_{N_{rs}}$ the probability of emission of N photons in a given momentum range, caused by a transition of the external system from the state α_r to the state α_s. Let $\bar{N}_{rs}$ be the average number of photons emitted in the same momentum range and in the same transition.

Then it may be asserted without need of direct calculation that in our approximation $W_{N_{rs}}$ is given by the Poisson distribution:

$$W_{N_{rs}} = \frac{\bar{N}_{rs}^{N}}{N!} \exp\left[-\bar{N}_{rs}\right]. \tag{I.1}$$

In fact let us consider all the processes in which a photon is emitted in the infinitesimal energy range dk_0, while eventually other photons are emitted in other energy ranges. Then we observe that each photon cannot interact with the other photons in this approximation, because we neglect the reaction of the photons on the charges, and photons can interact on each other only through

charges. So the emission of a photon in the energy range dk_0 is not affected from the emission of other photons in other energy ranges in the same transition. Therefore the emission of a photon in a given infinitesimal energy range is an event independent on the emission of other photons, so that we may define an emission probability of a photon per unit energy range, and one deduces in the usual way that the probability $W_{N_{rs}}$ of the emission of N photons is given by the Poisson distribution (I.1).

So the knowledge of $\bar{N}_{rs}$ is sufficient to individuate any transition probability.

Appendix II

We show here that (see Sect. 7):

$$\sum_{j\neq r} (A_{jr}(\boldsymbol{k})e)\, U^{e}_{sj}(T)\, \frac{1}{E_r - E_j - k_0}\,, \tag{II.1}$$

is finite in the neighbourhood of $k_0 = 0$.

From (33) we have:

$$\sum_j |(A_{jr}(\boldsymbol{k})e)|^2 = \sum_j |\langle \alpha_j | \int \mathrm{d}^3x \exp[-i\boldsymbol{k}\cdot\boldsymbol{x}] j_e(\boldsymbol{x}) | \alpha_r\rangle|^2 = \tag{II.2}$$

$$= \langle \alpha_r | \left| \left(\int \mathrm{d}^3x \exp[-i\boldsymbol{k}\cdot\boldsymbol{x}] \boldsymbol{j}(\boldsymbol{x}) \right) \cdot \boldsymbol{e} \right|^2 | \alpha_r \rangle\,.$$

So the sum $\sum_j' |(A_{jr}(0)e)|^2$ is equal to the expectation value in the state $|\alpha_r\rangle$ of the square of a component of the total electric current $\int \mathrm{d}^3x \boldsymbol{j}(\boldsymbol{x})$.

Now, if the theory has a meaning, the expectation value of this quantity in a bound state must be finite ([26]). So the expression (II.2) must be finite for $\boldsymbol{k} = 0$, and it is also finite in the neighbourhood of $\boldsymbol{k} = 0$ ([27]).

([26]) The fulfilment of this condition can be verified directly when the actual expression of $j(x)$ is given.

For instance in the case of one Dirac electron we have from (38) ($\boldsymbol{x}$ is here an operator):

$$\sum_j |(A_{jr}(\boldsymbol{k})e)|^2 = \sum_j |\langle \beta_j | \exp[-i\boldsymbol{k}\cdot\boldsymbol{x}](\gamma e) | \beta_r\rangle|^2 = \langle \beta_r | (\gamma e)(\gamma e) | \beta_r\rangle = \langle \beta_r | \beta_r\rangle = 1\,.$$

([27]) Indeed it may also be written:

$$\sum_j |(A_{jr}(\boldsymbol{k})e)|^2 = \int \mathrm{d}^3x\, \mathrm{d}^3x' \exp[-i\boldsymbol{k}\cdot(\boldsymbol{x}-\boldsymbol{x}')] \langle \alpha_r | j_e(\boldsymbol{x}) j_e(\boldsymbol{x}') | \alpha_r\rangle\,.$$

So it is a Fourier transform of a function of $\boldsymbol{x}$ which falls to zero exponentially as $|\boldsymbol{x}|$ tends to infinity, owing to the assumption that $|\alpha_r\rangle$ is a bound state.

So

$$\sum_{j\neq r} |(A_{jr}(\boldsymbol{k})e)|^2 \leqslant \sum_{j} |(A_{jr}(\boldsymbol{k})e)|^2 = A^2 , \tag{II.3}$$

where A is finite.

Moreover it is

$$\sum_{j} |U^e_{sj}(T)|^2 = 1 . \tag{II.4}$$

Let us call $\Delta E_{r(m)}$ the smallest of the quantities $|E_r - E_j|$, $j \neq r$. Let us suppose $k_0 \leqslant \varepsilon < \Delta E_{r(m)}$: Then from (II.4) it follows

$$\sum_{j\neq r} \left| U^e_{sj}(T) \frac{1}{E_r - E_j - k_0} \right|^2 \leqslant \frac{1}{(\Delta E_{r(m)} - E)^2} . \tag{II.5}$$

From (II.3) and (II.5) we have, using the Schwarz inequality:

$$\sum_{j\neq r} (A_{jr}(\boldsymbol{k})e)\, U^e_{sj}(T) \frac{1}{E_r - E_j - k_0} < \frac{A}{\Delta E_{r(m)} - \varepsilon} . \tag{II.6}$$

Therefore the expression (II.1) is finite when $k_0 \leqslant \varepsilon < \Delta E_{r(m)}$.

Appendix III

Let us suppose that the initial and final states $|\alpha_{r_0}\rangle$ and $|\alpha_{s_0}\rangle$ belong to multiplets $|\alpha_{r_i}\rangle$, $|\alpha_{s_j}\rangle$, $i, j = 0, 1, 2, \ldots$ of bound states, where the vectors in each multiplet have been chosen so as to be orthogonal each to other.

Then the two first terms of (41) become

$$\frac{1}{k_0}\left(\sum_j U^e_{s_0 r_j}(T) A_{r_j r_0}(\boldsymbol{k}) - \sum_i U^e_{s_i r_0}(T)\, A_{s_0 s_i}(\boldsymbol{k}) \exp[ik_0 T]\right) + \tag{III.1}$$

$$+ i\pi\delta(k_0)\left(\sum_j U^e_{s_0 r_j}(T) A_{r_j r}(\boldsymbol{k}) + \sum_i U^e_{s_i r_0}(T) A_{s_0 s_i}(\boldsymbol{k}) \exp[ik_0 T]\right) ,$$

whereas the remaining terms have the same form as in the case of non-degenerate states.

The argument given in Sect. 9 proves even in this case that $A_{r_0 r_0}(0) = 0$ and $A_{s_0 s_0}(0) = 0$.

However it is also $A_{r_j r_0}(0) = 0$ and $A_{s_0 s_i}(0) = 0$.

In fact from (33) we have:

$$A_{r_j r_0}(0) = \int \mathrm{d}^3 x \langle \alpha_{r_j} | j(\boldsymbol{x}) | \alpha_{r_0} \rangle . \tag{III.2}$$

Now

$$\langle \alpha_{r_j} | j(\boldsymbol{x}) | \alpha_{r_0} \rangle = \tag{III.3}$$

$$= \tfrac{1}{2} \left(\langle \alpha_{r_j} + \alpha_{r_0} | j(\boldsymbol{x}) | \alpha_{r_j} + \alpha_{r_0} \rangle - \langle \alpha_{r_j} | j(\boldsymbol{x}) | \alpha_{r_j} \rangle - \langle \alpha_{r_0} | j(\boldsymbol{x}) | \alpha_{r_0} \rangle \right) .$$

The only properties of $|\alpha_r\rangle$ used in Sect. **7** to prove that $\int \mathrm{d}^3 x \langle \alpha_r | j(\boldsymbol{x}) | \alpha_r \rangle = 0$ are that $|\alpha_r\rangle$ is stationary and bound. Now also $\langle \alpha_{r_j} + \alpha_{r_0}|$ has these two properties, therefore:

$$\int \mathrm{d}^3 x \langle \alpha_{r_j} + \alpha_{r_0} | j(\boldsymbol{x}) | \alpha_{r_j} + \alpha_{r_0} \rangle = 0 ,$$

and from (III.3) it follows $\boldsymbol{A}_{r_j r_0} = 0$.

So all the arguments given in Sect. **7** may be used to show that also in this case the expression (41) has the form (40) so that $\bar{N}_{r_0 s_0}$ is finite.

Appendix IV

Let us suppose that the external system possesses a continuum spectrum having energy eigenstates equal to the energies E_r, E_s of the initial and final bound states. Then in expression (41) the first two terms and the last term conserve their form, whereas the third and the fourth terms must be written with an integral besides the sum; so the following integrals must be added to the expression (41):

$$-\int \mathrm{d}p \, \varrho(p) A_{pr}(\boldsymbol{k}) U^{e}_{sp}(T) \frac{1}{E_r - E_p - k_0} + \tag{IV.1}$$

$$+ \int \mathrm{d}p \, \varrho(p) A_{sp}(\boldsymbol{k}) U^{e}_{pr}(T) \exp\left[- i(E_p - E_s - k_0) T \right] \frac{1}{E_p - E_s - k_0} +$$

$$+ i\pi \int \mathrm{d}p \, \varrho(p) A_{pr}(\boldsymbol{k}) U^{e}_{sp}(T) \delta(E_r - E_p - k_0) +$$

$$+ i\pi \int \mathrm{d}p \, A_{sp}(\boldsymbol{k}) U^{e}_{pr}(T) \exp\left[- i(E_p - E_s - k_0) T \right] \delta(E_p - E_s - k_0) .$$

The symbols used here are defined in Sect. **8**.

Now let us choose the energy E as one of the parameters p labelling the continuum eigenstates, and let q be the remaining parameters.

We suppose that the parameters q are chosen so that $\varrho(q, E)$ is a continuous function of E.

Then the first integral of (IV.1) becomes

$$\text{(IV.2)} \qquad \int \mathrm{d}q \int \mathrm{d}E\, \varrho(q, E) A_{(q,E)r}(\boldsymbol{k})\, U^{e}_{s(q,E)}(T)\, \frac{1}{E_r - E - k_0}\,.$$

This expression is certainly finite, for the argument of Appendix I, when an arbitrarily small domain $E_r - k_0 - \varepsilon < E < E_r - k_0 + \varepsilon$ is omitted in the integration over E. It remains then to prove the finiteness of

$$\text{(IV.3)} \qquad \int \mathrm{d}q \int_{E_r - k_0 - \varepsilon}^{E_r - k_0 + \varepsilon} \mathrm{d}E\, \varrho(E, q) A_{(q,E)r}(\boldsymbol{k})\, U^{e}_{s(q,E)}(T)\, \frac{1}{E_r - E - k_0}\,,$$

where ε is arbitrarily small (but finite).

Now (IV.3) is approximately equal to [28]:

$$\text{(IV.4)} \qquad \int \mathrm{d}q\, \varrho(E_r - k_0, q) A_{(q,E_r - k_0)r}(\boldsymbol{k})\, U^{e}_{s(q,E_r - k_0)}(T) \int_{E_r - k_0 - \varepsilon}^{E_r - k_0 + \varepsilon} \mathrm{d}E\, \frac{1}{E_r - E - k_0}\,.$$

Here the last integral must be interpreted as a principal value because the factor $1/(E_r - E - k_0)$ has been obtained from the formula

$$2\pi\delta(E_r - E - k_0) = \pi\delta(E_r - E - k_0) + \frac{i}{E_r - E - k_0}\,,$$

so that the expression (IV.4) is approximately zero, and therefore it is certainly finite. So the expression (IV.3) too is certainly finite.

The third integral in (IV.1) may be transformed analogously into

$$\text{(IV.5)} \qquad \int \mathrm{d}q \int \mathrm{d}E\, \varrho(q, E) A_{(q,E)r}(\boldsymbol{k})\, U^{e}_{s(q,E)}(T)\, \delta(E_r - E - k_0) =$$

$$= \int \mathrm{d}q\, \varrho(q, E_r - k_0) A_{(q,E_r - k_0)r}(\boldsymbol{k})\, U^{e}_{s(q,E_r - k_0)}(T)\,,$$

and it is certainly finite for the argument given in Appendix I.

---

[28] This statement uses the facts that $U_{s(q,E)}(T)$ is certainly a continuous function of E and that it is very reasonable to assume that also $A_{(q,E)r}(\boldsymbol{k})$ is a continuous function of E.

The application of the same arguments to the second and fourth integrals of (IV.1) is trivial; so the whole expression (IV.1) is finite.

Therefore even in this case the number of emitted photons results to be finite.

Appendix V

Let us apply the expression (48) to the case of a transition between two plane waves of momenta p_r, p_s.

Let us use the momentum $\boldsymbol{p}$ to label the unperturbed eigenstates.

Let the wave functions be normalized to one particle per unit volume, so that $\varrho(\boldsymbol{p}) = 1$:

$$\psi_p(\boldsymbol{x}) = u_{\boldsymbol{p}} \exp[i\boldsymbol{p}\cdot\boldsymbol{x}] .$$

Then (38) gives:

$$A_{\boldsymbol{p}_j\boldsymbol{p}_i}(\boldsymbol{k}) = ie(u_{\boldsymbol{p}_j}\gamma u_{\boldsymbol{p}_i})\int \mathrm{d}^3x \exp[i(\boldsymbol{p}_i - \boldsymbol{p}_j - \boldsymbol{k})\cdot\boldsymbol{x}] = ie(\bar{u}_{\boldsymbol{p}_j}\gamma u_{\boldsymbol{p}_i})\delta(\boldsymbol{p}_i - \boldsymbol{p}_j - \boldsymbol{k}) .$$

Now $(\bar{u}_{\boldsymbol{p}_j}\gamma u_{\boldsymbol{p}_i})$ is a continuous function of $\boldsymbol{p}_i$, $\boldsymbol{p}_j$; so for small k_0 it is

$$A_{\boldsymbol{p}_j\boldsymbol{p}_i}(\boldsymbol{k}) \simeq ie(\bar{u}_{\boldsymbol{p}_j}\gamma u_{\boldsymbol{p}_i})\delta(\boldsymbol{p}_i - \boldsymbol{p}_j - \boldsymbol{k}) = e\frac{p_i}{E_i}\delta(\boldsymbol{p}_i - \boldsymbol{p}_j - \boldsymbol{k}) .$$

Therefore (48) gives

$$\text{(V.1)}\quad \langle \alpha_s^{\text{out}} | j(k) | \alpha_r^{\text{in}} \rangle \simeq -eU_{sr}^e(T)\cdot$$

$$\cdot\left(\frac{p_r}{E_r}\int \mathrm{d}^3p\,\delta(\boldsymbol{p}_r - \boldsymbol{p} - \boldsymbol{k})\,\frac{1}{E_r - E - k_0} - \frac{p_s}{E_s}\int \mathrm{d}^3p\,\delta(\boldsymbol{p} - \boldsymbol{p}_s - \boldsymbol{k})\,\frac{1}{E - E_s - k_0}\right) =$$

$$= -eS_{sr}^e\left(\frac{p_r}{E_r}\,\frac{1}{E_r - E_{\boldsymbol{p}_r - \boldsymbol{k}} - k_0} - \frac{p_s}{E_s}\,\frac{1}{E_{\boldsymbol{p}_s + \boldsymbol{k}} - E_s - k_0}\right).$$

Now for small k_0 it is:

$$E_r - E_{\boldsymbol{p}_r - \boldsymbol{k}} \simeq \frac{\mathrm{d}E_r}{\mathrm{d}\boldsymbol{p}_r}\cdot\boldsymbol{k} = \frac{\boldsymbol{p}_r\cdot\boldsymbol{k}}{E_r} ,$$

$$E_r - E_{\boldsymbol{p}_r - \boldsymbol{k}} - k_0 \simeq \frac{\boldsymbol{p}_r\cdot\boldsymbol{k}}{E_r} - k_0 = \frac{1}{E_r}(\boldsymbol{p}_r\boldsymbol{k} - E_r k_0) = \frac{(p_r k)}{E_r} ,$$

so that (V.1) becomes

$$\langle \alpha_s^{\text{out}} | j(k) | \alpha_r^{\text{in}} \rangle = - e S_{sr}^{e} \left(\frac{p_r}{(p_r k)} - \frac{p_s}{(p_s k)} \right).$$

Substitution into (23) gives (49).

RIASSUNTO (*)

Risolviamo qui il problema dell'emissione di fotoni da un sistema generale quantizzato quando si trascuri la reazione dei fotoni sul sistema. Finora tale problema era stato risolto solo per il caso dell'emissione da un sistema classico. Deduciamo un'espressione generale per il numero medio di fotoni emessi in presenza di una transizione tra due stati arbitrari del sistema prodotto da una perturbazione dipendente dal tempo. La discussione di questa espressione porta a concludere che il numero medio di fotoni di bassa energia emessi in qualsiasi esperimento realmente eseguibile è finito: questa conclusione generalizza al caso di una sorgente quantizzata un risultato precedentemente ottenuto dall'autore per il caso di una sorgente classica. Inoltre, trascurando la reazione dei fotoni sulle cariche, dimostriamo qui che il numero medio di fotoni emessi è uguale al primo termine dello sviluppo in serie di potenze di e della probabilità di emissione di un fotone. L'applicazione di questa conclusione al caso della transizione tra due stati d'impulso definito mostra che la divergenza di Bloch-Nordsieck e la divergenza infrarossa del calcolo perturbativo hanno la loro origine nella divergenza della stessa espressione matematica, per quanto abbiano un significato fisico completamente differente. Finalmente dimostriamo che il problema studiato qui da un punto di vista generale non ha significato nel caso di una perturbazione indipendente dal tempo.

(*) *Traduzione a cura della Redazione.*

IL NUOVO CIMENTO Vol. XII, N. 3 1° Maggio 1959

The Worldwide Distribution of the $F2$ Layer Electron Density: Seasonal and Non-Seasonal Variations and Correlations with Solar Activity.

F. Mariani

Istituto Nazionale di Geofisica - Roma
Istituto di Fisica dell'Università - Roma

(ricevuto il 20 Dicembre 1958)

Summary. — The worldwide behaviour of the twelve-month period (seasonal and non-seasonal) variation of the maximum electron density N in the $F2$ layer appears noticeably different at noon and at midnight. In each case, it is controlled by the geomagnetic field and by the solar activity but, whilst at noon it shows large asymmetric features in the two hemispheres, at midnight, on the other hand, it is fairly symmetrical. It is not possible to account for the experimental results by assuming some external source of radiation producing non-seasonal effects. One is led to assume some terrestrial cause of asymmetry: for example, some effect of general circulation in the upper atmosphere. With respect to the correlation of electron density with solar activity, there appears again some noticeable asymmetry in the two hemispheres; in particular, the northern hemisphere appears more influenced by the solar hydrogen filaments, especially for increasing latitude. The explanation of these asymmetries, in terms of some direct influence of the sun, is also puzzling, so that, in this case, one is led to think of some more or less unknown effect of solar corpuscular (or electromagnetic) radiation on the upper atmosphere, for example on its movements or its conductivity. At the present stage of our knowledge, we cannot exclude the possibility of a similar cause for both the asymmetries of the twelve-month period variation and of the correlations with solar activity. Further observational evidence is required.

1. – Introduction.

A very important question in ionospheric physics is the study of the periodic and secular variations of the electron density, particularly those of the $F2$ layer which exhibit many interesting anomalies. Many authors have considered various aspects of these anomalies, but the problem of the seasonal

and non-seasonal variations of the electron density in the $F2$ layer, first considered by BERKNER-WELLS [1] and ECKERSLEY [2], requires a worldwide statistical investigation, to elucidate their dependence on geographical or geomagnetic latitudes, on solar activity, etc.

Such a statistical investigation is now possible, since we possess a nearly continuous collection of experimental data for many ionospheric observatories, adequately distributed over the Earth, and for time intervals sufficiently long to warrant a more definite experimental basis for future theoretical investigations.

2. – Experimental data and method of analysis.

We have used the ionospheric monthly median values of $foF2$ at noon and at midnight, taken from « Ionospheric data » volumes of the National Bureau of Standards; in our opinion, the use of median values is preferable to that of the mean values, because they are less influenced by perturbations; and we are principally interested in the « normal » behaviour of the $F2$ layer. With regard to the solar data, we have used the Wolf number R and sunspot areas A_g, respectively measured in the observatories of Zurich and Washington; for the other solar parameters we have used the values measured in the Astrophysical Observatory of Arcetri.

For the analysis of the data we have used Vercelli's selective method of periodogram analysis (VERCELLI [3,4]), which is based on symmetrical linear combinations, so that it does not alter the effective phase of every periodic component, while the corresponding amplitude is reduced for a known amount, depending on the coefficients of the linear combination. Thus one can obtain the correct phases and amplitudes. We have first applied the periodogram analysis to the series of median values of $N = (foF2)^2$, having first obtained the smoothed time series and, afterwards, the series representing the periodic component N_{12}, having a principal period of twelve months, and the secular component N, having the eleven-year period of the solar activity.

In effect, in the scheme we have used, together with the principal period of twelve months, there remain in the series of N_{12}, with amplitude comparable with that of the principal component, also the periodic waves of eight and ten months, which however, except the cases of Delhi at noon and of Singapore at midnight, will result practically absent. With the same method we have obtained the secular series for the solar parameters.

---

(1) L. V. BERKNER and H. W. WELLS: *Terr. Magn.*, **43**, 15 (1938).
(2) T. L. ECKERSLEY: *Terr. Magn.*, **45**, 25 (1940).
(3) F. VERCELLI: *Ric. Scient.*, **5** I, 364 (1934).
(4) F. VERCELLI: Memoria CCLXXXV of the « R. Comitato Talassografico » (1940).

We note that the values of N at noon may be considered approximately proportional to the ionization intensity just at the level of maximum electron density of the $F2$ layer.

Data from about thirty observatories have been used, as indicated in Table I, which gives their geographical and geomagnetic coordinates and their

TABLE I (*).

Observatory	Geomagn. coordinates		Geogr. coordinates		Magnetic dip
	Lat.	Long.	Lat.	Long.	
Resolute Bay	82 N	289 E	75 N	265 E	85 N
Reykjavik	70	71	64	338	76
Point Barrow	68	241	71	203	80
Kiruna	65	116	68	20	—
Anchorage	61	258	61	210	73
Lindau	52	94	52	10	66
Freiburg	50	90	48	8	64
Washington	50	350	39	283	71
San Francisco	44	298	37	238	62
White Sands	41	316	33	253	62
Baton Rouge	41	334	30	269	63
Wakkanai	35	206	45	142	60
Tokyo	25	206	36	140	50
Yamagawa	21	198	31	131	45
Maui	21	268	21	203	38
Delhi	19	149	29	77	43
Bombay	10	144	19	73	26
Madras	3	150	13	80	11
Guam	3	212	13	145	14
Huancayo	0.6 S	354 E	12 S	285 E	4 N
Leopoldville	3	84	4	15	33 S
Singapore	10	173	1 N	104	16
Rarotonga	21	274	21 S	200	38
Johannesburg	27	91	26	28	62
Brisbane	36	227	27	153	57
Watheroo	42	186	30	116	64
Canberra	44	225	35	149	65
Christchurch	48	253	44	173	68
Hobart	52	225	43	147	72
Decepcion	52	7	63	299	56
Port Lockroy	53	4	65	297	58
Campbell Is.	57	253	53	169	76
Terre Adelie	75	231	67	140	88

(*) The data of this table, sligthly different than those given by MARIANI (3) are desumed from the data collected by the C.S.A.G.I., now at our disposal. Moreover the table gives the correct coordinates of Christchurch which there, for an error of transcription, are mistaken.

magnetic inclinations. The experimental data at our disposal extend from January 1946 to December 1955. However the series of $\overline{N}$, N_{12}, etc., extends from January 1947 to December 1954; because in the method of linear combinations one loses part of the values of the starting series. Within this last interval we have selected, for the calculation of correlations, the interval May 1947–March 1954 which can be assumed as the complete decreasing stage of the last solar cycle. For some of the observatories indicated in the Table we have had at our disposal only shorter series of experimental data, so that the series of N_{12} and $\overline{N}$ are also shorter.

3. – Seasonal and non-seasonal variations.

3·1. *Behaviour of* N_{12}. – We have considered the experimental series of N at noon and at midnight: Fig. 1 shows the graphs of N_{12} at noon for the obser-

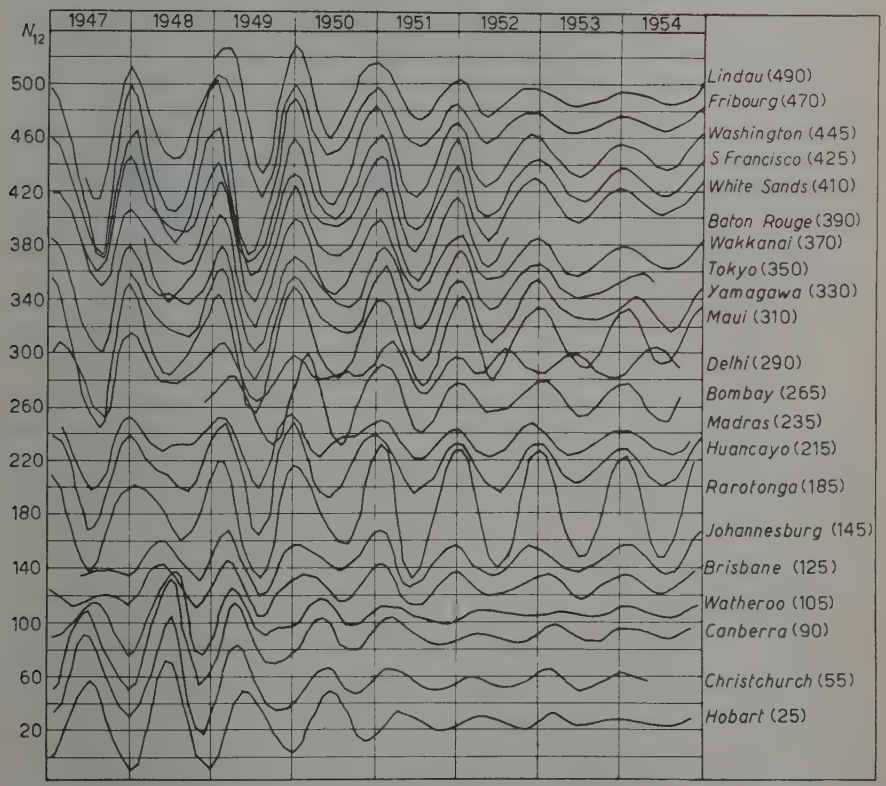

Fig. 1. – In this Figure and in the successive Figs. 2, 3, 4, 5, 6 the numbers within parentheses indicate the ordinate corresponding to the zero ordinate for every graph.

vatories whose series of data are about complete for the decreasing stage of the solar cycle, arranged according to the geomagnetic latitudes. We note the following principal features:

1) the amplitude of N_{12}, for symmetrical northern and southern latitudes, is clearly greater in the northern hemisphere;

2) in the northern hemisphere, the times of maximum or minimum amplitude show some slight tendency to be anticipated during the epochs of lower solar activity and at higher latitudes;

3) in the southern hemisphere, as far as the latitude of Brisbane, the component N_{12} exhibits a substantial phase-agreement with respect to the northern hemisphere; however, during the years 1947-1948 of higher solar activity, the behaviour of N_{12} at Johannesburg and Brisbane appears as a transition stage to the behaviour at observatories at greater southern latitudes, which clearly show a phase-shift of 180° with respect to the other observatories; on the other hand, with regard to the years 1949-1953, the times of maximum or minimum amplitude of N_{12} show a systematic tendency to be anticipated during the epochs of lower solar activity and at higher latitudes;

4) as a whole, the component N_{12} decreases for decreasing solar activity; between the geographical latitudes of S. Francisco and Rarotonga, an appreciable temporary diminution of amplitude is noted around June 1948 and June 1950; conversely, an increase of amplitude appears around June 1948 at Watheroo, Canberra, Christchurch and Hobart.

Concerning the behaviour of N_{12} at midnight we refer to Fig. 2, from which we can infer the following principal features:

1′) the amplitudes of N_{12}, for symmetrical northern and southern latitudes, are substantially the same;

2′) the times of maximum or minimum amplitude practically coincide with the solstitial months;

3′) there is a substantial phase-opposition for symmetrical northern and southern latitudes;

4′) as a whole, the component N_{12} decreases for decreasing solar activity.

Some further interesting features, that one can draw from Figs. 1-2, are the following:

5) the amplitudes of N_{12} are greater at noon than at midnight, in both the northern and southern hemisphere, with the exception, after 1949-1950, of the observatories at latitude higher than Brisbane;

6) the geomagnetic control of N_{12} either at noon or at midnight is clearly manifest; moreover there appears some « regional » behaviour, for example the noticeable attenuation of N_{12} at midnight in the observatories of Washington, San Francisco and White Sands, which are « regularly » distributed only with respect to the geomagnetic latitude.

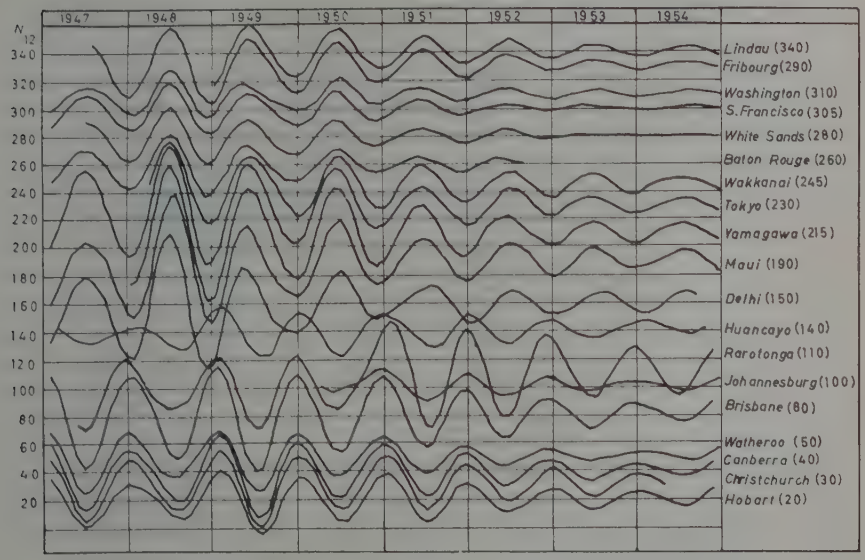

Fig. 2.

In order to obtain further information on N_{12} for very low and high latitudes, we now refer to Fig. 3, where the graphs are arranged according to the geographical latitude of the observatories, or else directly to the monthly median values of $foF2$. The graphs of Fig. 3, which refer to shorter time intervals, show the following features:

7) at noon, for equatorial and high southern latitudes, the component N_{12} reach maxima and minima respectively at approximately the December solstice and the June solstice, with the surprising exception of Singapore, where the reverse is the case.

For high northern latitudes the phase angle of N_{12} varies almost continually with increasing latitude so that, at Resolute Bay, N_{12} shows a « normal » behaviour, with summer maxima and winter minima, thus concluding the progressive phase shift already noted in the graph of Fig. 1. One notices a geographical rather than a geomagnetic control of N_{12}, at high latitudes.

As regards the amplitude of N_{12}, it appears approximately the same, at corresponding equal southern and northern latitudes.

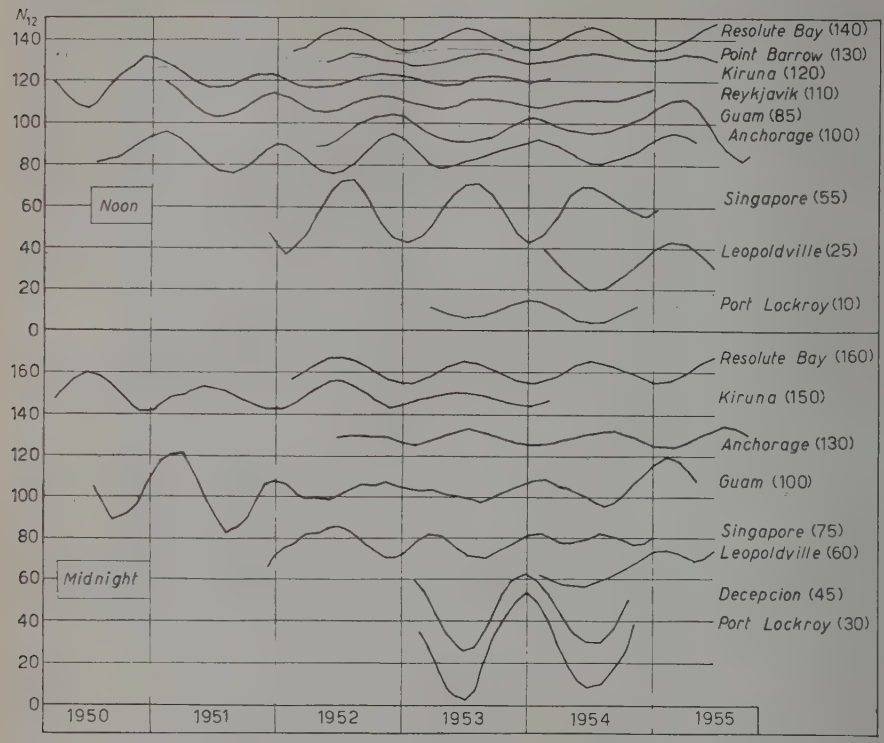

Fig. 3.

8) At midnight, the N_{12} shows phase-agreement at high and equatorial southern latitudes, again with the exception of Singapore, where a clear twelve month variation is not apparent. In respect to high northern latitudes, N_{12} shows « normal » summer maxima and winter minima. The amplitudes of N_{12} are much larger at high southern latitudes than at high northern latitudes. The graph of Guam is very interesting: although both the geographical and the geomagnetic latitudes are northern, N_{12} shows a substantial phase-agreement with the values relating to southern latitudes; thus, if one assumes the line of phase-inversion of N_{12} as « ionospheric equator » this appears rather different from the geomagnetic equator (as well as from the geographical equator). Our definition of « ionospheric equator », which can be considered rather similar to that given by APPLETON [5], seems however to lead to rather

[5] E. V. APPLETON: *Journ. Atmosph. Terr. Phys.*, **1**, 106 (1950).

different conclusions. Obviously a larger number of experimental data are necessary in order to derive the position of the ionospheric equator (or, perhaps, equators).

Concerning the behaviour of the electron density for higher southern latitudes we have had only shorter time intervals of data at our disposal: however, the visual inspection of monthly median values of $foF2$ for the observatories of Terre Adelie (February-December 1951) and Campbell Islands (April 1950-October 1951) seems to suggest for N_{12} characteristics similar to those of Decepcion and Port Lockroy. Another interesting fact is the systematic occurrence, for $foF2$, of values rather higher at midnight than at noon, during the winter at the observatories of Decepcion, Port Lockroy, Terre Adelie and Campbell Islands; no indication of any similar fact appears for the higher northern latitudes.

3·2. *Discussion.* – As a first conclusion, the comparison between the N_{12} relative to the various observatories, seems to suggest some interesting asymmetric features between the northern and the southern hemispheres, which, on the other hand, seem principally to concern the daylight side of the Earth.

In order to attempt some explanation of the observed anomalies, one has to remember the results and the discussion of BERKNER and WELLS: they studied the variations of the maximum electron density in the $F2$ layer at Washington and Watheroo during a period of about three years and inferred the presence of a non-seasonal variation of the electron density, having a principal period indistinguishable from one year and an amplitude about equal to that of the seasonal variation; the amplitude appeared to maintain an approximately fixed ratio to the average background ion density.

The authors showed that the non-seasonal effect could not be explained by the difference of latitude of the two stations from the equator, nor by the ellipticity of the Earth's orbit; on the other hand, also the non-homogeneity of data could not account for the non-seasonal variation. As regards the source of the effect the authors were unable to make any definite suggestion; they did not exclude that, for example, the effect might be associated with sidereal causes, or with the varying position of the Earth's magnetic moment with respect to the Sun, or with the circulation in the high atmosphere under the influence of the Earth's magnetic field. Some other observational evidence on the non-seasonal variation is due to ECKERSELY, who suggested some eventual association of the effect with JANSKY noise (JANSKY ([6,7])).

([6]) K. G. JANSKY: *P.I.R.E.*, **21**, 1387 (1933).
([7]) K. G. JANSKY: *P.I.R.E.*, **23**, 1158 (1935).

At this point, our extensive results allow us to draw some definite conclusions; for sake of simplicity we shall indicate as N_{12}^a and N_{12}^s, respectively, the non-seasonal (annual) and the seasonal components of N_{12}, the former in phase-agreement between the northern and southern hemispheres, the latter with a phase-shift of 180°. As is well known, it is still difficult to conclude whether the « normal » seasonal behaviour of the F_2 electron density is the one with summer maxima and winter minima, or viceversa: for this reason, in the theoretical analysis of the worldwide variation of N_{12}, we have considered as « normal » seasonal variation the cases of both summer or winter maxima.

At first, we have assumed a sidereal source or, at least, some association with some sidereal phenomenon to account for the non-seasonal effect. If it is so, we should have to expect that the effect depends upon the sidereal time: thus, if it is maximum at midday in December and January (*i.e.*, midwinter, northern hemisphere), it should also be a maximum at midnight in June and July (*i.e.*, midsummer, northern hemisphere). In effect, if the behaviour of N_{12} at noon can suggest some sidereal dependence of the non-seasonal variation, the behaviour at midnight clearly disagrees with such a hypothesis, because in the southern hemisphere the component N_{12} is a maximum in December and January, *i.e.* in the austral summer; on the other hand, also during daylight, at very high northern latitudes, N_{12} reaches its maximum in June and July, as it does during the night.

Moreover, any scheme of interpretation must give account of the phase opposition that N_{12} shows at latitudes higher than that of Brisbane (in particular that of Watheroo, whose data were considered by BERKNER and WELLS) with respect to the northern latitudes, during the period of maximum solar activity; moreover, another singular aspect of the behaviour of N_{12} is the gradual phase-shift depending on the latitude or on the solar activity, which is not clearly understood in the scheme of seasonal and non-seasonal variations of N, both exhibiting solstitial maxima and minima.

A last *a priori* objection that one can raise is the intensity required for the possible sidereal source of radiation, which would have to be of the same order as the solar radiation. However, one can assume the effective presence of two N_{12}^a and N_{12}^s components of about the same order, both reaching their maxima and minima in the solstitial months, and study their superposition in all the possible cases: we do not wish to labour this matter because, as can easily be verified, in every case, some systematic phase-disagreement or amplitude difference is obtained between the experimental and the expected behaviour of N_{12} in the two hemispheres.

As a first result of our discussion, the possibility of some important sidereal effect on the ionization of the $F2$ layer may be excluded. We can thus concentrate our attention on solar or terrestrial causes: as we have seen, the non-

seasonal irregularities occur essentially during daytime so that in order to explain them we are led to study in some detail the relations between solar radiation and our atmosphere.

In effect there is a non-seasonal variation of solar radiation due to the variation of the distance of the Earth from the Sun, which is a minimum at the December solstice and maximum at the June solstice: however, the difference of solar intensity in the two periods does not exceed a few per cent, so that one is led to infer the effective existence of some asymmetric property of the $F2$ layer in the two hemispheres, principally or exclusively during daytime. We shall consider the question again in Section **5**.

4. – Correlation between electron density in the $F2$ layer and solar activity.

4'1. *First case: at noon.* – We begin by considering the secular behaviour of N and its correlations with the Sun. For the parameters characterizing solar activity we have selected, together with the Wolf number R and the sunspot area A_R, also the areas of the hydrogen flocculi and filaments, respectively indicated with A_Φ and A_F, which are quiescent phenomena reappearing on the solar disc also for many consecutive rotations.

If we plot the secular variations of N and of R, A_R, A_Φ, A_F (which we indicate with a bar: $\overline{N}$, $\overline{R}$, etc.) as functions of time, some interesting « similarity » in the behaviours of $\overline{N}$ and A_F is apparent (Fig. 4): in particular two corre-

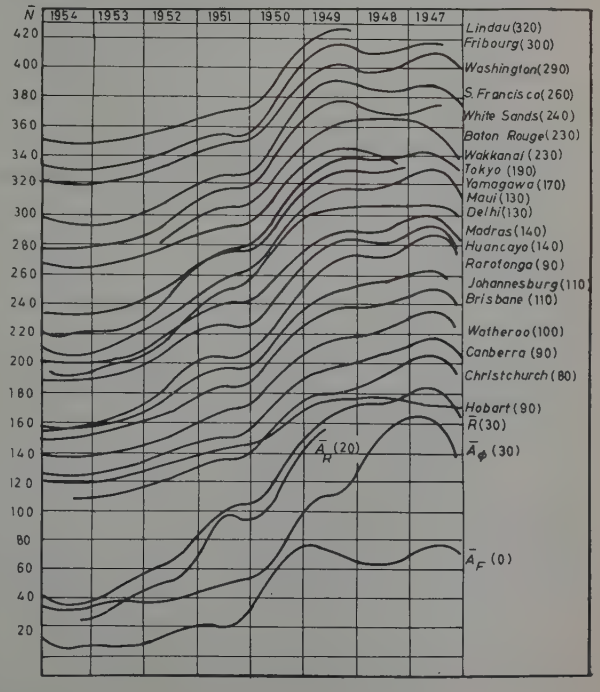

Fig. 4. – The areas $\overline{A}_F$ and $\overline{A}_\Phi$ are the projected areas, expressed in 10^{-4} of the solar disc; the areas $\overline{A}_R$ are expressed in $1/(16.09)\cdot 10^6$ of the solar disc.

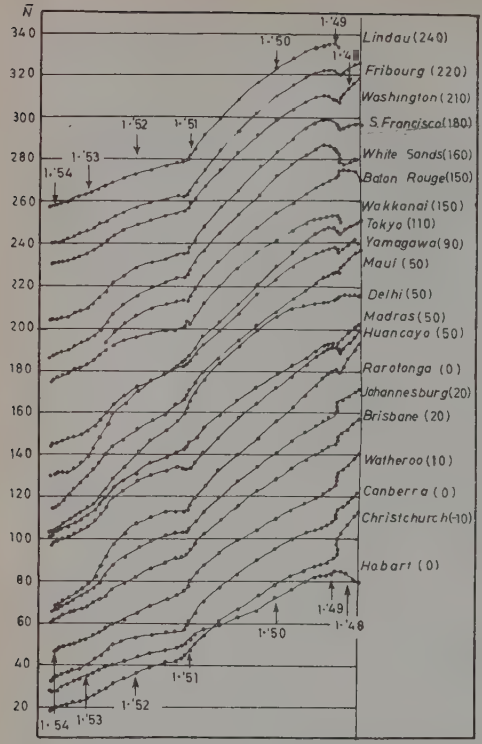

Fig. 5. – In this Figure and in the successive Figs. 6,7 the arrows indicate the date: for example 1·'50 indicates January 1950. The black points are the values of $\bar{N}$ for odd months.

sponding relative maxima and an intermediate minimum in the northern hemisphere; in the southern hemisphère, instead, such « similarity » is not present with the exception of Huancayo and Rarotonga.

Some better information is given by Fig. 5 and Fig. 6 which supply respectively the graphs of $\bar{N}$ $(\bar{R})$, and of $\bar{A}_\Phi(\bar{R})$ and $\bar{A}_F(\bar{R})$; we do not give the graph of $\bar{A}_R(\bar{R})$ which, except for some very small fluctuation, is well represented by the linear relation $\bar{A}_R = 16.09\,\bar{R}$, so that, as a consequence, one can infer that the behaviour of $\bar{N}(\bar{R})$ is identical with that of $\bar{N}(\bar{A}_R)$; a remarkable correlation between $\bar{N}$ and $\bar{A}_F$ appears again and more clearly; conversely, no striking correlation between $\bar{N}$ and $\bar{A}_\Phi$, appears, so that we shall disregard every dependence between $\bar{N}$ and $\bar{A}_\Phi$.

Moreover, one can infer that the correlation between $\bar{N}$ and $\bar{A}_F$ seems to increase for increasing northern latitudes; however, some increased dependence of $\bar{N}$ upon $\bar{A}_F$ appears also at the observatories of Christchurch and Canberra. Finally, both in the northern and southern hemisphere, a sudden variation of the slope around the beginning of 1951 is apparent at about the same time as a similar sudden variation of the slopes of $\bar{A}_\Phi$ and $\bar{A}_F$.

In order to study the foregoing results, it may be observed as a preliminary question that, in effect, the monthly median and mean values N

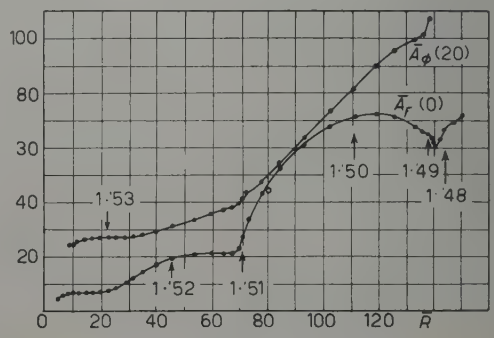

Fig. 6.

and R are referred to the conventional terrestrial month, so that they would have to be replaced by the analogous values N^* and R^* referred to the solar month; a calculation has, therefore, been made of the new series of solar month median and mean values N^* and R^*, for Washington: the new graphs of $\bar{N}^*(\bar{R}^*)$, as can be seen in Fig. 7, reproduce the features of the graphs shown in Fig. 5, so that one can infer that the features of the secular variation of $\bar{N}$ have some substantial physical meaning.

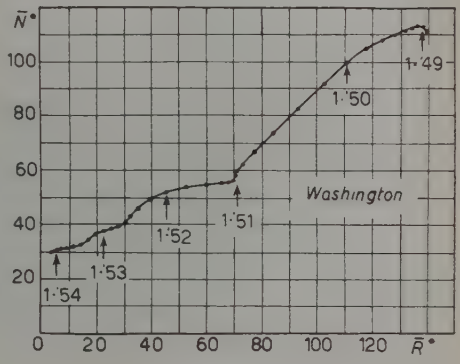

Fig. 7.

We have therefore assumed a multiple linear regression of $\bar{N}$ on $\bar{R}$ and $\bar{A}_F$, expressed in the form:

$$(1) \qquad \bar{N} = \bar{N}_0(1 + \beta\bar{R} + \gamma\bar{A}_F)$$

and the simple linear regression of $\bar{N}$ on $\bar{R}$ and $\bar{N}$ on $\bar{A}_F$

$$(2) \qquad \bar{N} = \bar{N}_0(1 + \alpha\bar{R}) ,$$

$$(3) \qquad \bar{N} = \bar{N}_0(1 + \delta\bar{A}_F) .$$

Table II shows the values of $\bar{N}_0$, α, β, γ, δ, the simple correlation coefficients r_{NR}, r_{NA_F} and the partial correlation coefficients $r_{NR.A_F}$, $r_{NA_F.R}$ (which will henceforth be indicated by the simpler symbols r_{12}, r_{13}, $r_{12.3}$, $r_{13.2}$, attributing the indices 1, 2, 3 respectively to N, R, A_F), calculated according to the standard linear correlation methods (OSTLE [8]); we also give, the standard deviations of the partial regression coefficients; finally, we supply the mean values α_0, β_0, γ_0, δ_0 of α, β, γ, δ for the eight observatories of the southern hemisphere and the corresponding standard deviations σ_α, σ_β, σ_γ, σ_δ together with the mean values A_0, B_0, Γ_0, Δ_0 for eight observatories located at symmetrical northern geomagnetic latitudes, which are indicated in italics.

One sees in the Table that the coefficients α, δ, β have a statistical meaning, while this is not the case for all the coefficients γ which cannot at first sight be considered significantly different from zero in the southern hemisphere (other than at Maui and Baton Rouge in the northern hemisphere): there might be some tendency of γ to increase in value for higher southern lati-

---

([8]) B. OSTLE: *Statistics in Research* (Ames, Iowa, 1954).

TABLE II.

Observatory	$N = N_0(1 - \alpha B)$		$N = N_0(1 - \Delta_0 \tau)$		$N = N_0(1 - \beta B - \gamma \Delta_0 \tau)$			r_{12}	r_{13}	$r_{12.3}$	$r_{13.2}$
	N_0	α	N_0	Δ_0	N_0	β	γ				
London	17.5	.0354 ± .0016	23.0	.0467 ± .0020	19.5	.0147 ± .0041	.0310 ± .0070	.968	.973	.551	.630
Freiberg	19.8	.0329 ± .0008	23.9	.0520 ± .0017	20.5	.0196 ± .0020	.0243 ± .0039	.988	.980	.840	.706
Washington	20.6	.0310 ± .0006	24.9	.0489 ± .0016	21.2	.0199 ± .0015	.0205 ± .0029	.992	.980	.908	.752
San Francisco	24.8	.0288 ± .0006	29.6	.0462 ± .0015	25.5	.0183 ± .0016	.0196 ± .0031	.990	.980	.875	.708
White Sands	30.5	.0237 ± .0005	35.2	.0393 ± .0013	31.2	.0149 ± .0014	.0167 ± .0027	.990	.979	.860	.697
Baton Rouge	30.6	.0231 ± .0007	43.1	.0281 ± .0019	31.2	.0194 ± .0018	.0063 ± .0037	.985	.937	.862	.218
Wakkanai	27.1	.0223 ± .0004	31.1	.0366 ± .0015	27.5	.0115 ± .0008	.0199 ± .0017	.988	.986	.929	.916
Tokyo	34.9	.0226 ± .0003	41.0	.0365 ± .0013	35.6	.0175 ± .0010	.0096 ± .0017	.996	.975	.961	.688
Yamagawa	45.6	.0181 ± .0003	52.0	.0296 ± .0012	46.2	.0135 ± .0007	.0086 ± .0014	.995	.972	.953	.725
Maui	70.8	.0119 ± .0002	78.3	.0199 ± .0010	70.7	.0125 ± .0004	.0011 ± .0007	.998	.957	.980	.227
Delhi	60.2	.0138 ± .0003	65.9	.0240 ± .0009	60.9	.0095 ± .0009	.0082 ± .0018	.990	.975	.859	.598
Madras	53.4	.0128 ± .0002	58.3	.0223 ± .0009	53.8	.0094 ± .0003	.0066 ± .0007	.998	.972	.985	.718
		$A_0 = .0236$		$\Delta_0 = .0370$		$B_0 = .0149$	$\Gamma_0 = .0154$				
Huancayo	40.8	.0174 ± .0002	46.5	.0287 ± .0012	41.1	.0153 ± .0008	.0040 ± .0014	.997	.968	.959	.403
Rarotonga	60.6	.0142 ± .0002	67.1	.0242 ± .0011	60.7	.0136 ± .0007	.0012 ± .0012	.997	.962	.921	.153
Johannesburg	38.5	.0191 ± .0002	44.7	.0306 ± .0013	38.6	.0184 ± .0006	.0012 ± .0013	.998	.963	.976	.151
Brisbane	32.5	.0207 ± .0003	37.9	.0333 ± .0014	32.7	.0182 ± .0009	.0048 ± .0017	.997	.968	.957	.407
Watheroo	27.3	.0238 ± .0004	32.7	.0374 ± .0016	27.5	.0215 ± .0014	.0043 ± .0027	.995	.964	.934	.237
Canberra	25.0	.0247 ± .0005	29.7	.0392 ± .0016	25.3	.0204 ± .0017	.0081 ± .0034	.991	.966	.894	.356
Christchurch	18.5	.0340 ± .0008	23.7	.0498 ± .0023	18.3	.0305 ± .0022	.0082 ± .0044	.989	.960	.859	.216
Hobart	25.1	.0160 ± .0003	28.4	.0265 ± .0012	25.2	.0146 ± .0014	.0027 ± .0027	.993	.962	.909	.196
		$\alpha_0 = .0212$		$\delta_0 = .0337$		$\beta_0 = .0191$	$\gamma_0 = .0043$				
		$\sigma_\alpha = .0059$		$\sigma_\delta = .0077$		$\sigma_\beta = .0050$	$\sigma_\gamma = .0025$				

tudes; however, this fact is not observed at Hobart and, on the other hand, it is not supported by the latitudinal variation of the partial correlation coefficient $r_{13.2}$.

Concerning the latitudinal variation of α and δ, there appear some analogies, obviously less evident, with the variation of γ, while the coefficients β can be considered fairly symmetrical in the two hemispheres and little dependent upon the latitude.

These features of α, β, γ, δ can better be seen, if we assume the mean values α_0, β_0, γ_0, δ_0 as « normal » values and σ_α, σ_β, σ_γ, σ_δ as « normal » deviations: it clearly appears that the more significant dependence upon the latitude is that of the coefficient γ, which is larger in the northern hemisphere and increases for increasing values of the geomagnetic latitude.

In regard to the correlation coefficients, one sees that, again with the exception of Maui and Baton Rouge for the northern hemisphere, the values of $r_{13.2}$ are clearly greater in the northern than in the southern hemisphere.

The extended results of Table II seem to support the preliminary conclusions of a preceding paper (MARIANI ([9])) of some different dependence or « sensibility » of the two hemispheres to the activity of hydrogen filaments (or to some other solar phenomenon closely connected). It may be interesting to compare our results with those of other authors: for example ALLEN ([10]) who considered only six observatories (Fairbanks, Brisbane, San Juan, Maui, San Francisco, Baton Rouge) without any distinction of the northern from the southern ones, obtained for α a mean value $\alpha = 0.0200$ which can be considered in good agreement with our results (our mean value for the four observatories of Brisbane, Maui, San Francisco, Baton Rouge gives $\alpha = 0.0211$); with regard to the results of GALLET and RAWER ([11]), the values calculated by their formula giving the dependence upon the magnetic inclination are, respectively, for Freiburg, San Francisco, White Sands, Wakkanai, Tokyo and Yamagawa, the values $\alpha = 0.0186$, 0.0185, 0.0183, 0.0178, 0.0161, 0.0156 which do not agree well with our values.

With regard to the values of $\overline{N}_0$, the statistical errors of which are of the order of a few per cent, it appears that they are not rigorously symmetrical around the geomagnetic equator: Fig. 8 shows the values of $\overline{N}_0$ for the case of multiple correlation arranged, in the upper part according to the geomagnetic latitude (black dots) or the magnetic inclination (crosses), and in the lower part according to the sum of geomagnetic and geographical latitudes (black dots); in this latter case, a greater symmetry of $\overline{N}_0$ is apparent; this fact is physically interesting because it shows that, in effect, although the abscissae

([9]) F. MARIANI: *Journ. Atmosph. Terr. Phys.*, **10**, 240 (1957).
([10]) C. W. ALLEN: *Terr. Magn.*, **53**, 433 (1948).
([11]) R. GALLET and K. RAWER: *Ann. Geophys.*, **6**, 104 (1950).

are somewhat conventional, the electron density in the $F2$ layer varies either with the geomagnetic or with the geographical latitudes (*i.e.* with the mean zenithal angle); moreover, some of the coefficients α, γ, δ appear in a better order, if we rearrange the observatories according to the sum of the two latitudes.

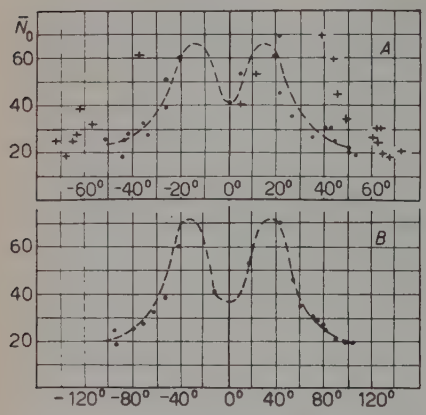

Fig. 8. – The dotted lines are symmetrical lines approximately fitting the calculated values. The northern latitudes and dips are positive.

A singular case is represented by the values of $\bar{N}_0$ at Christchurch which appear smaller than the others: this fact occurs systematically in all the single and multiple correlations, so that one is led to assume some particular local situation; the smaller value of $\bar{N}_0$ accounts in some way for the greater values of α, β, γ, δ.

Concerning the latitudinal variation of $\bar{N}_0$, we can also consider the result of BHAR ([12]) who has depicted the true relation between noon values of $foF2$ and the magnetic dip for the last sunspot minimum, by eliminating the effect of solar zenithal distance variation: he plotted the noon values of $foF2$ against the magnetic dip for many observatories, keeping the solar zenithal distance χ as a fixed parameter (instead of the equinox or any other time of the year); there remains an asymmetry in the two hemispheres which seems to increase for increasing values of χ_{noon} (particularly for $\chi_{\text{noon}} = 20°$ and $= 30°$): more precisely, there appears a maximum of $foF2$ at about $30° \div 40°$ of magnetic dip, larger in the northern than in the southern hemisphere.

Our results seem instead to suggest a more regular variation of $\bar{N}_0$ exhibiting two fairly symmetrical maxima.

In order to infer some further information on the north-south asymmetries, the simple and multiple correlations of the monthly values of $N - N_{12}$ with the monthly values of R and A_F have been calculated. The seasonal and non-seasonal variations of N have been subtracted, because it seems that these variations, although *a priori* they may be correlated with the solar activity, are strongly influenced by factors other than the solar activity (*i.e.* the variation of the zenithal angle of the Sun, the height variation of the generalized recombination coefficient, etc.). In these new correlations, three linear re-

([12]) J. N. BHAR: *Journ. Atmosph. Terr. Phys.*, **10**, 168 (1957).

gression laws have been assumed, expressed in the form:

$$N - N_{12} = (N - N_{12})_0(1 + \alpha' R) \; ; \tag{4}$$

$$N - N_{12} = (N - N_{12})_0(1 + \delta' A_F) \; ; \tag{5}$$

$$N - N_{12} = (N - N_{12})_0(1 + \beta' R + \gamma' A_F) \; . \tag{6}$$

The deductions one can draw from the results of the calculation, collected in Table III, substantially agree with those drawn from Table II; the simple and multiple correlation coefficients now seem fairly symmetrical in the two hemispheres; as regards the partial correlation coefficients, there appears some difference between the two hemispheres: $r'_{12.3}$, as a whole, is slightly greater in the southern hemisphere; $r'_{13.2}$, on the other hand, is symmetrical for lower and mean latitudes, while, for higher northern latitudes, it reaches values rather greater than at symmetrical southern latitudes.

With regard to the coefficients α', β', γ', δ' there appears again some clear tendency for α', δ' and particularly for γ' to increase in value for increasing northern latitude; in this case, the values of γ' appear statistically significant, also in the southern hemisphere; moreover, one sees again the small dependence of β' on latitude and its similarity in the two hemispheres.

With regard to the results relating to Christchurch, the values of $(N - N_{12})_0$ are again smaller than the other values.

The general diminution of the correlation coefficients is obviously due to the effect of the variables that we have excluded from our calculation; instead, a rather surprising feature is the remarkable increase of the values of the partial correlation coefficients $r_{13.2}$, with respect to the values of Table I, for the southern hemisphere.

Finally, we have considered the correlations of the series of $N - N_{12} - \overline{N}$ and $R - \overline{R}$, $A_F - \overline{A}_F$, according to the linear regression laws:

$$N - N_{12} - \overline{N} = (N - N_{12} - \overline{N})_0 + a(R - \overline{R}) \; ; \tag{7}$$

$$N - N_{12} - \overline{N} = (N - N_{12} - \overline{N})_0 + d(A_F - \overline{A}_F) \; ; \tag{8}$$

$$N - N_{12} - \overline{N} = (N - N_{12} - \overline{N})_0 + b(R - \overline{R}) + c(A_F - \overline{A}_F) \; . \tag{9}$$

In these correlations, obviously, the values of $(N - N_{12} - \overline{N})_0$ are very small and oscillate around zero. In Table IV we show the ratios α'', β'', γ'', δ'' of the coefficients a, b, c, d to the corresponding values of $(N - N_{12})_0$ obtained in the regression of $N - N_{12}$ on R and A_F: in this manner, the values of a, b, c, d appear more or less conveniently « weighted »; moreover, we have indicated in the Table the correlation coefficients.

TABLE III.

Observatory	$N-N_{12}=(N-N_{12})_0(1+\alpha' R)$		$N-N_{13}=(N-N_{13})_0(1+\delta' A_F)$		$N-N_{12}=(N-N_{12})_0(1+\beta' R+\gamma' A_F)$			r'_{12}	r'_{13}	$r'_{12.3}$	$r'_{13.2}$	$r'_{1.23}$
	$(N-N_{12})_0$	α'	$(N-N_{13})_0$	δ'	$(N-N_{12})_0$	β'	γ'					
Lindau	17.1	.0361±.0022	23.8	.0436±.0025	17.1	.0190±.0027	.0343±.0045	.901	.908	.640	.672	.947
Freiburg	23.7	.0256±.0016	28.3	.0410±.0025	22.0	.0149±.0028	.0285±.0053	.873	.873	.511	.513	.908
Washington	24.1	.0245±.0014	28.6	.0395±.0022	22.4	.0143±.0024	.0271±.0045	.891	.891	.560	.560	.927
San Francisco	29.2	.0226±.0014	33.6	.0377±.0022	27.2	.0123±.0023	.0268±.0044	.878	.887	.511	.562	.920
White Sands	35.2	.0188±.0011	40.9	.0304±.0019	33.5	.0115±.0019	.0185±.0036	.885	.873	.561	.493	.909
Baton Rouge	42.7	.0139±.0014	52.4	.0201±.0020	39.6	.0087±.0019	.0147±.0033	.792	.786	.485	.463	.841
Wakkanai	29.1	.0198±.0016	33.3	.0327±.0025	27.3	.0104±.0024	.0241±.0045	.821	.839	.445	.512	.872
Tokyo	39.9	.0184±.0012	46.8	.0291±.0021	38.1	.0119±.0023	.0165±.0043	.854	.832	.502	.389	.878
Yamagawa	49.5	.0156±.0011	59.0	.0228±.0020	47.9	.0110±.0018	.0116±.0034	.845	.800	.555	.357	.867
Maui	76.4	.0102±.0007	85.4	.0165±.0014	74.9	.0073±.0013	.0071±.0025	.850	.806	.529	.301	.865
Delhi	66.4	.0112±.0007	72.1	.0197±.0013	64.3	.0063±.0013	.0119±.0024	.864	.863	.493	.487	.898
Madras	58.0	.0109±.0007	64.4	.0181±.0013	56.6	.0072±.0012	.0089±.0023	.875	.846	.556	.401	.897
		$A'_0=.0202$		$\Delta'_0=.0310$		$B'_0=.0114$	$\Gamma'_0=.0204$					
Huancayo	43.7	.0154±.0008	51.2	.0239±.0016	42.4	.0108±.0015	.0114±.0029	.896	.854	.622	.398	.914
Rarotonga	66.1	.0119±.0007	75.2	.0189±.0014	64.7	.0085±.0014	.0082±.0026	.869	.823	.567	.328	.884
Johannesburg	42.3	.0162±.0009	50.0	.0249±.0017	41.0	.0114±.0016	.0119±.0030	.897	.855	.626	.398	.915
Brisbane	36.6	.0169±.0009	43.5	.0260±.0017	35.4	.0119±.0016	.0126±.0031	.901	.860	.635	.413	.919
Watheroo	30.8	.0197±.0010	38.3	.0284±.0020	29.8	.0149±.0019	0.125±.0036	.905	.849	.660	.360	.918
Canberra	27.9	.0206±.0012	34.5	.0303±.0021	26.8	.0150±.0022	.0147±.0042	.888	.843	.606	.367	.904
Christchurch	21.6	.0274±.0015	28.9	.0365±.0026	20.6	.0211±.0028	.0171±.0053	.899	.841	.644	.337	.911
Hobart	28.9	.0122±.0009	34.2	.0176±.0017	28.5	.0104±.0017	.0043±.0032	.839	.755	.570	.151	.843
		$\alpha'_0=.0175$		$\delta'_0=.0258$		$\beta'_0=.0130$	$\gamma'_0=.0116$					
		$\sigma_{\alpha'}=.0047$		$\sigma_{\delta'}=.0057$		$\sigma_{\beta'}=.0037$	$\sigma_{\gamma'}=.0036$					

TABLE IV.

Observatory	α''	δ''	β''	γ''	r''_{12}	r''_{13}	$r''_{12.3}$	$r''_{13.2}$	$r''_{1.23}$
Lindau	.0203±.0052	.0207±.0057	.0200±.0049	.0235±.0072	.489	.420	.460	.385	.593
Freiburg	.0082±.0032	.0168±.0048	.0055±.0035	.0181±.0065	.274	.361	.174	.297	.421
Washington	.0041±.0029	.0167±.0042	.0006±.0031	.0210±.0058	.154	.402	.022	.377	.402
San Francisco	.0069±.0028	.0177±.0042	.0038±.0030	.0195±.0055	.263	.422	.133	.399	.441
White Sands	.0065±.0021	.0112±.0034	.0049±.0023	.0107±.0043	.319	.345	.230	.267	.411
Baton Rouge	.0057±.0021	.0105±.0031	.0041±.0023	.0115±.0042	.326	.394	.221	.318	.460
Wakkanai	.0042±.0040	.0138±.0057	.0028±.0043	.0160±.0071	.122	.275	.078	.260	.287
Tokyo	.0076±.0030	.0138±.0048	.0055±.0033	.0136±.0061	.268	.310	.183	.242	.356
Yamagawa	.0052±.0026	.0080±.0040	.0042±.0029	.0078±.0050	.225	.227	.175	.179	.284
Maui	.0040±.0017	.0066±.0028	.0031±.0018	.0056±.0034	.251	.250	.183	.181	.306
Delhi	.0031±.0015	.0085±.0025	.0016±.0016	.0085±.0030	.218	.352	.113	.303	.368
Madras	.0029±.0015	.0052±.0024	.0022±.0016	.046±.0029	.219	.233	.153	.174	.277
Huancayo	.0070±.0019	.0097±.0031	.0057±.0021	.0081±.0038	.373	.327	.295	.231	.431
Rarotonga	.0042±.0017	.0063±.0028	.0033±.0018	.0052±.0034	.259	.240	.195	.168	.306
Johannesburg	.0070±.0020	.0125±.0031	.0050±.0021	.0121±.0039	.359	.410	.258	.329	.473
Brisbane	.0062±.0020	.0091±.0031	.0050±.0022	.0078±.0040	.326	.306	.251	.219	.387
Watheroo	.0088±.0024	.0093±.0037	.0078±.0026	.0071±.0049	.378	.267	.318	.161	.407
Canberra	.0096±.0027	.0105±.0042	.0084±.0029	.0082±.0055	.367	.269	.268	.227	.398
Christchurch	.0112±.0031	.0135±.0045	.0103±.0034	.0076±.0064	.371	.240	.274	.132	.391
Hobart	.0017±.0017	.0015±.0027	.0024±.0018	.0033±.0035	.109	.063	.139	.107	.134

Although the statistical errors on the ratios α'', β'', γ'', δ'' are very great, there remains however some indication of an asymmetric « sensibility » of the two hemispheres to the hydrogen filaments.

4·2. *Second case: at midnight.* – The study of the correlations can be carried out in a similar manner, using the corresponding midnight series of N.

There again appears the discontinuity of the slope about the beginning of 1951: however, the dependence of $\bar{N}$ upon the areas A_F is noticeable also in some observatories where it is fairly negligible at noon, so that, as a whole, the systematic asymmetries found at noon are practically absent; however, we must consider that, in effect, the midnight electron density depends upon the diurnal ionization intensity but, as in the phenomena of hysteresis, it is highly influenced by the foregoing behaviour of the diurnal $F2$ layer so that, from the physical point of view, the consideration of the correlations of nightly electron density with solar activity cannot be very significant. If, instead, we fix our attention on the behaviour of the maximum electron density, as a whole, we may assume that the asymmetric properties of the $F2$ layer in the two hemispheres are substantially and clearly present during daylight.

4·3. *Discussion.* – From the foregoing analysis, it may be concluded that the dependence on the solar activity of the maximum electron density is fairly well expressed by the double correlation of N with R (or A_R) and A_F; it is very interesting to notice that the north-south asymmetries of the correlations with solar activity, especially the one with the hydrogen filaments during daylight, show some interesting parallelism with the north-south asymmetries in the behaviour of N_{12}, which are present only during daylight.

In order to explain the above mentioned asymmetries, the presence of some solar radiation could be assumed, principally or exclusively reaching the northern hemisphere: if one excludes the direct effect of an electromagnetic radiation, which is more or less symmetrical around the Sun's and the Earth's equators, one could imagine some continuous asymmetrical corpuscular radiation; if, on the other hand, one excludes that this corpuscular radiation may reach the northern and the southern hemispheres with different intensity, as an effect produced by the geomagnetic field, one could imagine some selective effect determined, for example, by some geoelectric field: in this case, considering for example a dipole field, one might be forced to assume a primary corpuscular radiation composed of only positive (or only negative) particles or, in every case, having a net (positive or negative) charge different from zero.

Now, as it was pointed out by Simpson ([13]), if a variable geoelectric field

([13]) J. A. Simpson: *Ann. Geophys.*, **11**, 305 (1955).

is to be assumed, in order to explain the cosmic radiation variations, the necessary geoelectric potential is of the order of $2 \cdot 10^7$ to $4 \cdot 10^8$ V. A Coulomb field is excluded for, as FERRARO has shown, its potential cannot be higher than 10^2 V, otherwise, with higher fields, the ionospheric layers would tend to blow away; there remains the other alternative of a radial electric field produced by ring currents or cylindrical current sheets, as considered by NAGASHIMA [14] and others. However, one has to remember that these calculations substantially refer to the disturbed conditions associated with magnetic storms and, on the other hand, that the calculated fields appear at least of an order of magnitude too small to account for the observed variations. Further arguments indicate the hypothesis of a geoelectric field as being highly improbable: indeed, the minimum energy necessary for a primary particle in order to reach the fairly low geomagnetic latitude of $40° \div 50°$ is of the order of some GeV; such a degree of energy is sufficient for the penetration of the atmosphere, so that the cosmic ray intensity at sea level, or, better, at high latitude, would exhibit some asymmetry in the two hemispheres, contrarily to the known experimental data. Moreover, many authors (FIROR [15], etc.) have shown that the geographical distribution of the intensity of cosmic rays, as it has been possible to confirm on the occasion of solar flares, sufficiently agrees with the expected distribution of an extraradiation coming from a solar source and substantially subjected to the influence of only the geomagnetic field.

An other possibility is the presence of some low energy radiation which is continuously accelerated near the Earth to the ionosphere by some local electric field and whose effects interest only the upper atmosphere where it is absorbed. In this case, some relation of this radiation with the aurora could be present.

If this would not be the case, one could perhaps attribute, as in the case of the asymmetric features of N_{12}, the origin of the observed latitudinal anomalies to some terrestrial effect, more indirectly influenced by the solar activity.

5. – Further discussion and conclusions.

As it has already been said, there appears some parallelism between the latitudinal asymmetries of $\bar{N}$ (or $N - N_{12}$ or $N - N_{12} - \bar{N}$) and N_{12}. A dependence of $\bar{N}$ and N_{12} upon solar activity is indisputable; however, some remarkable features of the latitudinal dependence may seem influenced in a

(14) K. NAGASHIMA: *Journ. Geomagn. Geoelectr.*, **3**, 100 (1951).
(15) J. W. FIROR: *Phys. Rev.*, **94**, 1017 (1954).

rather indirect manner. A tentative suggestion is that of considering the effects induced in the ionospheric electron densities by the general circulation of the upper atmosphere.

We, at first, consider the effects of the atmospheric tides: enough observational evidence on tidal phenomena is furnished by current literature, especially with regard to the diurnal anomalous effects on *foF*2. Martyn's theory (MARTYN ([16])) of atmospheric tides in the ionosphere can give a solid base for accounting for such anomalies in a determined place; however, if one accepts his point of view, in order to explain the latitudinal variations, and particularly the north-south asymmetries of N_{12}, one has to imagine some asymmetric latitudinal characteristics of the tidal movements. As MARTYN ([17]) has shown, in order to explain the behaviour of *foF*2 at Cape York, Brisbane, Canberra and Hobart, one can assume the presence of two spherical harmonics ψ_2^2, ψ_3^2 (semidiurnal components) in the general expression of the velocity potential. At first sight, one might think that the features of N_{12}, particularly those relating to its phase-angle, varying so differently with the latitude at noon and at midnight, could be explained by assuming also the presence of the diurnal terms ψ_1^1, ψ_2^1 in the velocity potential considered above.

We have thus attempted to frame in some detail the experimental behaviour of N_{12} in such a scheme, assuming the presence of the terms ψ_1^1, ψ_2^1, ψ_2^2, ψ_3^2 in the velocity potential; however, we have not been able to obtain some complete agreement of experimental and theoretical results. In effect, it must be considered that the terms ψ_n^0 present in the general expression of the velocity potential are seasonal or annual terms, while, as a result of the discussion, of Section **3**, this does not seem the case of N_{12}. On the other hand, the corrections introduced by the presence of the geomagnetic field render the tidal circulation substantially symmetrical around the geomagnetic instead of around the geographical equator, because the effective asymmetries they introduce in the two hemispheres are negligible.

There remains the possibility that a mechanism of the Martyn tipe is effective, but that the circulation in the upper atmosphere is not well expressed in terms of spherical harmonics potential or that an asymmetric, non-uniform, conductivity is present.

In other words, it may be suggested that the observed north-south asymmetries of N_{12}, may be interpreted as the effect induced by the geomagnetic field on the worldwide circulation of the upper atmosphere, which may be more or less different in the two hemispheres. In effect, the « regional » behaviour we have observed in N_{12} may perhaps be an indication of some regional cha-

---

([16]) D. F. MARTYN: *Proc. Roy. Soc.*, A **189**, 241 (1947).
([17]) D. F. MARTYN: *Proc. Roy. Soc.*, A **194**, 445 (1948).

racteristic of this general circulation. Moreover, other experimental results seem to support the hypothesis of some different characteristic of the northern with respect to the southern hemisphere: on discussing the anomalous variations of the maximum electron density in the $F2$ layer, SATO ([18]) also has indicated some asymmetries between the two hemispheres in the ratio r of noon median values of the electron density in the minimum cos χ month to that in the maximum cos χ month, at various latitudes. This ratio is greater than unity for northern latitudes higher than 10°, at sunspot minimum, and becomes larger for higher northern latitudes, at sunspot maximum. The ratio r is larger for higher geographical latitudes, more for northern than for southern latitudes; moreover, the seasonal anomaly is amplified on a worlwide scale during sunspot maximum far more than during sunspot minimum. SATO has finally shown that the seasonal anomaly of $foF2$ cannot be accounted for merely by the vertical drift.

On the other hand, SCHWERDTFEGER and PROHASKA ([19]) have pointed out the occurrence of remarkable latitudinal asymmetries on the mean of the amplitude of the semiannual pressure oscillation and of its ratio to the amplitude of the annual oscillation.

Obviously, the above outlined point of view requires further observational data. The most important questions which must be exhaustively studied are:

i) the behaviour of $\overline{N}$ and N_{12} and the correlations with solar activity, for observatories located in the equatorial belt and at high northern, and particularly at high southern, latitudes;

ii) the worldwide distribution of the ionospheric winds, their diurnal and seasonal or non-seasonal variations; with regard to this question, some other research on the regular (not necessarily seasonal) tidal movements can be very useful. Moreover, one cannot disregard the possibility of a more or less regular slipping back of the upper atmosphere, with respect to the motion of the lower atmosphere and of the Earth: this effect should equally interest both hemispheres.

It will thus be very advantageous that the intensified researches on ionospheric physics (and on allied branches) during the International Geophysical Year may be continued regularly in the future.

An extensive statistical study of *all* the ionospheric data for the years 1938-1958 and of their correlation with other significant solar parameters is in preparation. The numerical calculation is now in progress by the Electronic Computer of the « Centro di Studi sulle Calcolatrici Elettroniche » of the University of Pisa.

([18]) T. SATO: *Journ. Geomagn. Geoelectr.*, **6**, 99 (1954).
([19]) W. SCHWERDTFEGER and F. PROHASKA: *Journ. Met.*, **13**, 217 (1956).

* * *

I take this opportunity of thanking Mr. W. B. CHADWICK, Chief, Regular Propagation Services Section, Radio Propagation Physics Division of the National Bureau of Standards, who very kindly and quickly sent me many ionospheric data and CRPL-reports. My sincere thanks are also due to Prof. E. JARGENCE and Prof. W. DIEMINGER, who have speedily complied with my requests for data.

RIASSUNTO

L'andamento globale della variazione di periodo 12 mesi della densità elettronica massima nello strato $F2$ risulta sensibilmente differente a mezzogiorno, e a mezzanotte. In ogni caso, essa è controllata dal campo magnetico terrestre e dall'attività solare ma, mentre a mezzogiorno mostra notevoli asimmetrie tra i due emisferi, al contrario a mezzanotte, le sue caratteristiche sono simmetriche. Non risulta possibile attribuire tale diversità di comportamento della parte illuminata e della parte oscura della Terra all'effetto di qualche sorgente esterna di radiazione. Si è indotti a pensare in termini di qualche asimmetria di origine terrestre: per es. di asimmetrie nella circolazione generale dell'alta atmosfera. Quanto alla correlazione con l'attività solare, di nuovo appaiono sensibili asimmetrie tra i due emisferi N e S; in particolare, l'emisfero N appare maggiormente soggetto all'influenza dei filamenti cromosferici solari, in misura tanto maggiore quanto maggiore è la latitudine geomagnetica. L'interpretazione di questa asimmetria in termini di una diretta influenza del Sole sullo strato $F2$ costituisce un grosso problema; si è indotti a pensare a qualche effetto più o meno sconosciuto di una radiazione corpuscolare (o elettromagnetica) incidente sull'alta atmosfera, che ne influenzi per esempio i movimenti o la conducibilità. Allo stato attuale delle conoscenze, in attesa di ulteriore e qualificato materiale sperimentale, non si può escludere la possibilità che ambedue i tipi di asimmetria, quella relativa alla variazione di periodo 12 mesi e quella relativa alla correlazione con l'attività solare, siano determinate da una medesima causa.

IL NUOVO CIMENTO Vol. XII, N. 3 1° Maggio 1959

The Interactions of Positive K-Mesons with Nuclei in Photographic Emulsion at Energies in the Region (240 ÷ 300) MeV.

D. Keefe, A. Kernan, A. Montwill
University College - Dublin

M. Grilli, L. Guerriero, G. A. Salandin
Istituto di Fisica dell'Università - Padova
Istituto Nazionale di Fisica Nucleare - Sezione di Padova

(ricevuto il 29 Dicembre 1958)

Summary. — Interactions of K^+-mesons with emulsion nuclei have been observed in a scan of 185 m of track. The analysis yielded information on scattering reactions K^+-p and K^+-n and charge-exchange reactions. An energy dependence of the three cross-sections up to 350 MeV was obtained from the collected data of different laboratories working with emulsion technique. The phase-shift analysis in the 300 MeV region shows a contribution of $T=0$ state of the same order of magnitude as that of $T=1$ state. An interference seems to be present between the P-waves of the two states, depressing the K^+-n scattering cross-section and raising the charge-exchange cross-section.

1. – Introduction.

The results of many investigations on the interactions of K^+-mesons in nuclear emulsions in the region from very low energies up to about 200 MeV

have been published recently ([1-17]). The results have been found to be well described in terms of the optical model for complex nuclei. From the interactions with the Hydrogen and other nuclei in the emulsion, certain features of the elementary interactions with free protons and « free » neutrons were inferred notably the slow rise in the K^+ proton interaction ($T = 1$ only), and the much faster rise in the K^+ neutron cross-section ($T = 1$ and $T = 0$) from a value at low energies which suggested that there was probably only a very small $T = 0$ part.

The present experiment was designed to extend, by an essentially similar technique, the investigation of the K^+ meson interactions to the energy region (240 ÷ 300) MeV. Attention was again concentrated on the magnitude of the interaction cross-section as a function of the energy, the ratio of the number of Charge-Exchange to non-Charge-Exchange events, and the collisions with

---

([1]) J. M. LANNUTTI, W. W. CHUPP, G. GOLDHABER, S. GOLDHABER, E. HELMY, E. ILOFF, A. PEVSNER and R. RITSON: *Phys. Rev.*, **101**, 1617 (1956).

([2]) N. N. BISWAS, L. CECCARELLI-FABBRICHESI, M. CECCARELLI, K. GOTTSTEIN, N. C. VARSHNEYA and P. WALOSCHEK: *Nuovo Cimento*, **5**, 123 (1957).

([3]) G. COCCONI, G. PUPPI, G. QUARENI and A. STANGHELLINI: *Nuovo Cimento*, **5**, 172 (1957).

([4]) M. BALDO-CEOLIN, M. CRESTI, N. DALLAPORTA, M. GRILLI, L. GUERRIERO, M. MERLIN, G. A. SALANDIN and G. ZAGO: *Nuovo Cimento*, **5**, 393 (1597).

([5]) B. BHOWMIK, D. EVANS, S. NILSSON, D. J. PROWSE, F. ANDERSON, D. KEEFE, A. KERNAN and J. LOSTY: *Nuovo Cimento*, **6**, 440 (1957).

([6]) M. WIDGOFF, A. PEVSNER, D. FOURNET-DAVIS, D. M. RITSON, R. SCHLÜTER and V. P. HENRY: *Phys. Rev.*, **107**, 1430 (1957).

([7]) T. F. HOANG, M. F. KAPLON and R. CESTER: *Phys. Rev.*, **107**, 1698 (1957).

([8]) D. FOURNET-DAVIS: *Phys. Rev.*, **106**, 816 (1957).

([9]) C. MARCHI, G. QUARENI, A. VIGNUDELLI, G. D'ASCOLA and S. MORA: *Nuovo Cimento*, **6**, 1790 (1957).

([10]) B. SECHI-ZORN and G. T. ZORN: *Phys. Rev.*, **108**, 1098 (1957).

([11]) J..M. LANNUTTI, S. GOLDHABER, G. GOLDHABER, W. W. CHUPP, S. GIAMBUZZI, C. MARCHI, G. QUARENI and A. WATAGHIN: *Reports of the Padua-Venice Conference* (September 1957), III, 1.

([12]) M. GRILLI, L. GUERRIERO, M. MERLIN and G. A. SALANDIN: *Reports of the Padua-Venice Conference* (September 1957), III, 16.

([13]) N. N. BISWAS, M. CECCARELLI and N. SCHMITZ: *Reports of the Padua-Venice Conference* (September 1957), III, 25.

([14]) L. T. KERTH, T. F. KYCIA and L. VAN ROSSUM: *Reports of the Padua-Venice Conference* (September 1957), III, 28.

([15]) G. IGO, D. G. RAVENHALL, J. J. TIEMANN, W. W. CHUPP, G. GOLDHABER, S. GOLDHABER, J. M. LANNUTTI, and R. M. THALER: *Phys. Rev.*, **109**, 2133 (1958).

([16]) B. BHOWMIK, D. EVANS, S. NILSSON, D. J. PROWSE, F. ANDERSON, D. KEEFE, A. KERNAN, N. N. BISWAS, M. CECCARELLI, P. WALOSCHEK, J. E. HOOPER, M. GRILLI and L. GUERRIERO: *Nuovo Cimento*, **5**, 994 (9157).

([17]) M. GRILLI, L. GUERRIERO, M. MERLIN, and G. A. SALANDIN: *Nuovo Cimento*, **10**, 205 (1958).

Hydrogen nuclei in the emulsion. In addition, a new feature present at this energy was the possibility of π-meson production, the threshold for this process in the collision of a K-meson with a stationary nucleon being 220 MeV. Some preliminary reports of this work have been given at the Geneva Conference (1958) and elsewhere ([18-20]).

2. – Experimental details.

2·1. *Exposure conditions.* – The plates used were from a stack (K_4^+) of 240 Ilford G-5 600 μm strips 20 cm $\times$ 17.5 cm, exposed to the Berkeley separated K^+-meson beam (nominal momentum = 625 MeV/c), processed at Bristol, and shared among the laboratories of Bristol, Dublin U.C., and Padua. The number of K-particles entering each emulsion strip at the shorter edge was about 100. The π/K ratio varied from place to place in the beam and generally was between 1:1 and 3:1. The development was reasonably high—a minimum blob-density of about 22.1 blobs/100 μm—the development gradient was only a few percent at most, and the distortion was negligible for the range of energy determination considered in this experiment. In addition, the values of minimum blob-density in different plates were remarkably similar.

2·2. *Selection and analysis of events.* – The tracks were chosen for following by scanning in a line at right angles to the beam direction. This line was chosen at 10 mm from the beam entry point for one part of the experiment and 15 mm for the other, in order to allow the identification of the primaries of stars found close to the pick-up line by multiple scattering measurements. Each track was blob-counted under $\times$100 objective over a distance of 2 mm, which was sufficient for an efficient selection of the heavy meson tracks. The blob density at this momentum was very close to minimum (22.1 blobs per 100 μm) for K-mesons. As an additional check on the choice of track and the correctness of tracing through, a large sample of tracks was again blob counted after it had been followed through for about 8 cm where the expected ionization for K-particle tracks was about 31 blobs/100 μm.

In all cases, when an interaction was found, identification of the primary was demanded. If one of the tracks emerging from the star was definitely identified as a K-meson, the primary, must also have been a K^+-meson. In

---

([18]) M. Grilli, L. Guerriero, M. Merlin, Z. O'Friel and F. A. Salandin: *Nuovo Cimento*, **10**, 163 (1958).

([19]) D. Keefe, A. Kernan and A. Montwill: *Nuovo Cimento*, **10**, 538 (1958).

([20]) D. Evans, F. Hassan, K. K. Nagpaul, M. D. Shafi, E. Helmy, J. H. Mulvey D. J. Prowse and D. H. Stork: *Nuovo Cimento*, **10**, 168 (1958).

all other cases, scattering measurements were carried out on the primary track to determine its mass. Only in 8 cases out of 365 was the identity of the primary found to be other than a K-meson (5 π-mesons, 2 protons, 1 cosmic-ray star with outgoing prong in the K-beam direction). To correct for tracks followed, which were due to other particles, the total track length was reduced by 2%. (The mean free path for π-meson and proton interactions is somewhat smaller than for the K^+-meson).

In the case of each star found, every prong was, if possible, followed to rest and its end examined for evidence of decay. The energy and direction of emission of the prong was recorded. In cases where a particle left the stack, its mass was determined by measurement of increase of ionization as a function of range, or, if flat enough, by measurements of $(\bar{\alpha}, b^*)$.

2·3. *Estimation of the primary energy.* – The mean energy of the incoming beam and its inherent spread in energy were estimated in two ways. Firstly, a sample of 45 K-meson tracks was chosen at random and they were followed for 20 cm—that is, nearly to the edge of the stack—and ionization measurements made. In this way, the mean residual range at that point was found to be 9.2 cm and the standard deviation of the range distribution 2.8 cm (see Fig. 1). Taking into account the errors due to straggling and the ionization measurements, the energy at entry of the beam turns out to be 310 MeV and the spread ~ 20 MeV. The second method involved the estimation of the primary K-meson energy in each of the K-Hydrogen events by simply summing the energies of the outgoing proton and K-meson. The K-meson energy at the point of interaction can be corrected up quite reliably to give the energy at the entry point and each individual estimate is good to a few MeV. The distribution in values thus found for our 13 events is shown in Fig. 2. The mean value at entry derived therefrom was (303 ± 4.5) MeV, and the spread, ~ 16 MeV. Accordingly the mean energy at entry was assumed to be 306 MeV.

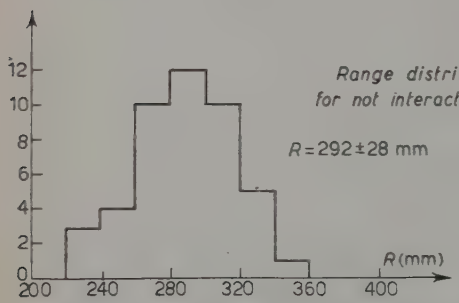

Fig. 1.

Since it was desirable to divide the data into two energy groups, $\lesssim 270$ MeV, individual energy estimates were required for the primaries of every star and here somewhat different methods were used by the two groups. The Dublin

group took simply the expected value at the star, based on the distance of the event from the edge of the stack and the assumed average beam energy at entry. Thus each primary estimate is uncertain by about ± 18 MeV.

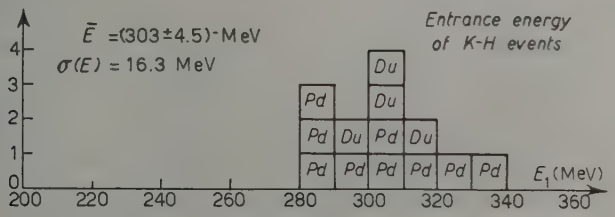

Fig. 2.

The Padua group determined the energy of the primary K-meson at each interaction directly by a grain-count along 2 mm of track combined, when necessary with multiple scattering measurements over 2 cm. The accuracy of this energy determination was $\pm 6\%$.

The energy distribution so determined for interacting K's turns out to be in agreement with that deduced for non-interacting K's, as was expected as the energy dependence of the interaction cross-section is slight. The experimental spread of $\pm 6\%$ coupled with the real energy spread of the beam results in some energy estimates less than 240 MeV and greater than 300 MeV. Because of such uncertainties it is clear that when a division of the data is made at 270 MeV, there will be an inevitable « spill-over » of events close to 270 MeV from the lower energy category to the higher one and *vice versa*. The number of events involved is small and the effect on the results is negligible, since the mean free path varies only slightly, and the energy distribution is close to symmetric.

3. – Experimental results.

3·1. *General considerations.* – In all, 185 m of K-meson track have been scanned, and 13 K-Hydrogen events, 203 nuclear inelastic scatters, 91 charge-exchange events, 7 « stops », 37 decays in flight and 12 further inelastic unanalysable events were observed. The full details of these events are tabulated in Appendix I and the main features are summarized in Table I-*a* for the two energy intervals (240÷270) MeV and (270÷300) MeV. A « stop » is defined as an event where the K-particle stops without any prongs or decay product being apparent. It is reckoned that two of the observed « stops » were due to a decay-in-flight where the secondary particle escaped detection. The results on K-H events are given in Table I-*b*.

From Table I it can be seen that the measured mean free paths for the various processes in emulsion are:

M.F.P. for K-H collisions	$14.2^{+6.5}_{-3.9}$	(240 ÷ 300) MeV
M.F.P. for inelastic collisions (excluding K-H events) (scatterings + charge-exchange)	0.61 ± 0.05	(240 ÷ 270) MeV
	0.58 ± 0.05	(270 ÷ 300) MeV
M.F.P. for inelastic scatterings . . .	0.84 ± 0.07	(240 ÷ 270) MeV
	0.92 ± 0.08	(270 ÷ 300) MeV
M.F.P. for charge-exchange collisions	2.25 ± 0.33	(240 ÷ 270) MeV
	1.56 ± 0.20	(270 ÷ 300) MeV

TABLE I (*a*).

Energy interval														Spurious Events
	(240 ÷ 270) MeV							(270 ÷ 300) MeV						
Labt.	Inelastic scatters	Ch.Ex. with prongs	Stops (*)	K-H	Unanalyzable	Decays in flight	Pathlength (m)	Inelastic scatters	Ch.Ex. with prongs	Stops (*)	K-H	Unanalizable	Decays in flight	Pathlength (m)	(π and p stars)
Pa.	58	21	1	5	2	10	53.5	50	30	—	4	6	11	55.5	3
Du.	52	18	2	2	2	6	40.7	43	22	4	2	2	10	35.0	5
Total	110	39	3 (2)	7	4	16	94.2	93	52	4 (3)	6	8	21	90.5	8

(*) Two stops were due to a decay in flight where the secondary particle escaped detection.

TABLE I (*b*). – K-*Hydrogen collisions*.

Number of events	E_1	$\chi_{c.m.}$	Number of events	E_1	$\chi_{c.m.}$
Pd. 99	250	38°	Pd. 678	230	76°
Pd. 192	260	94°	Pd. 1428	240	86°
Pd. 99	250	38°	Pd. 678	230	76°
Pd. 192	260	94°	Pd. 1428	240	86°
Pd. 386	270	106°	Du. 220/14	245	80°
Pd. 620	232	135°	Du. 181/7	274	108°
Pd. 637	265	76°	Du. 202/27	283	136°
Pd. 802	325	44°	Du. 217/21	233	98°

The Ratio of Charge Exchange/Non-Charge Exchange events in the lower energy is: 0.37 ± 0.07 and in the higher energy interval 0.59 ± 0.10.

Only one case of π-meson production in a K^+-nucleus collision was observed: this star had one prong—the emergent π^+-meson—and the experimental details are described fully in [18].

Fig. 3 shows the world data on the K-H angular distribution, $d\sigma p/d\Omega$, including the 13 events found in the present work. Fig. 4 is a scatter diagram of the inelasticity, $\Delta E/E$, against the laboratory angle of scattering, θ_{Lab}, for the 203 inelastic events.

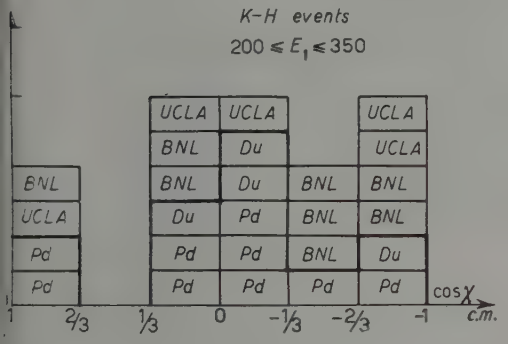

Fig. 3.

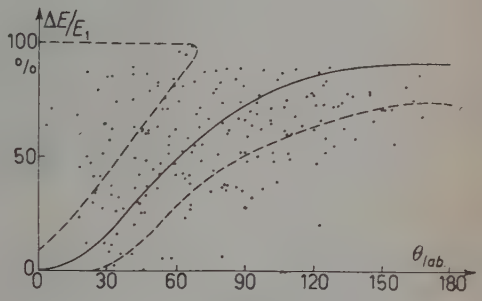

Fig. 4.

4. – Discussion of results.

4·1. *The mean free path for inelastic scattering.* – In Fig. 5 are shown the values at different energies of the mean free path of K^+ mesons in emulsion

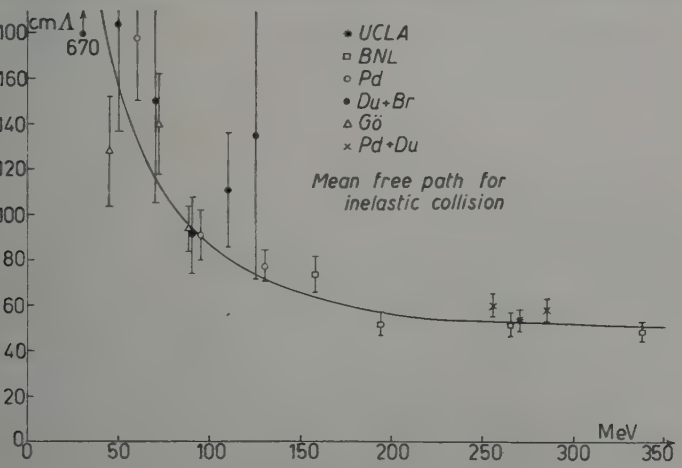

Fig. 5.

obtained in the present work and at various laboratories (K-Hydrogen events are excluded) ([1-20]). The value of the mean free path is seen to decrease with energy, and at low energy (< 130 MeV) this decrease is well explained in terms of the Pauli exclusion principle which prohibits low momentum transfers to bound nucleons. The continued decrease at higher energies is not explicable in the same terms but is due as discussed below to an increase in the K^+-bound-nucleon cross-section.

4·2. *The frequency of charge exchange interactions.* – Fig. 6 shows the available world data on the ratio of charge-exchange (CE) to non-charge-exchange (NCE) interactions. The points at 245 MeV and 280 MeV have

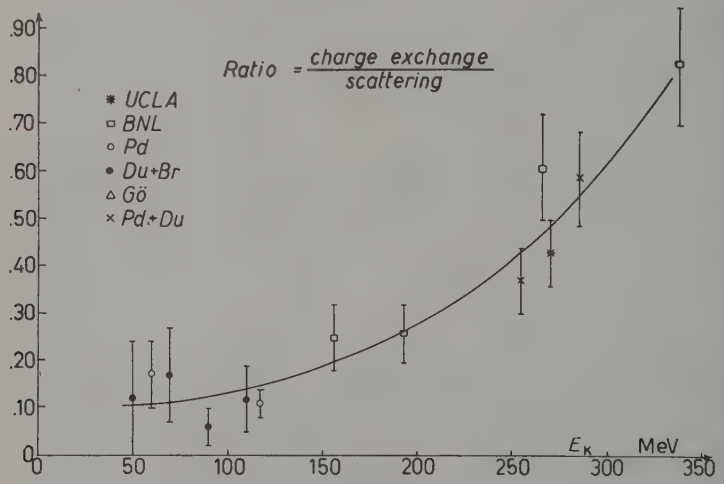

Fig. 6.

been obtained in the present experiment. It can be seen that while all the results below 200 MeV *could* have been consistent with the value 0.2 predicted by the Charge Independence Hypothesis for the case of a vanishing $T = 0$ interaction, the higher energy points lie substantially above this value and the rapid rise seems established. Since an emerging K-particle may have had more than one collision within the nucleus its chance of suffering charge exchange is greater than in just a single collision with an « average » bound nucleon. Fig. 7 shows the experimental curve of Fig. 6 after correction for double scattering—and represents the CE/NCE ratio for a single collision with an average

bound nucleon. At the energies considered in the present experiment double scattering occurs in about 40% of cases ([21]).

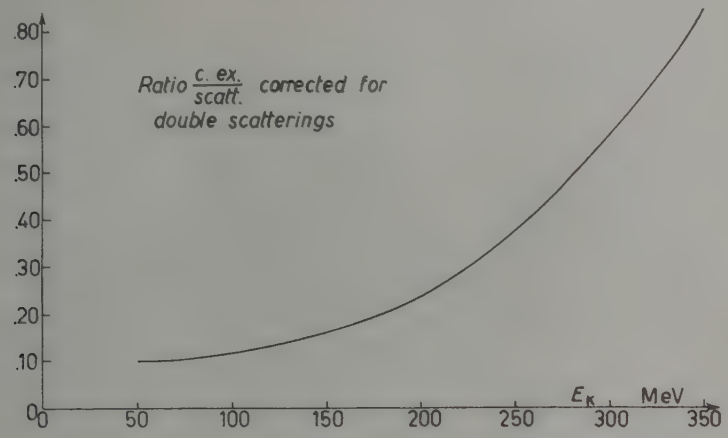

Fig. 7.

4·3. *The* K^+*-nucleon cross section.* – Adding our data to those reported at the Geneva Conference the K-proton cross-section results to be (21.3 ± 4) mb in the energy interval $(200 \div 350)$ MeV Fig. 8 shows the results on the total cross-

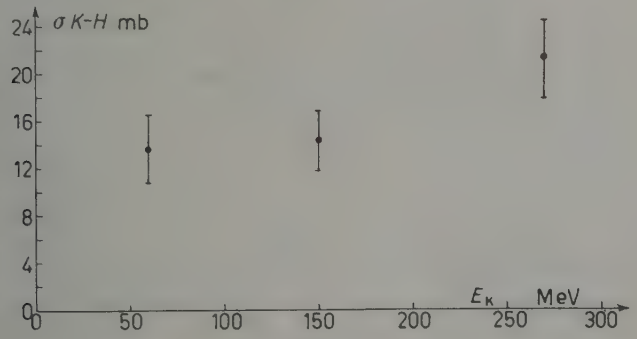

Fig. 8.

section, σ_p, at different energies. It is likely that there is a genuine rise in σ_p in the high energy region.

One can now deduce the K-neutron cross-section, σ_n, by using the mean free paths given above in Section 3. Firstly the M.F.P. must be decreased

([21]) K. A. Brueckner, R. Serber and K. M. Watson: *Phys. Rev.*, **84**, 258 (1951).

by a factor $(1 - V_c/E_k) \simeq 0.96$, to correct for the effect of electrostatic repulsion, where V_c = average Coulomb potential at the nuclear surface.

In order to deduce the cross-section on the average free nucleon, allowance must be made for the effects of the Pauli exclusion principle and of shading. The former correction at these energies is less than 10% if the angular cross-section in the C.M. system is assumed to be not too far from isotropic but the shading correction is much larger and depends on the assumptions made about the nuclear size and shape. Estimates of nuclear sizes and shapes vary very widely and clearly have a precise meaning only in relation to the experimental context. Whether one takes a one-parameter or two-parameter « shape », it appears that the magnitudes of the parameters will depend on the energy and nature of the bombarding particle. Since there is no evidence for a long range K-nucleon force and the energy involved is fairly high, we have chosen the simple homogeneous model with radius $R = r_0 A^{\frac{1}{3}}$, and have calculated results for $r_0 = 1.36$ fermi, 1.25 fermi and 1.15 fermi. The middle value 1.25 fermi, is in fair agreement with the high energy neutron and proton scattering data where a homogeneous matter distribution seems to be a good choice (cf. GLASSGOLD, ref. (22)). In addition the calculation has been carried out for a nuclear density distribution:

$$\varrho(R) = \frac{\varrho_0}{1 + \exp[R - R_0/d]},$$

with $R_0 = 1.04 A^{\frac{1}{3}}$ fermi and $d = 0.57$ fermi as used by IGO *et al.* (15). The results based on this shape factor are very close to those corresponding to $r_0 = 1.25$ fermi.

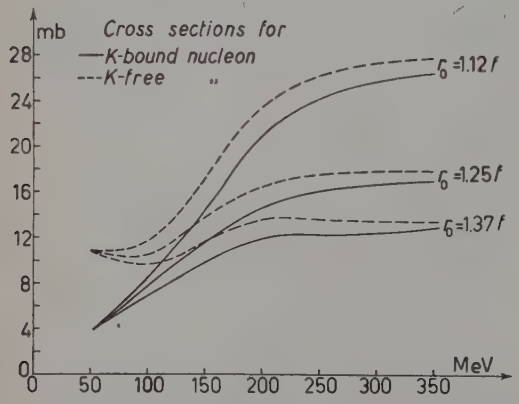

Fig. 9.

Fig. 9 shows the K^+-nucleon cross-section deduced from data reported in Fig. 5 as described above for different assumptions and one can see how sensitive the magnitudes are to changes in r_0. The curves show the variation in $\sigma(\bar{N})$ before and after correction for the effects of the Pauli exclusion principle (isotropic cross-section). For the following calculations we have assumed $r_0 = 1.25$ fermi.

(22) *Intern. Congress on Nuclear Sizes and Density Distribution*, in *Rev. Mod. Phys.*, 30, April (1958).

Using now the ratio (Charge-Exchange/Non-Charge-Exchange) at different energies, $\sigma(\overline{N})$ has been resolved into two parts, one corresponding to inelastic scattering—which can occur from either protons or neutrons —and the other corresponding to charge-exchange—which can of course arise only in a collision with a neutron (see Fig. 10). So by this means we can obtain directly σ_n(CE), the partial cross-section on a neutron for charge-exchange scattering alone.

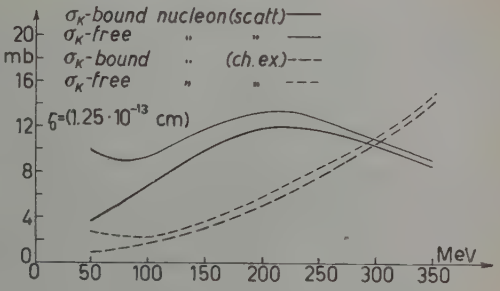

Fig. 10.

In order to determine the other partial cross-section on neutrons, that is, for non-charge exchange scattering, σ_n(NCE), one can use the fact that the atomic nuclei in emulsion are composed approximately of 54% neutrons and 46% protons. Thus

$$\sigma(\overline{N}) = 0.46\,\sigma_p + 0.54\,\sigma_n\,,$$

where

$$\sigma_n = \sigma_n(\mathrm{CE}) + \sigma_n(\mathrm{NCE}) = \text{Total cross-section on a neutron.}$$

Using the cross-section on an average nucleon corrected for the Pauli principle, $\sigma(\overline{N})$, and the K-p cross-section from the Hydrogen scatters, σ_p, the total cross-section on a «free» neutron, σ_n, may be deduced. Thus σ_n(NCE) may also be derived.

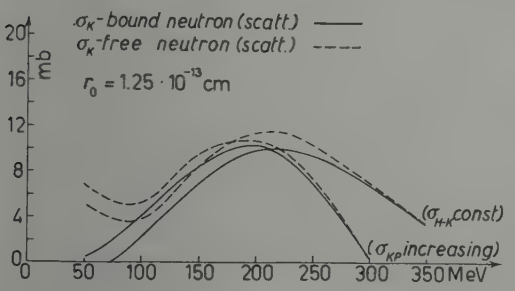

Fig. 11.

However, the data of Fig. 8 cannot be taken as positive proof of a rise in σ_p with energy, so the calculation of σ_n(NCE) has been carried out under the two assumptions: (*a*) that σ_p increases with E_k according to the data quoted in Fig. 8; (*b*) that σ_p is independent of energy below 300 MeV and has the value 15.7 mb. The behaviour of σ_n(NCE) so deduced is shown in Fig. 11 and it clearly passes through a maximum around 220 MeV independently of the

assumption (*a*) or (*b*). At present it appears that assumption (*a*) is a better approximation to the truth than (*b*).

4·4. *The* K-*nucleon differential cross-section.* – The distribution in center-of-mass scattering angle χ_{CM} has been shown in Fig. 3 for the 13 K-Hydrogen collisions reported in the present work and 13 other events found in other laboratories. The forward/backward ratio is $\frac{5}{8}$ for the Du-Pd data and 10/16 for the world data.

In the high-energy inelastic interactions of K^+-mesons with nuclei the picture of collisions occurring with just single nucleons within nuclear matter seems to hold quite well so that in principle one could learn something of the differential cross-section on the « average » bound nucleon. Apart, however, from the complication that a nucleon is in general moving with a considerable momentum when struck, in practice a substantial fraction of the K^+-mesons undergoes more than one collision within the nucleus. In Fig. 4 it can be seen that over 30% of the points lie outside the limits of $(\Delta E/E, \theta)$ allowed for collisions with a nucleon of a Fermi gas ($p_{max} = 241$ MeV/c) and presumably they correspond to multiple collisions. The occurrence of a large amount of secondary scattering will smear considerably the laboratory distribution of single scatterings and this effect is difficult to estimate. The distribution in the values of θ observed is shown in Fig. 12 together with that computed for single scattering from a Fermi gas, assuming $(d\sigma/d\Omega)_{CM}$ to be isotropic. The calculated distribution is slightly more peaked than the experimental one, but when the smearing effect due to multiple scattering is taken into account the calculated distribution will be less peaked, and that seems to indicate a $(d\sigma/d\Omega)_{CM}$ (K-free nucleon) a litte peaked in the forward direction.

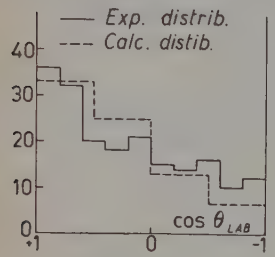

Fig. 12.

4·5. *Decays in flight.* – 37 examples of K^+-mesons decaying in flight with a visible secondary track have been observed. From the depth distribution of both the decays in flight and the stops it is estimated that two events classified as « stops » were decays in flight in which the secondary product escaped observation.

Thus the estimated total number of events occurring in 185 m of track is 39. Since the mean velocity of the K mesons is 0.764 c, the lifetime turns out to be $(2.1 \pm 0.3) \cdot 10^{-8}$ s seen in the laboratory frame. Dividing this by the time dilatation factor 1.55 gives the lifetime estimate for K^+ mesons at rest $(1.37 \pm 0.22) \cdot 10^{-8}$ s.

4·6. *A tentative phase shift-analysis.* – According to the Gell-Mann–Nishijima scheme, the only reactions expected from conservation of isotopic spin and strangeness considerations, are the following:

$$\mathrm{K^+ + p \to K^+ + p} \qquad T = 1$$

$$\mathrm{K^+ + n \to K^+ + n} \qquad T = 1 \text{ and } T = 0$$

$$\mathrm{K^+ + n \to K^0 + p} \qquad T = 1 \text{ and } T = 0 .$$

If we assume that only S and $P_{\frac{1}{2}}$ and $P_{\frac{3}{2}}$ waves are responsible for the interactions and define

$$a_{00} = \exp[i\delta_{00}] \sin \delta_{00} ,$$

a the scattering amplitude in the $T = 0$, $l = 0$, state (the second indices 0, 1, 3, signify S, $P_{\frac{1}{2}}$, $P_{\frac{3}{2}}$ waves respectively), the total and differential cross-sections can be written in the following way:

(A) $$\sigma = 4\pi\lambda^2(A + \tfrac{1}{3}C) ,$$

(B) $$\frac{\mathrm{d}\sigma}{\mathrm{d}\Omega} = \lambda(A + B\cos\theta + C\cos^2\theta) ,$$

where $2\pi\lambda =$ de Broglie wave length and

(i)) $$A_p = (a_{10})^2 + (a_{13} - a_{11})^2$$

(i) $$B_p = 2\,\mathrm{Re}\,[a_{10}^*(2a_{13} + a_{11})]$$

(iii) $$C_p = (2a_{13} + a_{11})^2 - (a_{13} - a_{11})^2$$

for proton scattering and

(iv) $$A_{cc}^n = \tfrac{1}{4}(a_{10} \pm a_{00})^2 + \tfrac{1}{4}[(a_{13} - a_{11}) \pm (a_{03} - a_{01})]^2$$

(v) $$B_{cc}^n = \tfrac{1}{2}\,\mathrm{Re}\,(a_{10} \pm a_{00})^*[(2a_{13} + a_{11}) \pm (2a_{03} + a_{01})]$$

(vi) $$C_{cc}^n = \tfrac{1}{4}[(2a_{13} + a_{11}) \pm (2a_{03} + a_{01})]^2 - \tfrac{1}{4}[(a_{13} - a_{11}) \pm (a_{03} - a_{01})]^2$$

for neutron scattering, and neutron charge-exchange respectively. (Positive signs for scattering).

Low energy results. From low energy data obtained in previous work ([4,5,16,17,23]) we can assume that:

([23]) O. R. Price, D. M. Stork and H. K. Tictro: *Phys. Rev., Letters*, **1**, 212 (1958).

1) The most important contribution to the K-nucleon cross-section is from the $T = 1$ state in the S-wave. $\delta_{10} < 0$ because the nuclear potential is repulsive.

2) The contribution from the $T = 0$ state is smaller and is from a P-wave which gives a backward peaked K-neutron cross-section. Therefore δ_{01} must be positive (Eq. (v), $P_{\frac{3}{2}}$ terms neglected).

High energy results. In analysing the high energy data, we can tentatively assume that the contribution of the $P_{\frac{3}{2}}$ waves is negligible. With this hypothesis, we can justify the maximum found for the K-neutron scattering cross-section at high energy, by assuming that the P-wave in the $T = 1$ state increases rapidly for energies > 200 MeV.

If the phaseshift δ_{11} is negative, destructive interference will result between a_{01} and a_{11} which will lower the K-neutron cross-section for scattering. Constructive interference will take place for charge exchange (change of sign in (iv), (v) and (vi)). This agrees with the experimental data (Fig. 10).

The experimentally found increase in the K-H cross-section supports the hypothesis of a rapid rise of the a_{11} contribution for E_k greater than 200 MeV. Other supporting evidence for the above is obtained from the forward peak in the differential cross-section for K-nucleon scattering in the laboratory system (Fig. 12). This distribution was flat at low energies.

Assuming that $\delta_{01} = -\delta_{11}$ in the energy region ~ 300 MeV, (as the neutron scattering cross-section seems to have a very small value (Fig. 11)), it is possible, from the charge-exchange cross-section at this energy (Fig. 10) and correcting for the Pauli principle, to obtain a value for the scattering amplitude. Thus we obtained a P-wave contribution for proton scattering at 270 MeV of ~ 6.3 mb (taking $r_0 = 1.25 \cdot 10^{-13}$ cm). On adding this to 13.5 mb, the assumed S-wave contribution, a value of 19.8 mb obtained for the expected K-H cross-section at this energy, in good agreement with the experimental value of (21.3 ± 4) mb.

Using the K-H cross section results, with an S-wave contribution of ~ 13.5 mb, it is possible to calculate the P-wave phase-shift, in order to obtain a cross-section of 21 at high energy. We have thus calculated the expected K-H differential cross-section in the C.M. system. This gave a pronounced forward-peak, which does not agree with experimental data at present available (*).

Similar conclusions can be obtained by considering the $P_{\frac{1}{2}}$ contribution to be negligible in comparison with $P_{\frac{3}{2}}$. The main difference lies in the fact

(*) *Note added in proofs.* – In a recent paper [24], indications are given in favour of a forward peaking in the K^+-p cross-section.

[24] T. F. KYCIA, L. T. KERTH and R. G. BAENDER: *Bull. Am. Phys. Soc.*, **4**, 25 (1959).

that term C in eqn. (iii) no longer vanishes, and an even more anisotropic K-H differential cross-section is obtained.

In addition to the above difficulty, we have had to assume that the P-wave in the $T=1$ state, with a negative phase-shift (δ_{11}) corresponding to a repulsive potential, increases more rapidly than the P-wave of the $T=0$ state, which has a positive phase shift. This point is difficult to interpret theoretically.

5. – Elastic scattering.

In a sub-sample of 75.7 metres of track followed, a total of 167 elastic scatters was observed with plane projected angles greater than 2°. These were classified in intervals of the space scattering angle, and the differential cross-section derived for each interval.

Angular interval	2° ÷ ÷3°	3° ÷ ÷4°	4° ÷ ÷5°	5° ÷ ÷6°	6° ÷ ÷7°	7° ÷ ÷8°	8° ÷ ÷10°	10° ÷ ÷12°	12° ÷ ÷14°	14° ÷ ÷19°
No. of events	27	19	22	19	16	13	17	20	8	6
$10^{-3}\,d\sigma/d\Omega$ (mb/sr)	59.5	14.3	10.3	6.8	4.5	3.2	1.7	1.5	0.6	0.14

Using the optical model, and assuming various values of the nuclear potential, theoretical curves of the elastic differential cross-section have been calculated by EVANS *et al.* ([20]). The points obtained in this experiment lie on an average about 25% higher than those found by these authors in a scan of 49 m of track and therefore reinforce their argument in favour of a substantial repulsive potential at these energies.

6. – Conclusions.

1) At higher energies the contribution of the $T=0$ state becomes approximately of the same importance as that of the $T=1$ state. This fact can be deduced from the rise in the charge-exchange cross-section which reaches approximately the same value as the K-H cross-section (Figs. 8 and 10).

2) The K-H cross-section seems to increase as the K-meson energy increases (from $\sim$ 14 mb at (20 ÷ 200) MeV to $\sim$ 21 mb at (200 ÷ 350) MeV). The errors in the determination are rather large but if the increase is established, one can assume that at least a P-wave interaction is present in the $T=1$ state.

3) There appears to be a maximum for the bound neutron scattering cross-section at about $E_k = 210$ MeV. This could be interpreted as an interference between two P-waves. A resonance can be excluded, because no maximum has been found for the charge-exchange cross-section in the same region.

* * *

We wish to thank Prof. E. J. LOFGREN and his collaborators for such a successful exposure of the stack. For processing and developing the plates our thanks are due to Prof. C. F. POWELL and the Bristol Group.

We are grateful to Prof. N. DALLAPORTA, Drs. C. CEOLIN, G. PATERGNANI and L. TAFFARA (Padua) and to Prof. T. E. NEVIN (Dublin) for many suggestions and interesting discussions during our work. To Messrs. M. BERNO, A. BENAZZI, V. CHIARATTI, V. CHIEREGATO, B. DAINESE, G. GESUATO, A. MANNELLINO and Miss A. MARCHETTI (Padua) and Misses P. LEAHY, B. MAHER, Y. RICHARDS and M. SMITH (Dublin) special thanks are due for their assistance in the scanning and analysis of events.

Finally we wish to acknowledge the cordial exchange of information with the laboratories of Bologna, Bristol, Brookhaven and Los Angeles.

APPENDIX

Scattering

No. events	No. of prongs	E_1	$\Delta E/E$	E prongs (*)	θ_k
		Dublin			
Du 170/11	4	285	63	104	133°
Du 220/11	5	269	51	76	51°
Du 175/8	1	276	42	30	53°
Du 177/14	3	295	62	56	83°
Du 175/22	$1+e$	289	49	24	110°
Du 170/23	$3+R$	258	84	17	86°
Du 194/5	0	292	87	—	72°
Du 194/15	4	256	78	19	134°
Du 185/19	2	252	69	46	95°
Du 186/16	0	275	71	—	6°
Du 185/23	$1+R$	238	49	12	42°
Du 186/19	2	293	63	76	42°
Du 187/4	0	283	84	—	104°
Du 185/13	$0+R$	255	6	—	80°

(*) «E prongs» is the total energy of the stable prongs.

Scattering (continued).

No. events	No. of prongs	E_1	$\Delta E/E$	E prongs (*)	ϑ_1
Du 194/9	3	267	83	5	68°
Du 177/19	1	286	86	240	41°
Du 191	1	284	29	82	66°
Du 196/19	$2 + R$	250	12	11	29°
Du 175/23	4	274	27	25	66°
Du 196/17	$1 - e$	281	60	4	48°
Du 204/6	$3 - e$	249	81	80	88°
Du 176/14	1	261	5	7	58°
Du 191/9	1	257	66	16	123°
Du 191/6	1	285	34	30	25°
Du 180/2	$0 - R$	262	29	—	50°
Du 203/19	1	257	25	55	46°
Du 170/18	2	291	85	30	30°
Du 170/33	0	253	61	—	48°
Du 191/19	$3 - R$	241	81	19	68°
Du 178/34	1	258	58	82	125°
Du 179/5	3	288	79	16	144
Du 220/5	$3 + 2R$	283	66	84	101°
Du 191/21	0	246	89	—	127°
Du 183/10	1	279	84	230	59°
Du 203/2	3	272	83	18	125°
Du 203/11	2	267	74	92	88°
Du 202/18	1	282	71	5	154°
Du 184/6	0	262	38	—	81°
Du 204/1	1	250	85	170	119°
Du 184/11	1	260	42	5	68°
Du 199/12	5	258	57	57	31°
Du 181/5	2	267	75	61	41°
Du 188/7	1	263	39	54	104°
Du 207/1	1	248	11	7	32°
Du 184/9	2	239	74	79	34°
Du 202/11	0	289	82	—	51°
Du 198/15	4	285	52	92	88°
Du 200/16	$0 + R$	234	67	—	87°
Du 200/24	2	273	48	121	71°
Du 208/14	1	261	68	21	17°
Du 219/5	1	243	79	86	48°
Du 189/30	1	259	71	26	150°
Du 219/14	1	292	12	8	21°
Du 219/2	$4 + R$	242	74	27	132°
Du 219/4	1	273	89	28	41°
Du 199/11	1	285	78	62	119°
Du 189/15	3	290	89	57	82°
Du 183/9	1	251	28	4	90°
Du 215/6	1	246	47	8	58°

(*) «E prongs» is total energy of the stable prongs.

Scattering (continued).

No. events	No. of prongs	E_1	$\Delta E/E$	E prongs (*)	θ_k
Du 201/26	4	274	78	125	134°
Du 198/6	3	275	73	43	82°
Du 191/36	3	271	75	47	88°
Du 207/13	2	243	66	42	90°
Du 197/14	4	265	86	113	120°
Du 197/7	2	253	48	72	88°
Du 191/32	2	243	77	200	58°
Du 191/34	2	265	65	22	88°
Du 210/8	3	283	77	45	117°
Du 210/2	2	281	75	179	163
Du 208/3	$1+2R$	236	68	108	112°
Du 211/8	3	285	72	43	107°
Du 214/13	3	284	59	42	57°
Du 188/14	0	248	81	—	160°
Du 216/15	1	284	47	104	23°
Du 218/6	1	236	75	9	142°
Du 181/14	4	295	55	40	129°
Du 202/22	4	265	60	37	82°
Du 189/13	1	259	30	14	30°
Du 217/10	2	237	71	9	151°
Du 217/4	3	266	87	88	106°
Du 200/12	$0+R$	237	7	—	36°
Du 217/1	1	275	52	80	125°
Du 208/2	0	290	45	—	18°
Du 176/42	1	243	56	60	155°
Du 205/26	$2+R$	260	50	6	95°
Du 218/2	1	293	89	80	88°
Du 205/12	$3+R$	247	96	17	61°
Du 208/4	$1+R$	238	60	130	47°
Du 200/4	3	295	66	103	146°
Du 203/27	$3+R$	269	68	37	49°
Du 216/16	2	300	20	50	122°
Du 206/16	2	248	64	11	93°
Du 219/10	$0+R$	286	47	—	59°
Du 188/23	1	278	35	109	75°
Du 219/7	2	287	58	73	65°
		Padua			
Pd 7	1	380	37	37	32°
Pd 24	0	275	35	—	25°
Pd 58	$1+R$	248	23	9	64°
Pd 60	$0+R$	210	0	—	46°
Pd 61	$1+R$	242	30	70	24°

(*) «E prongs» is total energy of the stable prongs.

Scattering (continued).

No. events	No. of prongs	E_1	$\Delta E/E$	E prongs (*)	θ_k
Pd 73	$0+e$	262	88	—	98°
Pd 79	$4+e$	250	85	109	32°
Pd 80	1	280	33	47	47°
Pd 105	$3+R$	338	78	56	144°
Pd 114	$3+R$	242	81	135	52°
Pd 172	$2+R$	282	52	58	90°
Pd 162	$0+R$	250	36	—	98°
Pd 209	3	247	64	39	115°
Pd 180	1	222	50	—	21°
Pd 228	3	230	47	57	121°
Pd 211	$0+R$	317	44	—	50°
Pd 248_1	2	300	41	10	24°
Pd 250	$0+R$	200	5	—	54°
Pd 375	3	260	71	23	54°
Pd 396	1	282	87	65	21°
Pd 407	2	235	77	10	96°
Pd 412	$2+R$	220	51	38	28°
Pd 321	$3+R$	205	71	42	56°
Pd 323	1	210	24	38	57°
Pd 325	$0+R$	320	36	—	42°
Pd 264	0	240	61	—	74°
Pd 257	0	255	37	—	47°
Pd 341	0	430	16	—	34°
Pd 347	3	257	86	74	166°
Pd 444	2	310	74	115	61°
Pd 462	$3+R$	235	—	36	—
Pd 477	2	325	42	30	44°
Pd 509	3	230	52	49	67°
Pd 512	1	240	52	50	102°
Pd 529	$2+R$	230	52	13	109°
Pd 531	$0+R$	235	48	—	103°
Pd 539	4	240	69	43	69°
Pd 590	1	245	77	200	120°
Pd 593	0	200	7	—	41°
Pd 599	0	268	48	—	91°
Pd 615	1	240	42	—	60°
Pd 621	$5+4R$	430	51	82	78°
Pd 630	1	260	20	62	42°
Pd 643	3	333	88	52	77°
Pd 652	0	295	25	—	45°
Pd 662	$1+e$	275	40	82	64°
Pd 664	$0+e$	275	48	—	47°
Pd 669	2	317	73	16	124°
Pd 694	$4+R$	250	82	59	124°
Pd 700	$4+R$	298	54	28	65°

(*) « E prongs » is total energy of the stable prongs.

Scattering (continued).

No. events	No. of prongs	E_1	$\Delta E^1 E$	E prongs (*)	θ_k
Pd 706	1	300	58	—	138°
Pd 728	1	308	55	66	57°
Pd 732	2	290	73	131	131°
Pd 760	3	215	62	20	120°
Pd 774	$0+R+e$	280	67	—	74°
Pd 776	2	250	74	121	95°
Pd 787	$1+3R$	350	37	13	80°
Pd 801	2	330	78	29	76°
Pd 824	1	277	74	21	80°
Pd 844	3	255	65	25	80°
Pd 861	1	310	26	16	34°
Pd 864	3	287	71	18	101°
Pd 870	1	244	80	—	77°
Pd 872	3	230	70	76	92°
Pd 887	1	317	86	135	47°
Pd 895	0	280	35	—	89°
Pd 745	$1+R$	242	60	86	110°
Pd 725	2	245	56	29	103°
Pd 908	1	232	23	7	18°
Pd 947	$2+R$	307	89	212	112°
Pd 966	4	262	52	44	63°
Pd 970	3	212	62	113	32°
Pd 993	0	242	27	—	28°
Pd 994	1	210	38	33	66°
Pd 999	3	285	30	11	43°
Pd 1017	2	210	55	20	71°
Pd 1031	1	248	27	8	37°
Pd 1058	1	285	32	31	35°
Pd 1080	3	230	62	64	97°
Pd 1130	1	215	51	90	57°
Pd 1146	$0+R$	242	29	—	44°
Pd 1169	2	228	8	19	31°
Pd 1172	2	400	87	85	122°
Pd 1193	1	340	83	200	79°
Pd 1204	1	375	41	57	27°
Pd 1208	5	255	65	51	101°
Pd 1264	$1+R$	290	36	10	52°
Pd 1267	$3+2R$	270	55	48	68°
Pd 1298	5	305	61	81	107°
Pd 1308	$0+e$	260	2	—	33°
Pd 1314	$4+R$	258	62	20	60°
Pd 1318	$1+R$	210	38	3	82°
Pd 1327	1	292	66	145	90°
Pd 1335	$0+R$	260	44	—	76°
Pd 1356	$2+e$	360	79	57	26°

(*) «E prongs» is total energy of the stable prongs.

Scattering continued.

No. events	No. of prongs	E_1	ΔE E	E prongs (*)	ϑ_1
Pd 1382	$2+R$	255	77	13	137°
Pd 1385	1	310	68	155	167°
Pd 1389	1	305	33	75	32
Pd 1392	1	260	35	24	82°
Pd 899	1	210	32	8	93°
Pd 1412	2	285	73	15	121°
Pd 1426	1	307	59	3	91°
Pd 1432	$0-R$	105	60	—	108°
Pd 1433	$2+R$	245	75	140	108°
Pd 1434	1	290	71	3	70°
Pd 1438	$4+R$	288	61	57	45°
Pd 1459	1	270	63	112	70°
Pd 1474	1	285	63	13	52°

(*) «E prongs» is total energy of the stable prongs.

Charge-Exchange

No. events	No. of prongs	E_1	Enegy of fastest protons	θ of fastest protons
		Dublin		
Du 220/8	$2+R$	182	1	23°
Du 177/3	3	282	52	62°
Du 175/11	$2+R$	260	107	38°
Du 193/3	4	293	12	63°
Du 175/2	$2+e$	282	4	107°
Du 185/24	4	251	29	46°
Du 186/21	$3+\bar{\alpha}$	285	45	29°
Du 186/22	1	290	5	149°
Du 187/11	3	262	38	60°
Du 191/5	$2+R$	278	32	78°
Du 193/2	3	234	15	53°
Du 202/6	5	289	96	29°
Du 191 11	$2-R$	265	8	138°
Du 176 8	$3-R$	252	9	72°
Du 202 15	$2-R$	293	8	66°
Du 179 4	$1-R$	289	9	108°
Du 178 35	2	272	165	63°
Du 184 23	2	244	74	93°
Du 193 16	3	263	47	72°
Du 186 18	1	269	95	49°
Du 184 10	3	263	7	77°

Charge-Exchange (*continued*).

No. events	No. of prongs	E_1	Energy of fastest protons	θ of fastest protons
Du 198/4	6	281	15	48°
Du 205/1	$2 + R$	275	91	52°
Du 198/9	$3 + R$	290	80	51°
Du 204/5	$1 + R$	253	3	104°
Du 202/4	$2 + R$	287	53	30°
Du 219/11	5	280	51	108°
Du 207/21	3	281	27	50°
Du 191/27	3	271	16	73°
Du 219/3	$3 + R$	287	112	31°
Du 205/10	$2 + R$	239	116	25°
Du 218/1	1	275	10	147°
Du 201/35	1	285	86	25°
Du 183/24	1	236	115	32°
Du 184/31	1	289	93	30°
Du 213/9	1	242	92	20°
Du 176/38	2	243	25	20°
Du 216/17	4	250	23	63°
Du 177/20	$1 + R$	250	82	59°
Du 200/35	$3 + R$	295	46	76°
		Padua		
Pd 18	$3 + R$	255	54	30°
Pd 28	6	270	36	38°
Pd 46	2	277	45	48°
Pd 54	3	210	12	—
Pd 55	$4 + R$	275	7	—
Pd 66	$0 + e$	350	—	—
Pd 84	2	307	170	57°
Pd 88	$1 + e$	242	150	31°
Pd 103	$1 + R$	262	12	—
Pd 126	2	225	58	52°
Pd 210	3	262	199	10°
Pd 203	$2 + e$	250	160	16°
Pd 371	2	238	80	69°
Pd 451	$3 + R$	260	168	24°
Pd 471	2	310	50	32°
Pd 510	5	440	127	24°
Pd 519	5	330	165	144°
Pd 571	3	300	80	67°
Pd 432	2	282	245	42°
Pd 557	2	200	72	69°
Pd 632	$1 + R$	318	180	98°
Pd 709	5	310	27	88°
Pd 778	5	300	40	54°
Pd 791	1	240	16	75°

Charge-Exchange (*continued*).

No. events	No. of prongs	E_1	Energy of fastest protons	θ of fastest protons
Pd 823	2	270	240	55°
Pd 853	$2+R$	245	13	34°
Pd 555	$3+R$	262	70	127°
Pd 755	$2+R$	210	8	—
Pd 340	1	280	225	15°
Pd 907	$3+2R$	286	35	120°
Pd 913	4	210	34	63°
Pd 980	$1+e$	245	10	92°
Pd 1009	4	262	19	82°
Pd 1014	$3+R$	300	45	43°
Pd 1068	5	210	52	14°
Pd 1084	3	330	11	—
Pd 1102	1	250	72	49°
Pd 1103	5	272	50	22°
Pd 1143	$2+R$	325	19	125°
Pd 1144	1	270	130	43°
Pd 1159	3	275	29	177°
Pd 1170	$3+R$	215	80	35°
Pd 1199	$1+R$	380	133	39°
Pd 1224	$1+R$	282	230	23°
Pd 1280	$2+R$	278	54	92°
Pd 1281	5	260	56	86°
Pd 1309	7	300	97	103°
Pd 1330	2	270	43	67°
Pd 1357	4	262	74	35°
Pd 1360	2	280	19	45°
Pd 1480	1	302	27	99°
Pd 1527	$2+R$	350	18	36°

RIASSUNTO

Sono state analizzate le interazioni relative a 185 m di traccia di mesoni K⁻ osservati in emulsione nucleare. Si sono ottenute informazioni sulle reazioni di scattering K⁻-p e K⁺-n e di cambio carica. Basandosi su tutti i dati in emulsione raccolti nei vari laboratori, si è determinata la dipendenza dell'energia delle 3 sezioni d'urto fino a 350 MeV. L'analisi in fasi mostra che verso i 300 MeV il contributo dello stato $T=0$ è dello stesso ordine di grandezza di quello dello stato $T=1$. All'interferenza tra onde P di questi due stati si può attribuire l'aumento della sezione d'urto di cambio carica e la diminuzione della sezione d'urto di scattering su neutrone.

IL NUOVO CIMENTO Vol. XII, N. 3 1° Maggio 1959

Partial Wave Analysis of the Production of Boson Pairs.

S. Ciulli (*) and J. Fischer (**)

Joint Institute for Nuclear Research - Dubna

(ricevuto l'11 Gennaio 1959)

Summary. — Partial wave analysis for boson pair production on nucleons is made. The corresponding angular operators, which characterize the spin and angular dependence of the S-matrix, are expressed with the help of the Legendre polynomials and tabulated. Simultaneously a general method of calculating the angular operators is given for processes containing more than four particles, in which cases the straightforward method leads to very lengthy calculations.

1. – Introduction.

Boson production processes as pion and photon pair production, radiative pion scattering etc., have been intensively investigated during the last years. The theoretical bibliography on this subject may be divided into two parts: one containing pure-theoretical treatises, which solve the problem by means of the Chew-Low method or dispersion relations, and the other consisting of works which use some semiempirical postulates concerning the dynamical character of the process, such as assumptions on the existence of resonant states.

For both these methods, it is useful to study the angular and charge dependence of the S-matrix. In the first case, one obtains in this way a set of independent equations for the energy-dependent coefficients; in the latter case, one can write directly the amplitude of the assumed resonant state as a function of angular and isotopic variables.

(*) On leave of absence from the Institute for Atomic Physics, Bucarest.

(**) On leave of absence from the Physical Institute of the Czechoslovak Academy of Sciences, Prague.

To perform this angular and isotopic analysis, it is sufficient to know the general laws of conservation, without assuming anything concerning the dynamics of the reaction. The result of such an analysis is a set of orthonormal polynomials, which can also be used for the phase analysis of the experimental data. This is especially important for processes with an interaction character which is not very well known.

In the present paper, the ordinary space structure of the S-matrix is studied for processes which may be described with the help of the following formula

$$\mathrm{b} + \mathrm{N} \to \sum_{i=1}^{n} \mathrm{b}_i + \mathrm{N} , \tag{1}$$

where N denotes the nucleon and b, b_i bosons of any kind. For processes of the type $\mathrm{b}-\mathrm{N} \to \mathrm{b}'-\mathrm{N}$ this analysis has been made by RITUS [1]. However, the straightforward generalization of his method to the case of more particles leads to lengthy and cumbersome calculations. For instance, for $n = 2$ in (1) almost two hundred terms must be calculated and for higher values of n the calculations are practically impossible. We give a method for simplifying this procedure, namely by reducing the production of n bosons to that of $n-1$ bosons. We demonstrate it for $n = 2$, but it has general validity ($n = 2$ is chosen only to deal with simple formulae). For the same value of n we have calculated the explicit form of the angular operators. The resulting polynomials are given in the Tables I, II and III for different coupling schemes of the final angular momenta.

Readers interested only in the practical use of these Tables can omit Sections **3** and **4**, which deal with the calculation formalism of the angular operators in the boson-boson and boson-nucleon coupling schemes respectively.

2. – The angular operators.

Let the initial state of our system be characterized by the total angular momentum J, its z-component M and by the eigenvalues (i) of a system of quantities which together with J and M form a complete set of commuting observables. Then, the initial state will be described by the following ket-vector

$$|JM(i)\rangle .$$

Similarly, the final state will be described by

$$|J'M'(f)\rangle ,$$

(1) V. I. RITUS: *Žu. Èksp. Teor. Fiz. SSSR*, **32**, 1536 (1957); English in *Soviet Physics* (*JETP*), **5**, 1249 (1957).

where the symbols have an analogical meaning to that of J, M, (i) respectively. The operator which describes the transition $|JM(i)\rangle \to |J'M'(f)\rangle$ is defined by

$$|J'M'(f)\rangle\langle JM(i)| .$$

Consequently, the S-matrix can be expressed as follows

$$S = \sum a(J'M'(f); JM(i))\, |J'M'(f)\rangle\langle JM(i)| , \tag{2}$$

where $a(J'M'(f); JM(j))$ determines the « breadth » of the corresponding channel. Doing the partial wave analysis, we shall be concerned only with the angular momentum part of the channel labels (i), (f) and we shall omit any explicit reference to other quantities such as energy, isotopic spin etc., which would be included in the a-coefficients. Due to the three-dimensional rotational invariance of the S-matrix, the right-hand side of (2) may be written in the following form:

$$\sum_{J(f)(i)} a(J(f)(i)) \sum_{M=-J}^{+J} |JM(f)\rangle\langle JM(i)| ,$$

where

$$\sum_{M=-J}^{J} |JM(f)\rangle\langle JM(i)| = \hat{\mathcal{F}}(J(f)(i)) \tag{3}$$

are the so-called angular operators of the reaction (see [1]); they determine the angular and spin dependence of the S-matrix. They are orthogonal with one another and are normalized in the following way:

$$\underset{\substack{\text{over}\\ \text{spins}}}{\text{tr}} \int_{\substack{\text{over all}\\ \text{angles}}} \hat{\mathcal{F}}^{+}(J'(f')(i'))\, \hat{\mathcal{F}}(J(f)(i)) = (2J+1)\, \delta_{JJ'} \delta_{(f)(f')} \delta_{(i)(i')} ,$$

if the initial and the final state eigenfunctions are normalized to 1.

Before calculating the explicit form of (3) for reactions belonging to the type (1), let us remark that if we know the angular operators for b, b_i (see (1)) having spin zero, then those for spin one may be obtained by operating with:

$$\frac{1}{\sqrt{l_k(l_k+1)}} \frac{\partial}{\partial \boldsymbol{k}} \qquad \text{for the electric multipole ,}$$

$$\frac{-i}{\sqrt{l_k(l_k+1)}} \left[\boldsymbol{k} \frac{\partial}{\partial \boldsymbol{k}}\right] \qquad \text{for the magnetic multipole and}$$

$$\boldsymbol{k} \qquad \text{for the « longitudinal » multipole ,}$$

on the corresponding angular operators. Therefore we calculate only the angular operators for b and b_i having spin zero, and we do not suppose any definite parity for them. (So, if some of the b, b_i are π-mesons, the corresponding angular operators are obtained by postulating the internal oddness of these particles.) In this particular case, the set (i) of the initial eigenvalues consists of the spin $\sigma = \frac{1}{2}$ of the nucleon and the orbital momentum l of the ingoing boson. The symbol (f), in the two-boson case, represents by itself either

(I) $$\sigma' = \tfrac{1}{2}, \quad l_1, \quad l_2, \quad L \quad \text{where} \quad \hat{\boldsymbol{L}} = \hat{\boldsymbol{l}}_1 + \hat{\boldsymbol{l}}_2$$

or

(II) $$\sigma' = \tfrac{1}{2}, \quad l_1, \quad j, \quad l_2 \quad \text{where} \quad \hat{\boldsymbol{j}} = \hat{\boldsymbol{\sigma}}' + \hat{\boldsymbol{l}}_1 .$$

Both these coupling schemes must give the same information about the process, if transitions from all possible initial to all possible final states are considered, *i.e.* if no one from the a-coefficients is neglected. Mathematically, this is an evident fact because of the completeness of the orthonormal set of the angular operators both in Case (I) and in Case (II). In practical calculations, however, we deal always only with certain non-complete subsets of these sets, having to restrict ourselves to a finite number of terms in (2). Then, the two coupling schemes are no more equivalent and we must choose that of them which gives a better approximation to the ideal case. This depends, naturally, on the distribution of the a-coefficients in (2): if only few of them are large and the others small, then it is sufficient to consider only a small number of channels for obtaining a true picture of the reality. If, on the contrary, we deal with such a coupling in which all or many a's are large, the calculations approach very slowly to the real case. Thus, this practical reason gives a criterion in choosing the coupling.

Besides this practical argument, from the physical point of view, the fact that in a given coupling scheme only a small number of channels are important, gives a deeper insight into the understanding of the nature of the process. Indeed, the existence of such resonant states cannot be predicted by means of general group-theoretical methods, but is in a direct connection with the dynamical properties of the interaction. For instance, it is to be expected that the isobaric state $(\frac{3}{2}, \frac{3}{2})$ of the nucleon will play an important role in processes in which at least one π-meson is present, as it is the case for nucleon-nucleon collisions and for elastic scattering of pions [2].

[2] We refer the reader to the clear discussion on this topic contained in the paper of R. F. PEIERLS: *Phys. Rev.*, **111**, 1373 (1958).

In general, we can say that the choice of the coupling scheme is determined by the interaction: if in a system of three particles, a certain pair interacts much stronger than other pairs, it may be considered approximately as a shortly-living subsystem with spin equal to the vectorial sum (according to the vector model) of angular momenta of these particles. Naturally, by specifying the spin eigenvalue of this subsystem we determine, simultaneously, the coupling scheme of the angular momenta. This situation is quite analogous to that in an atom, in which the angular momenta may be coupled either according to the (LS)-scheme or according to the (jj)-scheme.

3. – The boson-boson coupling.

In the case of the boson-boson coupling, the final state may be written as follows

$$|JMl_1l_2L\tfrac{1}{2}\rangle = \sum_{\mu'=-\frac{1}{2}}^{\frac{1}{2}} C_{JM}^{LM-\mu'\frac{1}{2}\mu'}\, \mathcal{Y}_{LM-\mu'}^{l_1l_2} |\tfrac{1}{2}\mu'\rangle ,$$

where

$$\mathcal{Y}_{LM-\mu'}^{l_1l_2}(\boldsymbol{q},\boldsymbol{r}) = \sum_{\lambda_1=-l_1}^{l_1} C_{LM-\mu'}^{l_1\lambda_1 l_2 M-\mu'-\lambda_1} Y_{l_1\lambda_1}(\boldsymbol{q}) Y_{l_2 M-\mu'-\lambda_1}(\boldsymbol{r}),$$

is the orbital eigenfunction of the outgoing bosons and $|\frac{1}{2}\mu'\rangle$ is the spin eigenfunction of the nucleon. If we write the initial state also as a Clebsch-Gordan combination of the angular momenta of the ingoing particles, we find that the angular operator (3) has the following form

$$\hat{\mathcal{F}}(Jl_1l_2L\tfrac{1}{2}l_2) = \sum_{\mu'=-\frac{1}{2}}^{\frac{1}{2}} \sum_{\mu=-\frac{1}{2}}^{\frac{1}{2}} \mathcal{L}_{\mu'\mu} |\tfrac{1}{2}\mu'\rangle\langle\tfrac{1}{2}\mu| , \tag{4}$$

where

$$\mathcal{L}_{\mu'\mu} = \sum_{M} C_{JM}^{LM-\mu'\frac{1}{2}\mu'} C_{JM}^{l_2M-\mu\frac{1}{2}\mu}\, \mathcal{Y}_{LM-\mu'}^{l_1l_2}(\boldsymbol{q},\boldsymbol{r}) Y_{LM-\mu}^{*}(\boldsymbol{p}) , \tag{5}$$

will be called the orbital operator and

$$|\tfrac{1}{2}\mu'\rangle\langle\tfrac{1}{2}\mu| = \begin{cases} \dfrac{1 \pm \sigma_z}{2}, & \text{for } \mu' = \mu = \pm\dfrac{1}{2}, \\ \dfrac{\sigma_x \pm i\sigma_y}{2}, & \text{for } \mu' = -\mu = \pm\dfrac{1}{2}, \end{cases} \tag{6}$$

will be called the spin operator (σ_x, σ_y, σ_z are the Pauli matrices); $\boldsymbol{p}$, $\boldsymbol{q}$ and $\boldsymbol{r}$ are unit vectors parallel to the momenta of the b, b_1 and b_2-particles respectively.

Comparing this with formula (5.II) of [1] we see that the angular operators (4) have the same form as those for the elastic scattering of (parityless) pions on nucleons; the only difference is that the orbital eigenfunction of the final pion is replaced here by the $\mathcal{Y}$-function. Therefore, all calculations are analogous to those for the elastic scattering, namely, the sum over $M = -J, \ldots +J$ in (5) can be reduced, by choosing the z-axis parallel to $\boldsymbol{p}$, to one term:

$$C^{L\mu-\mu'\frac{1}{2}\mu'}_{J\mu}\, C^{l,-\frac{1}{2}\mu}_{J\mu}\, \mathcal{Y}^{l_1 l_2}_{L\mu-\mu'}(\boldsymbol{q},\boldsymbol{r})\, \frac{\sqrt{2l+1}}{\sqrt{4\pi}}\,, \tag{7}$$

(because $M - \mu = 0$ in this co-ordinate frame). By inserting this expression in (4) we obtain the form of $\hat{\mathcal{F}}$ in a special frame and, using the rotational invariance of $\hat{\mathcal{F}}$, we can write it in an invariant form.

Let us perform the calculations in some more detail. The first Clebsch-Gordan coefficient in (7) is different from zero only for $J = L \pm \frac{1}{2}$ and the second one only for $J = l \pm \frac{1}{2}$. Furthermore, $\mu = \pm\frac{1}{2}$ and $\mu' = \pm\frac{1}{2}$ so that there are sixteen values of $\mathcal{L}_{\mu'\mu}$ for given l, L, l_1 and l_2. Let us remark now that the magnetic index $\mu - \mu'$ in (7) has only the values 1, 0 and -1, so that the $\mathcal{Y}$-function may be expressed with the help of the operator

$$\hat{\boldsymbol{L}} = \frac{1}{i}\left[\boldsymbol{q}\,\frac{\partial}{\partial \boldsymbol{q}}\right] + \frac{1}{i}\left[\boldsymbol{r}\,\frac{\partial}{\partial \boldsymbol{r}}\right],$$

in the following way

$$\sqrt{L(L+1)}\,\mathcal{Y}_{L,\pm 1} = \hat{L}_{\pm}\mathcal{Y}_{L0} \tag{8}$$

where $\hat{L}_{\pm} = \hat{L}_x \pm i\hat{L}_y$. Now, according to (6) and (7), the four terms on the right-hand side of (4) may be written as follows (we take, for example, the case $J = L + \frac{1}{2} = l + \frac{1}{2}$):

$$\begin{cases} \dfrac{L+1}{\sqrt{2L+1}}\,\mathcal{Y}^{l_1 l_2}_{L0}(\boldsymbol{q},\boldsymbol{r})\,\dfrac{1 \pm \sigma_z}{2}, & \text{for } \mu' = \mu = \pm\tfrac{1}{2}, \\ \text{and} & \\ \dfrac{1}{\sqrt{2L+1}}\,\hat{L}_{\mp}\mathcal{Y}^{l_1 l_2}_{L0}(\boldsymbol{q},\boldsymbol{r})\,\dfrac{\sigma_x \pm i\sigma_y}{2}, & \text{for } \mu' = -\mu = \pm\tfrac{1}{2}. \end{cases} \tag{9}$$

They depend, evidently, on the co-ordinate frame chosen. In order to write them invariantly, let us define the vectors

$$\boldsymbol{P}_x = \boldsymbol{r} - \boldsymbol{p}\,\boldsymbol{p}\cdot\boldsymbol{r}\,, \qquad \boldsymbol{P}_y = [\boldsymbol{p}\boldsymbol{r}]\,,$$

which together with $\boldsymbol{p}$ form a carthesian system and are, in the $p_1 z$-frame, parallel to the x, y, z-axis respectively (the x-axis is chosen in the plane of the vectors $\boldsymbol{p}$, $\boldsymbol{r}$). Their lengths are $|\boldsymbol{P}_x| = |\boldsymbol{P}_y| = \sqrt{1-(\boldsymbol{p}\cdot\boldsymbol{r})^2}$, $|\boldsymbol{p}| = 1$. With the help of them, we can write (9) in the following invariant form:

$$\frac{L+1}{\sqrt{2L+1}}\,\mathcal{Y}_{L0}\,\frac{1\pm\boldsymbol{\sigma}\cdot\boldsymbol{p}}{2}\,,$$

$$-\frac{1}{|2\boldsymbol{P}_x|^2\sqrt{2L+1}}\,\boldsymbol{P}_{\mp}\cdot\hat{\boldsymbol{L}}\,\mathcal{Y}_{L0}\,\boldsymbol{P}_{\pm}\cdot\boldsymbol{\sigma}\,,$$

where $\boldsymbol{P}_{\pm} = \boldsymbol{P}_x \pm i\boldsymbol{P}_y$. Taking into account that

$$\frac{\boldsymbol{P}_-\cdot\hat{\boldsymbol{L}}\,\boldsymbol{P}_+\cdot\boldsymbol{\sigma} + \boldsymbol{P}_+\cdot\hat{\boldsymbol{L}}\,\boldsymbol{P}_-\cdot\boldsymbol{\sigma}}{2|\boldsymbol{P}_x|^2} = \sigma_x\hat{L}_x + \sigma_y\hat{L}_y\,,$$

and that $\hat{L}_z\mathcal{Y}_{L0} = 0$ we obtain the following form for the angular operator:

$$\hat{\mathcal{F}} = \frac{L+1}{\sqrt{2L+1}}\,\mathcal{Y}_{L0} + \frac{1}{\sqrt{2L+1}}\,\boldsymbol{\sigma}\cdot\hat{\boldsymbol{L}}\mathcal{Y}_{L0}\,. \tag{10}$$

In this form, the angular operator is still independent of the number of outgoing particles (for more particles it is only necessary to write more arguments behind $\mathcal{Y}_{L0}$). For the two particle case, we can write

$$\mathcal{Y}_{L0}^{l_1 l_2} = \sum_{\lambda_1=-l_1}^{l_1} C_{L0}^{l_1\lambda_1 l_2-\lambda_1}\,Y_{l_1\lambda_1}\,Y_{l_2-\lambda_1}\,. \tag{11}$$

For simplicity, we restrict ourselves to $l_1 = 0$ and 1, l_2 being arbitrary. We obtain for $l_1 = 0$

$$\mathcal{Y}_{l_2}^{0 l_2} = \frac{1}{\sqrt{4\pi}}\cdot Y_{l_2 0} = \frac{\sqrt{2l_2+1}}{4\pi}\,\mathcal{P}_{l_2}(\boldsymbol{p}\cdot\boldsymbol{r})\,,$$

and for $l_1 = 1$

$$\mathcal{Y}_{l_2+1}^{1 l_2} = \frac{\sqrt{3}}{4\pi\sqrt{l_2+1}}\left((l_2+1)\boldsymbol{p}\cdot\boldsymbol{q}\,\mathcal{P}_{l_2}(\boldsymbol{p}\cdot\boldsymbol{r}) - [\boldsymbol{p}\boldsymbol{q}]\cdot[\boldsymbol{p}\boldsymbol{r}]\mathcal{P}'_{l_2}(\boldsymbol{p}\cdot\boldsymbol{r})\right),$$

$$\mathcal{Y}_{l_2}^{1 l_2} = -i\frac{\sqrt{3}}{4\pi}\sqrt{\frac{2l_2+1}{l_2(l_2+1)}}\,\boldsymbol{p}\cdot[\boldsymbol{q}\boldsymbol{r}]\mathcal{P}'_{l_2}(\boldsymbol{p}\cdot\boldsymbol{r})\,,$$

$$\mathcal{Y}_{l_2-1}^{1 l_2} = -\frac{\sqrt{3}}{4\pi\sqrt{l_2}}\left(-l_2\boldsymbol{p}\cdot\boldsymbol{q}\,\mathcal{P}_{l_2}(\boldsymbol{p}\cdot\boldsymbol{r}) - [\boldsymbol{p}\boldsymbol{q}]\cdot[\boldsymbol{p}\boldsymbol{r}]\mathcal{P}'_{l_2}(\boldsymbol{p}\cdot\boldsymbol{r})\right),$$

where $\mathcal{P}_{l_2}(\boldsymbol{p}\cdot\boldsymbol{r})$ is the Legendre function of the order l_2.

By inserting them in (10) and in analogical expressions for $J = L \pm \frac{1}{2} = l \mp \frac{1}{2}$, $J = L - \frac{1}{2} = l - \frac{1}{2}$ we obtain sixteen different angular operators as given in Tables I and II.

4. – The boson-nucleon coupling.

In the case of the boson-nucleon coupling, the angular operator is given by a formula which is quite analogical to (4):

$$\hat{\mathcal{F}}(Jl_1l_2j\tfrac{1}{2}l\tfrac{1}{2}) = \sum_{\mu'=-\frac{1}{2}}^{\frac{1}{2}} \sum_{\mu=-\frac{1}{2}}^{\frac{1}{2}} \mathcal{L}_{\mu'\mu} |\tfrac{1}{2}\mu'\rangle\langle\tfrac{1}{2}\mu| \,. \tag{12}$$

However, we can easily see that this form of writing, in which the orbital and spin quantities are separated, is very disadvantageous in this case. Indeed, $\mathcal{L}_{\mu'\mu}$ in (12) have the following form:

$$\mathcal{L}_{\mu'\mu} = \sum_{M=-J}^{J} \sum_{m=-j}^{j} C_{JM}^{l_2M-mjm} C_{jm}^{l_1m-\mu'\frac{1}{2}\mu'} C_{JM}^{lM-\mu\frac{1}{2}\mu} Y_{l_2M-m}(\boldsymbol{r}) Y_{l_1m-\mu'}(\boldsymbol{q}) Y^*_{lM-\mu}(\boldsymbol{p}) \,. \tag{13}$$

If comparing it with (5) we see that (13) contains two summations (namely over M and over m), while (5) has only one, namely that over M. The second summation in (5) is involved implicitly, through $\mathcal{Y}$, which must be expressed through $Y(\boldsymbol{q})$ and $Y(\boldsymbol{r})$ according to (11). For this reason, even if the sum over M is eliminated in (13) by suitable choosing of the co-ordinate frame (as it was done in (5)), the sum over m remains. This circumstance, naturally, complicates considerably the calculations. Therefore it is more convenient to write (11) in another form:

$$\hat{\mathcal{F}}(Jl_1l_2j\tfrac{1}{2}l\tfrac{1}{2}) = \sum_{m=-j}^{j} \sum_{\mu=-\frac{1}{2}}^{\frac{1}{2}} \mathcal{K}_{m\mu} |jml_1\tfrac{1}{2}\rangle\langle\tfrac{1}{2}\mu| \,, \tag{14}$$

where

$$\mathcal{K}_{m\mu} = \sum_{M=-J}^{J} C_{JM}^{l_2M-mjm} C_{JM}^{lM-\mu\frac{1}{2}\mu} Y_{l_2M-m}(\boldsymbol{r}) Y^*_{lM-\mu}(\boldsymbol{p}), \tag{15}$$

and

$$|jml_1\tfrac{1}{2}\rangle = \sum_{\mu'=-\frac{1}{2}}^{\frac{1}{2}} C_{jm}^{l_1m-\mu'\frac{1}{2}\mu'} Y_{l_1m-\mu'}(\boldsymbol{q}) |\tfrac{1}{2}\mu'\rangle \,.$$

It is clear that all the four summs will subsist in (14), namely the two « small » (over μ and μ') (*) and the two « great » ones (over m and M). The

(*) One of them (μ') is contained implicitly through $|jml_1\tfrac{1}{2}\rangle$.

last two are responsible for the existence of a great amount of terms, which make all direct computations impossible. Nevertheless, (14) has the advantage of an explicit summation only over m, M being included in $\mathcal{K}_{m\mu}$, (see (15)).

To get rid of the summation over m, we have to take the vector $\boldsymbol{q}$ parallel to the z-axis; on the other hand, the expression for $\mathcal{K}_{m\mu}$ reduces to one term only in the co-ordinate frame in which $\boldsymbol{p}$ is parallel to the z-axis. Since $\mathcal{K}_{m\mu}$ is not invariant we must, having found its form in the $\boldsymbol{p}$ z-frame, transform into the $\boldsymbol{q}$ z-frame, in which (14) may easily be calculated. For this reason, we shall investigate the transformation properties of $\mathcal{K}_{m\mu}$. Let us consider the following angular operator

$$\hat{\mathcal{K}}(jl_2jl\tfrac{1}{2}) = \sum_{m=-j}^{j} \sum_{\mu=-\frac{1}{2}}^{\frac{1}{2}} \mathcal{K}_{m\mu} |jm\rangle\langle\tfrac{1}{2}\mu| .$$

The only difference between (16) and (14) is that $|jm\rangle$ in (16) is a pure spin function corresponding to spin j, while $|jml\tfrac{1}{2}\rangle$ in (14) is a combination of a spherical harmonic $Y_{lm-\mu}(\boldsymbol{q})$ and a one-half spin function $\tfrac{1}{2}\mu'$. The operators

$$|jm\rangle\langle\tfrac{1}{2}\mu|$$

describe the conversion of the nucleon into a particle with spin j. Thus, the $\hat{\mathcal{K}}$-operator defined by (16) describes the elastic scattering on a fermion the spin of which changes from $\frac{1}{2}$ to j.

The method consists now in the following: from (15), we find the form of $\mathcal{K}_{m\mu}$ in the $\boldsymbol{p}$ z-frame and inserting it in (16) we obtain the explicit form of $\hat{\mathcal{K}}$. Since $\hat{\mathcal{K}}$ is invariant, it has the same form in the $\boldsymbol{q}$ z-system. The form of $\mathcal{K}_{m\mu}$ in this system may now be obtained by means of a trace operation on the product of $\hat{\mathcal{K}}$ with the spin transition operators $|jm\rangle\langle\tfrac{1}{2}\mu|$, written in the $\boldsymbol{q}\|z$-system:

$$\text{(17)} \qquad \begin{cases} \hat{\mathcal{K}} = \sum_{m\mu} \mathcal{K}_{m\mu}(z\|\boldsymbol{p})\, |jm(z\|\boldsymbol{p})\rangle\langle\tfrac{1}{2}\mu(z\|\boldsymbol{p})| , \\ \mathcal{K}_{m\mu}(z\|\boldsymbol{q}) = \operatorname{tr}\left(\hat{\mathcal{K}} \cdot |\tfrac{1}{2}\mu(z\|\boldsymbol{q})\rangle\langle jm(z\|\boldsymbol{q})|\right) , \end{cases}$$

where $|\tfrac{1}{2}\mu(z\|\boldsymbol{q})\rangle$ and $|jm(z\|\boldsymbol{q})\rangle$ are the spin functions in the $\boldsymbol{q}$ z-frame, for spin $\frac{1}{2}$ and j respectively. In order to write easily these transition operators in different co-ordinate frames it is convenient to express them as linear combinations of the spin-tensors of Racah, which, as it is known, provide a basis for the corresponding matrix algebra. Moreover, they have the advantage

that their transformation properties are known, so that they can easily be written in the desired co-ordinate frame. The spin-tensors are defined as follows:

$$T^{I\xi}(j,\tfrac{1}{2}) = \sum_{\mu=-\frac{1}{2}}^{\frac{1}{2}} (-1)^{\frac{1}{2}-\mu} C^{j\xi-\mu\,\frac{1}{2}\mu}_{I\xi}\, |j\,\xi-\mu\rangle\langle\tfrac{1}{2}\mu| \tag{18}$$

and transform according to the irreducible representation of weight $2I+1$ of the three-dimensional rotation group (in our case $I=j+\frac{1}{2}$ or $I=j-\frac{1}{2}$.

Let us perform this calculation for $j=\frac{1}{2}$ and $j=\frac{3}{2}$, for which values the Clebsch-Gordan coefficients are tabulated (see [3]). We obtain, for $j=\frac{1}{2}$

$$T^{00}(\tfrac{1}{2}\tfrac{1}{2}) = \frac{1}{\sqrt{2}}\begin{pmatrix}1 & 0\\ 0 & 1\end{pmatrix}; \qquad T^{1,\pm1}(\tfrac{1}{2}\tfrac{1}{2}) = \mp\frac{\sigma_x \pm i\sigma_y}{2}, \qquad T^{1,0}(\tfrac{1}{2}\tfrac{1}{2}) = \frac{1}{\sqrt{2}}\sigma_z, \tag{19a}$$

and for $j=\frac{3}{2}$

$$\left.\begin{aligned}
&T^{11} = -\frac{1}{2}\begin{pmatrix}\sqrt{3} & 0\\ 0 & 1\\ 0 & 0\\ 0 & 0\end{pmatrix}, \quad T^{10} = -\frac{1}{2}\begin{pmatrix}0 & 0\\ \sqrt{2} & 0\\ 0 & \sqrt{2}\\ 0 & 0\end{pmatrix}, \quad T^{1\,-1} = -\frac{1}{2}\begin{pmatrix}0 & 0\\ 0 & 0\\ 1 & 0\\ 0 & \sqrt{3}\end{pmatrix};\\
&T^{22} = \begin{pmatrix}0 & 1\\ 0 & 0\\ 0 & 0\\ 0 & 0\end{pmatrix}, \quad T^{21} = -\frac{1}{2}\begin{pmatrix}1 & 0\\ 0 & -\sqrt{3}\\ 0 & 0\\ 0 & 0\end{pmatrix}, \quad T^{20} = -\frac{1}{2}\begin{pmatrix}0 & 0\\ \sqrt{2} & 0\\ 0 & -\sqrt{2}\\ 0 & 0\end{pmatrix},\\
&T^{21} = -\frac{1}{2}\begin{pmatrix}0 & 0\\ 0 & 0\\ \sqrt{3} & 0\\ 0 & -1\end{pmatrix}, \quad T^{2\,-2} = -\begin{pmatrix}0 & 0\\ 0 & 0\\ 0 & 0\\ 1 & 0\end{pmatrix}.
\end{aligned}\right\} \tag{19b}$$

In order to be able to write them in different co-ordinate frames, it is convenient to make use of the carthesian components T_i, T_{ik}, rather than the

---

[3] E. U. Condon and G. H. Shortley: *The Theory of Atomic Spectra* (London, 1935).

circularly polarized ones. They are connected by the following relations:

$$T^{1,\pm 1} = \mp \frac{T_x \pm iT_y}{\sqrt{2}}, \qquad T^{1,0} = T_z, \tag{20a}$$

$$\begin{cases} T^{2,\pm 2} = \dfrac{1}{2}(T_{xx} - T_{yy}) \pm iT_{xy}, \\ T^{2,\pm 1} = \mp (T_{xz} \pm iT_{yz}), \\ T^{2,0} = \dfrac{1}{\sqrt{6}}(2T_{zz} - T_{xx} - T_{yy}); \end{cases} \tag{20b}$$

(see Appendix). Now, if we use the relation inverse to (18) we can express, with the help of (20), the spin transition operators $|jm\rangle\langle \frac{1}{2}\mu|$ in their tensorial form. We obtain (omitting the labels j and $\frac{1}{2}$)

for $j = \frac{1}{2}$

$$\begin{cases} |\pm\tfrac{1}{2}\rangle\langle\pm\tfrac{1}{2}| = \dfrac{1}{\sqrt{2}}(T^{00} \pm T_z), \\ |\pm\tfrac{1}{2}\rangle\langle\mp\tfrac{1}{2}| = \dfrac{1}{\sqrt{2}}(T_x \pm iT_y). \end{cases} \tag{21a}$$

and for $j = \frac{3}{2}$

$$\begin{cases} |\pm\tfrac{3}{2}\rangle\langle\pm\tfrac{1}{2}| = \tfrac{1}{2}(T_{xz} \pm iT_{yz}) \pm \tfrac{1}{2}\sqrt{\tfrac{3}{2}}(T_x \pm iT_y), \\ |\pm\tfrac{1}{2}\rangle\langle\pm\tfrac{1}{2}| = \mp \dfrac{1}{2\sqrt{3}}(2T_{zz} - T_{xx} - T_{yy}) - \dfrac{1}{\sqrt{2}}T_z, \\ |\mp\tfrac{1}{2}\rangle\langle\pm\tfrac{1}{2}| = -\dfrac{\sqrt{3}}{2}(T_{xz} \mp iT_{yz}) \mp \dfrac{1}{2\sqrt{2}}(T_x \mp iT_y), \\ |\mp\tfrac{3}{2}\rangle\langle\pm\tfrac{1}{2}| = \mp\tfrac{1}{2}(T_{xx} - T_{yy}) + iT_{xy}. \end{cases} \tag{21b}$$

Now, we must compute $\mathcal{K}_{m\mu}$ both for $j = \frac{3}{2}$ and $j = \frac{1}{2}$. For $j = \frac{3}{2}$, there are eight possibilities of combining l_2 with j and l with $\sigma = \frac{1}{2}$, namely:

$$J = l_2 + \tfrac{3}{2} = l \pm \tfrac{1}{2},$$

$$J = l_2 + \tfrac{1}{2} = l \pm \tfrac{1}{2},$$

$$J = l_2 - \tfrac{1}{2} = l \pm \tfrac{1}{2},$$

$$J = l_2 - \tfrac{3}{2} = l \pm \tfrac{1}{2}.$$

For $j=\frac{1}{2}$, there are the following four possibilities:

$$J = l_2 + \tfrac{1}{2} = l \pm \tfrac{1}{2} ,$$

$$J = l_2 - \tfrac{1}{2} = l \pm \tfrac{1}{2} .$$

Let us perform the calculations for an example, say $J=l_2+\frac{3}{2}=l+\frac{1}{2}$, *i.e.* $l=l_2+1$. In the co-ordinate frame in which $z\|\boldsymbol{p}$ and the x-axis is chosen in the plane of the vectors $\boldsymbol{p}$, $\boldsymbol{r}$, we have, using the Clebsch-Gordan coefficients:

$$\mathcal{K}_{\frac{3}{2}\frac{1}{2}} = \frac{1}{4\pi}\sqrt{\frac{l_2(l_2+1)(l_2+2)}{2(l_2+1)(2l_2+2)(2l_2+3)}}\sqrt{\frac{l+1}{2l+1}}\,Y_{l_2,-1}(\boldsymbol{r})\sqrt{2l+1} =$$

$$= \frac{1}{4\pi}\frac{l_2+2}{\sqrt{(2l_2+2)(2l_2+3)}}\,r_-\,\mathcal{P}'_{l_2}(\boldsymbol{p}\cdot\boldsymbol{r})$$

This expression is to be multiplied by

$$\frac{1}{2}(T_{xz}+iT_{yz})+\frac{1}{2}\sqrt{\frac{3}{2}}(T_x+iT_y) .$$

Since, however,

$$\mathcal{K}_{\cdot\frac{3}{2}-\frac{1}{2}} = -\frac{1}{4\pi}\frac{l_2+2}{\sqrt{(2l_2+2)(2l_2+3)}}\,r_+\,\mathcal{P}'_{l_2}(\boldsymbol{p}\cdot\boldsymbol{r})$$

is to be multiplied by $\frac{1}{2}(T_{xz}-iT_{yz})-\frac{1}{2}\sqrt{\frac{3}{2}}(T_x-iT_y)$ and since $r_-=r_+=r_x$ in our system, the sum of these two terms gives

$$\frac{1}{4\pi}\frac{l_2+2}{\sqrt{2(l_2+2)(2l_2+3)}}\,\mathcal{P}'_{l_2}(\boldsymbol{p}\cdot\boldsymbol{r})\,r_x\frac{1}{2}\left(iT_{yz}+\sqrt{\frac{3}{2}}T_x\right).$$

This expression can be written in the following invariant form

$$\frac{1}{4\pi}\frac{l_2+2}{\sqrt{(2l_2+2)(2l_2+3)}}\,\mathcal{P}'_{l_2}(\boldsymbol{p}\cdot\boldsymbol{r})\frac{1}{2}\left(\sqrt{\frac{3}{2}}\boldsymbol{P}_x\cdot\boldsymbol{T}+i\boldsymbol{P}_y\cdot\overleftrightarrow{\boldsymbol{T}}\cdot\boldsymbol{p}\right).$$

In a similar way, terms containing $\mathcal{K}_{\pm\frac{3}{2},-\frac{1}{2}}$, $\mathcal{K}_{\pm\frac{1}{2},\pm\frac{1}{2}}$, $\mathcal{K}_{\pm\frac{1}{2},\mp\frac{1}{2}}$ are calculated. Sum-

ming all these contributions, one obtains the following expression for $\hat{\mathcal{R}}$:

$$\hat{\mathcal{R}} = \frac{1/(4\pi)}{\sqrt{(2l_2+2)(2l_2+3)}} \{-\sqrt{6}\,(l_2+2)(l_2+1)\boldsymbol{p}\cdot\boldsymbol{T}\,\mathcal{P}_{l_2}(\boldsymbol{p}\cdot\boldsymbol{r}) + \\ + (l_2+2)(\sqrt{6}\,\boldsymbol{P}_r\cdot\boldsymbol{T} - 2i\boldsymbol{P}_u\cdot\overleftrightarrow{\boldsymbol{T}}\cdot\boldsymbol{p})\,\mathcal{P}'_{l_2}(\boldsymbol{p}\cdot\boldsymbol{r}) + 2i\boldsymbol{P}_y\cdot\overleftrightarrow{\boldsymbol{T}}\cdot\boldsymbol{P}_x\mathcal{P}''_{l_2}(\boldsymbol{p}\cdot\boldsymbol{r})\}.$$

Similar expressions were obtained also for the other seven cases of $j=\frac{3}{2}$.

By the same method, also the $\hat{\mathcal{R}}$-operators for $j=\frac{1}{2}$ were obtained.

To find the $\hat{\mathcal{F}}$-operators, we make use of (17). It is easy to see that the orbital operators $\mathcal{L}_{\mu'\mu}$ may be written as follows

$$\mathcal{L}_{\mu'\mu} = \frac{1}{(4\pi)^{\frac{3}{2}}}\, C^{l_1 0 \frac{1}{2}\mu'}_{j\mu'}\sqrt{2l_1+1}\ \mathrm{tr}\,(\hat{\mathcal{R}}\,|\tfrac{1}{2}\mu\rangle\langle j\mu'|).$$

The trace operations can quickly be performed using the formulae

$$\mathrm{tr}\,(T_i^+ T_j) = \delta_{ij}\,,$$

$$\mathrm{tr}\,(T_{ij}^+ T_{kl}) = \tfrac{1}{2}(\delta_{ik}\delta_{jl}+\delta_{il}\delta_{jk})\,,$$

$$\mathrm{tr}\,(T_{ij}^+ T_k) = 0\,.$$

These relations have only a restricted domain of validity, but for our purpose one can use them without supplementary precautions (see Appendix).

For instance, for $j=\frac{3}{2}$ $(l_1=1)$, $J=l_2+\frac{3}{2}=l+\frac{1}{2}$ we obtain the following result, if we are working in the $\boldsymbol{q}\|z$-frame (*):

$$\mathcal{L}_{\frac{1}{2}\frac{1}{2}} = \frac{1}{(4\pi)^{\frac{3}{2}}}\frac{\sqrt{6}}{\sqrt{(2l_2+2)(2l_2+3)}}\{(l_2+1)(l_2+2)\boldsymbol{p}\cdot\boldsymbol{q}\,\mathcal{P}_{l_2} + \\ + (l_2+2)(i\boldsymbol{p}\cdot\boldsymbol{q}\,\boldsymbol{P}_y\cdot\boldsymbol{q} - \boldsymbol{P}_x\cdot\boldsymbol{q})\,\mathcal{P}'_{l_2} - i\boldsymbol{q}\cdot\boldsymbol{P}_y\,\boldsymbol{q}\cdot\boldsymbol{P}_x\mathcal{P}''_{l_2}\}.$$

The other orbital operators have a similar form or are somewhat more complicated. By multiplying $\mathcal{L}_{\mu'\mu}$ with $|\frac{1}{2}\mu'\rangle\langle\frac{1}{2}\mu|$ and summing over μ' and μ, we obtain the corresponding angular operator. The resulting angular operators are tabulated in Table I and Table III.

(*) The result is dependent on the co-ordinate frame.

All practical calculations of Section **3** and Section **4** were checked. Moreover, the normalization and orthogonality of each angular operator was verified by direct integration.

5. – Conclusion.

We must mention that the calculation of the angular operators is only the first step in investigating the S-matrix of a given process. To do the second one means to perform the same analysis in the isotopic space. The method of obtaining the corresponding « isotopic angular operators » is quite analogous, the only difference being that if one or more photons are present, the S-matrix is no more a scalar but rather a sum of a scalar and the third component of a vector. This means that instead of each angular operator in the ordinary space, there are one scalar and three vectorial operators in the isotopic space. So, the number of operators is greater, but the calculations are not more complicated because the whole procedure is quite automatical.

The third step consists in constructing the theory of interaction. This problem must be solved by other means than the first two, for instance, with the help of dispersion relations or of the Chew-Low equation. However, it should be mentioned that for the complete analysis of the reaction the first two steps are necessary, because only after having done them, one can compare the theory with the experiment. Indeed, if the angular analysis gives the explicit form of the angular operator $\hat{\mathcal{F}}(J, (f), (i))$ and the form of the S-matrix is obtained by use of the interaction theory, the experimentally observable coefficient $a(J(f)(i))$ is defined by the theoretical formula

$$a(J, (f), (i)) = \mathrm{tr} \int \hat{\mathcal{F}}^{+}(J, (f), (i))\, S\,,$$

where $\mathrm{tr}\int$ means integration over all continuous and sum over all discrete variables. In the isotopic space, the situation is quite analogous.

* * *

We would like to express our gratitude to Professor Ning Hu, Professor S. Titeica and Professor Ya. A. Smorodinsky for many illuminating discussions. We thank also Mr. V. G. Efimov for helpful conversation during this work.

Tables of the angular operators.

These Tables contain angular operators for processes of the type $b+N \to N+b_1+b_2$ (where b_1, b_2 and b are zero-spin bosons without definite parity) for $l_1=0$, 1 and l, l_2 being arbitrarily large. l, l_1 and l_2 are orbital quantum numbers of b, b_1 and b_2 respectively. L is the intermediate quantum number in the case of boson-boson coupling in the final state, ($\hat{\boldsymbol{L}}=\hat{\boldsymbol{l}}_1+\hat{\boldsymbol{l}}_2$), j is the intermediate quantum number in the case of boson-nucleon coupling in the final state, ($\hat{\boldsymbol{j}}=\hat{\boldsymbol{l}}_1+\hat{\boldsymbol{\sigma}}'$). $\boldsymbol{p}$, $\boldsymbol{q}$, $\boldsymbol{r}$ are unit vectors in the directions of the momenta of b, b_1, b_2 respectively. For practical reasons, we make use of an orthogonal set of (not normalized) vectors $\boldsymbol{P}_x=\boldsymbol{r}-\boldsymbol{p}\,\boldsymbol{p}\cdot\boldsymbol{r}$, $\boldsymbol{P}_y=[\boldsymbol{p}\boldsymbol{r}]$, $\boldsymbol{p}$.

$\mathcal{P}_{l_1}$ denotes the Legendre function depending on $\boldsymbol{p}\cdot\boldsymbol{r}=\cos\theta$; $\mathcal{P}'_{l_2}$ and $\mathcal{P}''_{l_2}$ are derivatives with respect to $(\boldsymbol{p}\cdot\boldsymbol{r})$.

If one of the bosons is a vectorial particle, the corresponding angular operators can be derived from ours by means of the following operations:

$$\frac{1}{\sqrt{l_k(l_k+1)}}\frac{\partial}{\partial\boldsymbol{k}} \qquad \text{for the electric multipole,}$$

$$\frac{-i}{\sqrt{l_k(l_k+1)}}\left[\boldsymbol{k}\frac{\partial}{\partial\boldsymbol{k}}\right] \qquad \text{for the magnetic multipole,}$$

$$\boldsymbol{k} \qquad \text{for the longitudinal multipole.}$$

Here $\boldsymbol{k}$ is the unitary momentum of the corresponding boson.

TABLE I.

$$\begin{cases} J=L+\frac{1}{2}=l+\frac{1}{2} & l_1=0 \quad L=l_2 \quad l=l_2 \\ J=l_2+\frac{1}{2}=l+\frac{1}{2} & l_1=0 \quad j=\frac{1}{2} \quad l=l_2 \end{cases}$$

$$\hat{\mathcal{F}}=(4\pi)^{-\frac{3}{2}}\{(l_2+1)\mathcal{P}_{l_2}+i\boldsymbol{\sigma}\cdot\boldsymbol{P}_y\mathcal{P}'_{l_2}\}$$

$$\begin{cases} J=L+\frac{1}{2}=l-\frac{1}{2} & l_1=0 \quad L=l_2 \quad l=l_2+1 \\ J=l_2+\frac{1}{2}=l-\frac{1}{2} & l_1=0 \quad j=\frac{1}{2} \quad l=l_2+1 \end{cases}$$

$$\hat{\mathcal{F}}=(4\pi)^{-\frac{3}{2}}\{-(l_2+1)\boldsymbol{\sigma}\cdot\boldsymbol{p}\mathcal{P}_{l_2}+\boldsymbol{\sigma}\cdot\boldsymbol{P}_x\mathcal{P}'_{l_2}\}$$

$$\begin{cases} J=L-\frac{1}{2}=l+\frac{1}{2} & l_1=0 \quad L=l_2 \quad l=l_2-1 \\ J=l_2-\frac{1}{2}=l+\frac{1}{2} & l_1=0 \quad j=\frac{1}{2} \quad l=l_2-1 \end{cases}$$

$$\hat{\mathcal{F}}=(4\pi)^{-\frac{3}{2}}\{-l_2\boldsymbol{\sigma}\cdot\boldsymbol{p}\mathcal{P}_{l_2}-\boldsymbol{\sigma}\cdot\boldsymbol{P}_x\mathcal{P}'_{l_2}\}$$

$$\begin{cases} J=L-\frac{1}{2}=l-\frac{1}{2} & l_1=0 \quad L=l_2 \quad l=l_2 \\ J=l_2-\frac{1}{2}=l-\frac{1}{2} & l_1=0 \quad j=\frac{1}{2} \quad l=l_2 \end{cases}$$

$$\hat{\mathcal{F}}=(4\pi)^{-\frac{3}{2}}\{l_2\mathcal{P}_{l_2}-i\boldsymbol{\sigma}\cdot\boldsymbol{P}_y\mathcal{P}'_{l_2}\}$$

TABLE II.

$J = L + \frac{1}{2} = l + \frac{1}{2} \quad l_1 = 1 \quad L = l_2 + 1 \quad l = l_2 + 1$

$$\hat{\mathcal{F}} = (4\pi)^{-\frac{3}{2}} \frac{\sqrt{3}}{\sqrt{(l_2+1)(2l_2+3)}} \{(l_2+1)((l_2+2)\boldsymbol{p}\cdot\boldsymbol{q} + i\boldsymbol{\sigma}\cdot[\boldsymbol{pq}])\,\mathcal{P}_{l_2} -$$
$$-((l_2+2)(\boldsymbol{P}_x\cdot\boldsymbol{q} - i\boldsymbol{\sigma}\cdot\boldsymbol{P}_y\boldsymbol{p}\cdot\boldsymbol{q}) - i\boldsymbol{\sigma}\cdot[\boldsymbol{pq}]\boldsymbol{p}\cdot\boldsymbol{r})\,\mathcal{P}'_{l_2} - i\boldsymbol{\sigma}\cdot\boldsymbol{P}_y\boldsymbol{P}_x\cdot\boldsymbol{q}\,\mathcal{P}''_{l_2}\}$$

$J = L + \frac{1}{2} = l - \frac{1}{2} \quad l_1 = 1 \quad L = l_2 + 1 \quad l = l_2 + 2$

$$\hat{\mathcal{F}} = (4\pi)^{-\frac{3}{2}} \frac{\sqrt{3}}{\sqrt{(l_2+1)(2l_2+3)}} \{-(l_2+1)((l_2+3)\boldsymbol{\sigma}\cdot\boldsymbol{p}\boldsymbol{p}\cdot\boldsymbol{q} - \boldsymbol{\sigma}\cdot\boldsymbol{q})\,\mathcal{P}_{l_2} +$$
$$+((l_2+2)(\boldsymbol{\sigma}\cdot\boldsymbol{p}\boldsymbol{P}_x\cdot\boldsymbol{q} + \boldsymbol{\sigma}\cdot\boldsymbol{P}_x\boldsymbol{p}\cdot\boldsymbol{q}) + (\boldsymbol{\sigma}\cdot\boldsymbol{q} - \boldsymbol{\sigma}\cdot\boldsymbol{p}\boldsymbol{p}\cdot\boldsymbol{q})\boldsymbol{p}\cdot\boldsymbol{r})\,\mathcal{P}'_{l_2} - \boldsymbol{\sigma}\cdot\boldsymbol{P}_y\boldsymbol{P}_x\cdot\boldsymbol{q}\,\mathcal{P}''_{l_2}\}$$

$J = L - \frac{1}{2} = l + \frac{1}{2} \quad l_2 = 1 \quad L = l_2 + 1 \quad l = l_2$

$$\hat{\mathcal{F}} = (4\pi)^{-\frac{3}{2}} \frac{\sqrt{3}}{\sqrt{(l_2+1)(2l_2+3)}} \{-(l_2+1)(l_2\boldsymbol{\sigma}\cdot\boldsymbol{p}\boldsymbol{p}\cdot\boldsymbol{q} + \boldsymbol{\sigma}\cdot\boldsymbol{q})\,\mathcal{P}_{l_2} +$$
$$+((l_2+1)\boldsymbol{\sigma}\cdot\boldsymbol{p}\boldsymbol{P}_x\cdot\boldsymbol{q} - (l_2+2)\boldsymbol{\sigma}\cdot\boldsymbol{P}_x\boldsymbol{p}\cdot\boldsymbol{q} - (\boldsymbol{\sigma}\cdot\boldsymbol{q} - \boldsymbol{\sigma}\cdot\boldsymbol{p}\boldsymbol{p}\cdot\boldsymbol{q})\boldsymbol{p}\cdot\boldsymbol{r})\mathcal{P}'_{l_2} + \boldsymbol{\sigma}\cdot\boldsymbol{P}_y\boldsymbol{P}_x\cdot\boldsymbol{q}\mathcal{P}''_{l_2}\}$$

$J = L - \frac{1}{2} = l - \frac{1}{2} \quad l_1 = 1 \quad L = l_2 + 1 \quad l = l_2 + 1$

$$\hat{\mathcal{F}} = (4\pi)^{-\frac{3}{2}} \frac{\sqrt{3}}{\sqrt{(l_2+1)(2l_2+3)}} \{(l_2+1)((l_2+1)\boldsymbol{p}\cdot\boldsymbol{q} - i\boldsymbol{\sigma}\cdot[\boldsymbol{pq}])\,\mathcal{P}_{l_2} -$$
$$-((l_2+1)\boldsymbol{P}_x\cdot\boldsymbol{q} + i(l_2+2)\boldsymbol{\sigma}\cdot\boldsymbol{P}_y\boldsymbol{p}\cdot\boldsymbol{q} + i\boldsymbol{\sigma}\cdot[\boldsymbol{pq}]\boldsymbol{p}\cdot\boldsymbol{r})\,\mathcal{P}'_{l_2} + i\boldsymbol{\sigma}\cdot\boldsymbol{P}_y\boldsymbol{P}_x\cdot\boldsymbol{q}\,\mathcal{P}''_{l_2}\}$$

$J = L + \frac{1}{2} = l + \frac{1}{2} \quad l_1 = 1 \quad L = l_2 \quad l = l_2$

$$\hat{\mathcal{F}} = (4\pi)^{-\frac{3}{2}} \frac{\sqrt{3}}{\sqrt{l_2(l_2+1)}} \{(i(l_2+1)\,\boldsymbol{P}_y\cdot\boldsymbol{q} - \boldsymbol{\sigma}\cdot\boldsymbol{r}\boldsymbol{p}\cdot\boldsymbol{q} + \boldsymbol{\sigma}\cdot\boldsymbol{q}\boldsymbol{p}\cdot\boldsymbol{r})\,\mathcal{P}'_{l_2} - \boldsymbol{\sigma}\cdot\boldsymbol{P}_y\boldsymbol{P}_y\cdot\boldsymbol{q}\,\mathcal{P}''_{l_2}\}$$

$J = L + \frac{1}{2} = l - \frac{1}{2} \quad l_1 = 1 \quad L = l_2 \quad l = l_2 + 1$

$$\hat{\mathcal{F}} = (4\pi)^{-\frac{3}{2}} \frac{-i\sqrt{3}}{\sqrt{l_2(l_2+1)}} \{((l_2+2)\boldsymbol{\sigma}\cdot\boldsymbol{p}\,\boldsymbol{P}_y\cdot\boldsymbol{q} + \boldsymbol{\sigma}\cdot[\boldsymbol{qr}])\,\mathcal{P}'_{l_2} - \boldsymbol{\sigma}\cdot\boldsymbol{P}_x\boldsymbol{P}_y\cdot\boldsymbol{q}\,\mathcal{P}''_{l_2}\}$$

TABLE II (*continued*).

$J = L - \frac{1}{2} = l + \frac{1}{2} \quad l_1 = 1 \quad L = l_2 \quad l = l_2 - 1$

$$\hat{\mathcal{F}} \quad (4\pi)^{-\frac{3}{2}} \frac{-i\sqrt{3}}{\sqrt{l_2(l_2+1)}} \{(l_2 \quad 1)\boldsymbol{\sigma}\cdot\boldsymbol{p}\boldsymbol{P}_r\cdot\boldsymbol{q} \quad \boldsymbol{\sigma}\cdot[\boldsymbol{q}\boldsymbol{r}])\mathcal{P}'_{l_2} + \boldsymbol{\sigma}\cdot\boldsymbol{P}_r\boldsymbol{P}_s\cdot\boldsymbol{q}\mathcal{P}_{l_2}\}$$

$J = L - \frac{1}{2} = l - \frac{1}{2} \quad l_1 = 1 \quad L = l_2 \quad l = l_2$

$$\hat{\mathcal{F}} \quad (4\pi)^{-\frac{3}{2}} \frac{\sqrt{3}}{\sqrt{l_2(l_2+1)}} \{(il_2\boldsymbol{P}_r\cdot\boldsymbol{q} + \boldsymbol{\sigma}\cdot\boldsymbol{r}\boldsymbol{p}\cdot\boldsymbol{q} \quad \boldsymbol{\sigma}\cdot\boldsymbol{q}\boldsymbol{p}\cdot\boldsymbol{r})\mathcal{P}'_{l_2} + \boldsymbol{\sigma}\cdot\boldsymbol{P}_q\boldsymbol{P}_s\cdot\boldsymbol{q}\mathcal{P}'_{l_2}\}$$

$J \quad L + \frac{1}{2} = l \quad \frac{1}{2} \quad l_1 \quad 1 \quad L = l_2 - 1 \quad l \quad l_2 \quad 1$

$$\hat{\mathcal{F}} \quad (4\pi)^{-\frac{3}{2}} \frac{\sqrt{3}}{\sqrt{l_2(2l_2-1)}} \{-l_2(l_2\boldsymbol{p}\cdot\boldsymbol{q} + i\boldsymbol{\sigma}\cdot[\boldsymbol{p}\boldsymbol{q}])\mathcal{P}_{l_2} -$$
$$(l_2\boldsymbol{P}_r\cdot\boldsymbol{q} + i(l_2 \quad 1)\boldsymbol{\sigma}\cdot\boldsymbol{P}_r\boldsymbol{p}\cdot\boldsymbol{q} \quad i\boldsymbol{\sigma}\cdot[\boldsymbol{p}\boldsymbol{q}|\boldsymbol{p}\cdot\boldsymbol{r})\mathcal{P}'_{l_2} \quad i\boldsymbol{\sigma}\cdot\boldsymbol{P}_q\boldsymbol{P}_r\cdot\boldsymbol{q}\mathcal{P}_{l_2}\}$$

$J = L + \frac{1}{2} = l - \frac{1}{2} \quad l_1 = 1 \quad L = l_2 - 1 \quad l = l_2$

$$\hat{\mathcal{F}} = (4\pi)^{-\frac{3}{2}} \frac{\sqrt{3}}{\sqrt{l_2(2l_2-1)}} \{l_2((l_2+1)\boldsymbol{\sigma}\cdot\boldsymbol{p}\boldsymbol{p}\cdot\boldsymbol{q} - \boldsymbol{\sigma}\cdot\boldsymbol{q})\mathcal{P}_{l_2} +$$
$$(l_2\boldsymbol{\sigma}\cdot\boldsymbol{p}\boldsymbol{P}_r\cdot\boldsymbol{q} \quad (l_2 \quad 1)\boldsymbol{\sigma}\cdot\boldsymbol{P}_r\boldsymbol{p}\cdot\boldsymbol{q} + (\boldsymbol{\sigma}\cdot\boldsymbol{q} \quad \boldsymbol{\sigma}\cdot\boldsymbol{p}\boldsymbol{p}\cdot\boldsymbol{q})\boldsymbol{p}\cdot\boldsymbol{r})\mathcal{P}'_{l_2} \quad \boldsymbol{\sigma}\cdot\boldsymbol{P}_r\boldsymbol{P}_s\cdot\boldsymbol{q}\mathcal{P}''_{l_2}\}$$

$J = L - \frac{1}{2} = l + \frac{1}{2} \quad l_1 = 1 \quad L = l_2 - 1 \quad l_2 = l_2 - 2$

$$\hat{\mathcal{F}} = (4\pi)^{-\frac{3}{2}} \frac{\sqrt{3}}{\sqrt{l_2(2l_2-1)}} \{l_2((l_2-2)\boldsymbol{\sigma}\cdot\boldsymbol{p}\boldsymbol{p}\cdot\boldsymbol{q} + \boldsymbol{\sigma}\cdot\boldsymbol{q})\mathcal{P}_{l_2} +$$
$$(l_2 \quad 1)(\boldsymbol{\sigma}\cdot\boldsymbol{p}\boldsymbol{P}_r\cdot\boldsymbol{q} + \boldsymbol{\sigma}\cdot\boldsymbol{P}_r\boldsymbol{p}\cdot\boldsymbol{q}) \quad (\boldsymbol{\sigma}\cdot\boldsymbol{q} \quad \boldsymbol{\sigma}\cdot\boldsymbol{p}\boldsymbol{p}\cdot\boldsymbol{q})\boldsymbol{p}\cdot\boldsymbol{r})\mathcal{P}'_{l_2} + \boldsymbol{\sigma}\cdot\boldsymbol{P}_r\boldsymbol{P}_s\cdot\boldsymbol{q}\mathcal{P}''_{l_2}\}$$

$J = L - \frac{1}{2} = l - \frac{1}{2} \quad l_1 = 1 \quad L = l_2 - 1 \quad l = l_2 - 1$

$$\hat{\mathcal{F}} = (4\pi)^{-\frac{3}{2}} \frac{\sqrt{3}}{\sqrt{l_2(2l_2-1)}} \{-l_2((l_2-1)\boldsymbol{p}\cdot\boldsymbol{q} - i\boldsymbol{\sigma}\cdot[\boldsymbol{p}\boldsymbol{q}])\mathcal{P}_{l_2} -$$
$$((l_2 \quad 1)(\boldsymbol{P}_r\cdot\boldsymbol{q} \quad i\boldsymbol{\sigma}\cdot\boldsymbol{P}_r\boldsymbol{p}\cdot\boldsymbol{q}) + i\boldsymbol{\sigma}\cdot[\boldsymbol{p}\boldsymbol{q}|\boldsymbol{p}\cdot\boldsymbol{r})\mathcal{P}'_{l_2} + i\boldsymbol{\sigma}\cdot\boldsymbol{P}_q\boldsymbol{P}_r\cdot\boldsymbol{q}\mathcal{P}''_{l_2}\}$$

TABLE III.

$$J = l_2 + \tfrac{1}{2} = l + \tfrac{1}{2} \qquad l_1 = 1 \qquad j = \tfrac{1}{2} \qquad l = l_2$$

$$\hat{\mathcal{F}} = -(4\pi)^{-\frac{3}{2}}\{(l_2+1)\boldsymbol{\sigma}\cdot\boldsymbol{q}\,\mathcal{P}_{l_2} + i(\boldsymbol{P}_y\cdot\boldsymbol{q} - i\boldsymbol{\sigma}\cdot[\boldsymbol{P}_y\boldsymbol{q}])\,\mathcal{P}'_{l_2}\}$$

$$J = l_2 + \tfrac{1}{2} = l - \tfrac{1}{2} \qquad l_1 = 1 \qquad j = \tfrac{1}{2} \qquad l = l_2 + 1$$

$$\hat{\mathcal{F}} = (4\pi)^{-\frac{3}{2}}\{(l_2+1)(\boldsymbol{p}\cdot\boldsymbol{q} - i\boldsymbol{\sigma}\cdot[\boldsymbol{p}\boldsymbol{q}])\,\mathcal{P}_{l_2} - (\boldsymbol{P}_x\cdot\boldsymbol{q} - i\boldsymbol{\sigma}\cdot[\boldsymbol{P}_x\boldsymbol{q}])\,\mathcal{P}'_{l_2}\}$$

$$J = l_2 - \tfrac{1}{2} = l + \tfrac{1}{2} \qquad l_1 = 1 \qquad j = \tfrac{1}{2} \qquad l = l_2 - 1$$

$$\hat{\mathcal{F}} = (4\pi)^{-\frac{3}{2}}\{l_2(\boldsymbol{p}\cdot\boldsymbol{q} - i\boldsymbol{\sigma}\cdot[\boldsymbol{p}\boldsymbol{q}])\,\mathcal{P}_{l_2} + (\boldsymbol{P}_x\cdot\boldsymbol{q} - i\boldsymbol{\sigma}\cdot[\boldsymbol{P}_x\boldsymbol{q}])\,\mathcal{P}'_{l_2}\}$$

$$J = l_2 - \tfrac{1}{2} = l - \tfrac{1}{2} \qquad l_1 = 1 \qquad j = \tfrac{1}{2} \qquad l = l_2$$

$$\hat{\mathcal{F}} = (4\pi)^{-\frac{3}{2}}\{-l_2\boldsymbol{\sigma}\cdot\boldsymbol{q}\,\mathcal{P}_{l_2} + i(\boldsymbol{P}_y\boldsymbol{q} - i\boldsymbol{\sigma}\cdot[\boldsymbol{P}_y\boldsymbol{q}])\,\mathcal{P}'_{l_2}\}$$

$$J = l_2 + \tfrac{3}{2} = l + \tfrac{1}{2} \qquad l_1 = 1 \qquad j = \tfrac{3}{2} \qquad l_2 = l_2 + 1$$

$$\hat{\mathcal{F}} = (4\pi)^{-\frac{3}{2}}\frac{\sqrt{3}}{2\sqrt{(l_2+1)(2l_2+3)}}\{(l_2+2)(l_2+1)(2\boldsymbol{p}\cdot\boldsymbol{q} + i\boldsymbol{\sigma}\cdot[\boldsymbol{p}\boldsymbol{q}])\,\mathcal{P}_{l_2} +$$
$$+ (l_2+2)(i(\boldsymbol{\sigma}\cdot\boldsymbol{P}_y\ \ \boldsymbol{p}\cdot\boldsymbol{q} + \boldsymbol{\sigma}\cdot\boldsymbol{p}\,\boldsymbol{P}_y\cdot\boldsymbol{q}) - (2\boldsymbol{P}_x\cdot\boldsymbol{q} + i\boldsymbol{\sigma}\cdot[\boldsymbol{P}_x\boldsymbol{q}]))\,\mathcal{P}'_{l_2} -$$
$$- i(\boldsymbol{\sigma}\cdot\boldsymbol{P}_x\boldsymbol{P}_y\cdot\boldsymbol{q} + \boldsymbol{\sigma}\cdot\boldsymbol{P}_y\boldsymbol{P}_x\cdot\boldsymbol{q})\,\mathcal{P}''_{l_2}\}$$

$$J = l_2 + \tfrac{3}{2} = l - \tfrac{1}{2} \qquad l_1 = 1 \qquad j = \tfrac{3}{2} \qquad l = l_2 + 2$$

$$\hat{\mathcal{F}} = (4\pi)^{-\frac{3}{2}}\frac{\sqrt{3}}{2\sqrt{(l_2+1)(2l_2+3)}}\{-(l_2+2)(l_2+1)(3\boldsymbol{\sigma}\cdot\boldsymbol{p}\,\boldsymbol{p}\cdot\boldsymbol{q} - \boldsymbol{\sigma}\cdot\boldsymbol{q})\,\mathcal{P}_{l_2} +$$
$$+ 2(l_2+2)(\boldsymbol{\sigma}\cdot\boldsymbol{P}_x\boldsymbol{p}\cdot\boldsymbol{q} + \boldsymbol{\sigma}\cdot\boldsymbol{p}\,\boldsymbol{P}_x\cdot\boldsymbol{q})\,\mathcal{P}'_{l_2} \quad (\boldsymbol{\sigma}\cdot\boldsymbol{P}_x\boldsymbol{P}_x\cdot\boldsymbol{q} \quad \boldsymbol{\sigma}\cdot\boldsymbol{P}_y\boldsymbol{P}_y\cdot\boldsymbol{q})\,\mathcal{P}''_{l_2}\}$$

$$J = l_2 + \tfrac{1}{2} = l + \tfrac{1}{2} \qquad l_1 = 1 \qquad j = \tfrac{3}{2} \qquad l = l_2$$

$$\hat{\mathcal{F}} = (4\pi)^{-\frac{3}{2}}\frac{1}{2\sqrt{l_2(2l_2+3)}}\{-l_2(l_2+1)(3\boldsymbol{\sigma}\cdot\boldsymbol{p}\,\boldsymbol{p}\cdot\boldsymbol{q} - \boldsymbol{\sigma}\cdot\boldsymbol{q})\,\mathcal{P}_{l_2}$$
$$(3(\boldsymbol{\sigma}\cdot\boldsymbol{P}_x\,\boldsymbol{p}\cdot\boldsymbol{q} + \boldsymbol{\sigma}\cdot\boldsymbol{p}\boldsymbol{P}_x\cdot\boldsymbol{q}) - i(2l_2+3)(2\boldsymbol{P}_y\cdot\boldsymbol{q} - i\boldsymbol{\sigma}\cdot[\boldsymbol{P}_y\boldsymbol{q}]))\,\mathcal{P}'_{l_2} -$$
$$+ 3(\boldsymbol{\sigma}\cdot\boldsymbol{P}_x\boldsymbol{P}_x\cdot\boldsymbol{q} - \boldsymbol{\sigma}\cdot\boldsymbol{P}_y\boldsymbol{P}_y\cdot\boldsymbol{q})\,\mathcal{P}''_{l_2}\}$$

TABLE III (*continued*).

$$J = l_2 + \tfrac{1}{2} = l - \tfrac{3}{2} \qquad l_1 = 1 \qquad j = \tfrac{3}{2} \qquad l = l_2 + 1$$

$$\hat{\mathcal{F}} = (4\pi)^{-\frac{3}{2}} \frac{1}{2\sqrt{l_2(2l_2+3)}} \{ l_2(l_2+1)(2\boldsymbol{p}\cdot\boldsymbol{q} + i\boldsymbol{\sigma}\cdot[\boldsymbol{p}\boldsymbol{q}])\,\mathcal{P}_{l_2} -$$
$$- (3i(l_2+2)(\boldsymbol{\sigma}\cdot\boldsymbol{P}_y\boldsymbol{p}\cdot\boldsymbol{q} + \boldsymbol{\sigma}\cdot\boldsymbol{p}\boldsymbol{P}_y\cdot\boldsymbol{q}) + l_2(2\boldsymbol{P}_x\cdot\boldsymbol{q} + i\boldsymbol{\sigma}\cdot[\boldsymbol{P}_x\boldsymbol{q}]))\,\mathcal{P}'_{l_2} +$$
$$+ 3i(\boldsymbol{\sigma}\cdot\boldsymbol{P}_x\boldsymbol{P}_y\cdot\boldsymbol{q} + \boldsymbol{\sigma}\cdot\boldsymbol{P}_y\boldsymbol{P}_x\cdot\boldsymbol{q})\,\mathcal{P}''_{l_2}\}$$

$$J = l_2 - \tfrac{1}{2} = l + \tfrac{1}{2} \qquad l_1 = 1 \qquad j = \tfrac{3}{2} \qquad l = l_2 - 1$$

$$\hat{\mathcal{F}} = (4\pi)^{-\frac{3}{2}} \frac{1}{2\sqrt{(l_2+1)(2l_2-1)}} \{ -l_2(l_2+1)(2\boldsymbol{p}\cdot\boldsymbol{q} + i\boldsymbol{\sigma}\cdot[\boldsymbol{p}\boldsymbol{q}])\,\mathcal{P}_{l_2} -$$
$$- (3i(l_2-1)(\boldsymbol{\sigma}\cdot\boldsymbol{p})\boldsymbol{P}_y\cdot\boldsymbol{q} + \boldsymbol{\sigma}\cdot\boldsymbol{P}_y\boldsymbol{p}\cdot\boldsymbol{q}) + (l_2+1)(2\boldsymbol{P}_x\cdot\boldsymbol{q} + i\boldsymbol{\sigma}\cdot[\boldsymbol{P}_x\boldsymbol{q}]))\,\mathcal{P}'_{l_2} -$$
$$- 3i(\boldsymbol{\sigma}\cdot\boldsymbol{P}_x\boldsymbol{P}_y\cdot\boldsymbol{q} + \boldsymbol{\sigma}\cdot\boldsymbol{P}_y\boldsymbol{P}_x\cdot\boldsymbol{q})\,\mathcal{P}''_{l_2}\}$$

$$J = l_2 - \tfrac{1}{2} = l - \tfrac{1}{2} \qquad l_1 = 1 \qquad j = \tfrac{3}{2} \qquad l = l_2$$

$$\hat{\mathcal{F}} = (4\pi)^{-\frac{3}{2}} \frac{1}{2\sqrt{(l_2+1)(2l_2-1)}} \{ l_2(l_2+1)(3\boldsymbol{\sigma}\cdot\boldsymbol{p}\boldsymbol{p}\cdot\boldsymbol{q} - \boldsymbol{\sigma}\cdot\boldsymbol{q})\,\mathcal{P}_{l_2} +$$
$$+ (3(\boldsymbol{\sigma}\cdot\boldsymbol{P}_x\boldsymbol{p}\cdot\boldsymbol{q} + \boldsymbol{\sigma}\cdot\boldsymbol{p}\boldsymbol{P}_x\cdot\boldsymbol{q}) + i(2l_2-1)(2\boldsymbol{P}_y\cdot\boldsymbol{q} + i\boldsymbol{\sigma}\cdot[\boldsymbol{P}_y\boldsymbol{q}]))\,\mathcal{P}'_{l_2} -$$
$$- 3(\boldsymbol{\sigma}\cdot\boldsymbol{P}_x\boldsymbol{P}_x\cdot\boldsymbol{q} - \boldsymbol{\sigma}\cdot\boldsymbol{P}_y\boldsymbol{P}_y\cdot\boldsymbol{q})\,\mathcal{P}''_{l_2}\}$$

$$J = l_2 - \tfrac{3}{2} = l + \tfrac{1}{2} \qquad l_1 = 1 \qquad j = \tfrac{3}{2} \qquad l_1 = l_2 - 2$$

$$\hat{\mathcal{F}} = (4\pi)^{-\frac{3}{2}} \frac{\sqrt{3}}{2\sqrt{l_2(2l_2-1)}} \{ l_2(l_2-1)(3\boldsymbol{\sigma}\cdot\boldsymbol{p}\boldsymbol{p}\cdot\boldsymbol{q} - \boldsymbol{\sigma}\cdot\boldsymbol{q})\,\mathcal{P}_{l_2} +$$
$$+ 2(l_2-1)(\boldsymbol{\sigma}\cdot\boldsymbol{P}_x\boldsymbol{p}\cdot\boldsymbol{q} + \boldsymbol{\sigma}\cdot\boldsymbol{p}\boldsymbol{P}_x\cdot\boldsymbol{q})\mathcal{P}'_{l_2} + (\boldsymbol{\sigma}\cdot\boldsymbol{P}_x\boldsymbol{P}_x\cdot\boldsymbol{q} - \boldsymbol{\sigma}\cdot\boldsymbol{P}_y\boldsymbol{P}_y\cdot\boldsymbol{q})\,\mathcal{P}''_{l_2}\}$$

$$J = l_2 - \tfrac{3}{2} = l - \tfrac{1}{2} \qquad l_1 = 1 \qquad j = \tfrac{3}{2} \qquad l = l_2 - 1$$

$$\hat{\mathcal{F}} = (4\pi)^{-\frac{3}{2}} \frac{\sqrt{3}}{2\sqrt{l_2(2l_2-1)}} \{ -l_2(l_2-1)(2\boldsymbol{p}\cdot\boldsymbol{q} + i\boldsymbol{\sigma}\cdot[\boldsymbol{p}\boldsymbol{q}])\,\mathcal{P}_{l_2} +$$
$$+ (l_2-1)(i(\boldsymbol{\sigma}\cdot\boldsymbol{P}_y\boldsymbol{p}\cdot\boldsymbol{q} + \boldsymbol{\sigma}\cdot\boldsymbol{p}\boldsymbol{P}_y\cdot\boldsymbol{q}) - (2\boldsymbol{P}_x\cdot\boldsymbol{q} + i\boldsymbol{\sigma}\cdot[\boldsymbol{P}_x\boldsymbol{q}]))\,\mathcal{P}'_{l_2} +$$
$$+ i(\boldsymbol{\sigma}\cdot\boldsymbol{P}_x\boldsymbol{P}_y\cdot\boldsymbol{q} + \boldsymbol{\sigma}\cdot\boldsymbol{P}_y\boldsymbol{P}_x\cdot\boldsymbol{q})\,\mathcal{P}''_{l_2}\}$$

Appendix

Relation (18) is a unitary transformation connecting the spin transition operators $|jm\rangle\langle\frac{1}{2}\mu|$ with the circularly polarized spin-tensors $T^{j+\frac{1}{2}}$ and $T^{j-\frac{1}{2}}$. We see from it that the circularly polarized spin-tensors are orthonormal:

$$\text{(A.1)} \qquad \operatorname{tr}\left((T^{I'\xi'})^{+}T^{I\xi}\right) = \delta_{I'I}\delta_{\xi'\xi} .$$

Further, we can use (18) for recognizing the transformation character of the spin transition operators $|\frac{3}{2}m\rangle\langle\frac{1}{2}\mu|$. For this purpose, we express T^2 and T^1 through the corresponding carthesian components T_{ik} and T_i. The relation between T^1 and T_i is well-known:

$$\text{(A.2)} \qquad \begin{cases} T^{1,\pm 1} = \mp\dfrac{1}{\sqrt{2}}\,(T_x \pm iT_y)\,, \\ T^{1,0} = T_z\,. \end{cases}$$

To find the relation between T^2 and T_{ik}, we express T^2 as a Clebsch-Gordan combination of two independent vectors. We obtain

$$\text{(A.3)} \qquad \begin{cases} T^{2,\pm 2} = \dfrac{1}{2}u_x v_x - \dfrac{1}{2}u_y v_y \pm \dfrac{i}{2}\,(u_x v_y + u_y v_x)\,, \\ T^{2,\pm 1} = \mp\dfrac{1}{2}\,(u_z v_x + u_x v_z) - \dfrac{i}{2}\,(u_y v_z + u_z v_y)\,, \\ T^{2,0} = -\dfrac{1}{\sqrt{6}}\,u_x v_x - \dfrac{1}{\sqrt{6}}\,u_y v_y + \sqrt{\dfrac{2}{3}}\,u_z v_z\,, \end{cases}$$

and

$$T^{0,0} = \frac{1}{\sqrt{3}}\,(u_x v_x + u_y v_y + u_z v_z)\,.$$

This is a unitary transformation between the circularly polarized tensors and the symmetrized pairs. The corresponding carthesian symmetrical tensor is defined by

$$\text{(A.4)} \qquad \begin{cases} T_{xx} = u_x v_x\,, \ \ldots \\ T_{xy} = T_{yx} = \frac{1}{2}\,(u_x v_y + u_y v_x)\,, \ \ldots \end{cases}$$

To make the transformation (A.4) unitary, we define also

$$\text{(A.5)} \qquad \begin{cases} \tilde{T}_{xx} = T_{xx} , \\ \tilde{T}_{xy} = \sqrt{2} T_{xy} . \end{cases}$$

In this way, $\tilde{T}_{ik}$ will be expressed through T^2 and $T^{00} \equiv T$ by a product U of two unitary transformations. However, being not contained in the relations (18) for $j = \frac{3}{2}$, T cannot be expressed through the spin transition operators $\frac{3}{2}m \langle \frac{1}{2}\mu$. Therefore, it must be constructed artificially, with the help of a supplementary vector, $\boldsymbol{p}$ say. For instance, let us take $T = \boldsymbol{p} \cdot \boldsymbol{T}$. Then

$$\text{(A.6)} \qquad \text{tr}\,(T^+ T^{2,\xi}) = 0 , \qquad \text{tr}\,(T^+ T) = 1 .$$

Hence, according to (A.1) and owing to the unitarity of U, $\tilde{T}_{ik}$ will be an orthonormal set of matrices

$$\text{(A.7)} \qquad \begin{cases} \text{tr}\,(\tilde{T}^+_{xx} \tilde{T}_{xx}) - \text{tr}\,(\tilde{T}^+_{xy} \tilde{T}_{xy}) = \ldots = 1 , \\ \textit{i.e.} \\ \text{tr}\,(T^+_{ij} T_{kl}) = \tfrac{1}{2}(\delta_{ik}\delta_{jl} + \delta_{il}\delta_{jk}) . \end{cases}$$

Combining now the three transformations (A.3), (A.4) and (A.5) we obtain the explicit form of the matrix

$$\text{(A.8)} \qquad U = \begin{array}{c} \begin{matrix} (xx) & (yy) & (zz) & (xy) & (yz) & (zx) \end{matrix} \\ \begin{pmatrix} \frac{1}{2} & -\frac{1}{2} & 0 & \frac{i}{\sqrt{2}} & 0 & 0 \\ 0 & 0 & 0 & 0 & -\frac{i}{\sqrt{2}} & -\frac{1}{\sqrt{2}} \\ -\frac{1}{\sqrt{6}} & -\frac{1}{\sqrt{6}} & \frac{2}{\sqrt{6}} & 0 & 0 & 0 \\ 0 & 0 & 0 & 0 & -\frac{i}{\sqrt{2}} & \frac{1}{\sqrt{2}} \\ \frac{1}{2} & -\frac{1}{2} & 0 & -\frac{i}{\sqrt{2}} & 0 & 0 \\ \frac{1}{\sqrt{3}} & \frac{1}{\sqrt{3}} & \frac{1}{\sqrt{3}} & 0 & 0 & 0 \end{pmatrix} \end{array}$$

This is the transformation matrix between $T^{2,\xi}$, T and $\tilde{T}_{ik}$

Similarly, from (A.2) it follows

$$\text{(A.9)} \qquad \text{tr}\,(T^+_i T_k) = \delta_{ik} .$$

However, T_i and T_{ik} will not be orthogonal one to another because T_{ik} contains T_i (through $T = \boldsymbol{p} \cdot \boldsymbol{T}$). By means of another choice of T, they can be made orthogonal, but in this way, either (A.6) or (A.7) or (A.9) would be violated. Nevertheless, this arbitrariness in choosing T_k is not embarrassing: being a linear combination of elements of the product representation $\mathcal{D}^{\frac{3}{2}} \times \mathcal{D}^{\frac{1}{2}}$, $\hat{\mathcal{R}}$ will not contain elements of the $\mathcal{D}^0$ representation so that terms containing T will cancel in all our expressions.

This is also the reason which enables us to take

$$\text{(A.10)} \qquad \text{tr}\,(T_i^+ T_{kl}) = 0\,,$$

in our calculations. This relation is correct for all angular operators $\hat{\mathcal{R}}$ because all non-orthogonal terms between T_i and T_{kl} are due to T.

RIASSUNTO (*)

Si fa una analisi parziale in onde per la produzione di coppie di bosoni su nucleoni. Gli operatori angolari corrispondenti, che caratterizzano completamente la dipendenza dallo spin e angolare della matrice S, si esprimono con l'ausilio dei polinomi di Legendre e si tabulano. Simultaneamente si dà un metodo generale per calcolare gli operatori angolari per processi interessanti più di quattro particelle, casi nei quali il metodo diretto conduce a calcoli assai laboriosi.

(*) *Traduzione a cura della Redazione.*

Magnetic and Crystallographic Analysis by Electron Diffraction.

S. YAMAGUCHI

Institute of Physical and Chemical Research - Tokyo

(ricevuto il 19 Febbraio 1959)

Summary. — The Lorentz effect observable in electron diffraction is utilized for measurement of the magnetization of ferromagnetic substances. In the present study, the martensitic transformed layer of austenitic stainless steel was studied magnetically and crystallographically by electron diffraction.

An electron beam is deflected in a magnetic field. This effect, *i.e.*, the Lorentz effect is observable in the diffraction pattern obtained from a ferromagnetic substance.

In order to know the conditions existing in the present experiment, a test piece of hard steel with the known remanence was studied by electron diffraction. The thin edge of a usual razor blade (10×10 mm) was employed as test piece. An electron beam grazed this sharp edge (minimum thickness of the truncated wedge: about 3 000 Å) to give rise to a diffraction pattern.

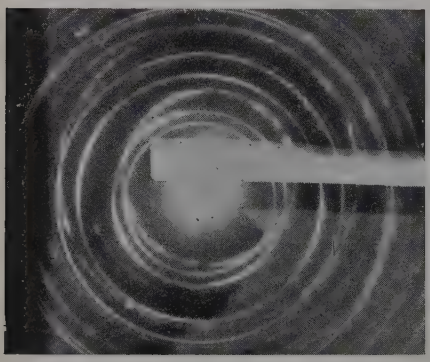

Fig. 1. – The diffraction patterns of hard steel and of gold are superposed. The rings are eccentric as a result of the Lorentz effect. Wavelength, 0.0292 Å. Camera length, 495 mm. Positive enlarged 2.3 times.

In order to measure the deflection of the incident beam caused by the magnetic field, a process of double exposure with a non-ferromagnetic substance was employed. A pattern of gold was beforehand photographed, and then that of the magnetic specimen was superposed on it. The wavelength of the incident electrons as well as the position of the photographic plate were fixed during this process. Fig. 1 was prepared with the hard steel and

with a gold foil. In Fig. 1, the diffraction rings of the ferromagnetic specimen and those of gold are eccentric as a result of the Lorentz effect.

Fig. 2 was obtained from two non-ferromagnetic substances, copper and gold, in the same process as for Fig. 1. All diffraction rings are concentric in Fig. 2, since there is no magnetic effect on the electrons. Fig. 2 corresponds to the successful result of a blank test for the magnetic analysis.

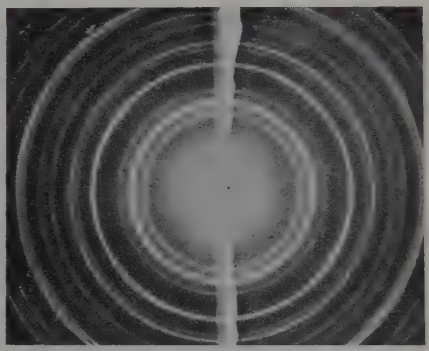

Fig. 2. – Copper and gold. All rings are concentric. No Lorentz effect. Wavelength. 0.0306 Å.

The deflection ΔZ of the incident beam is measurable from the ring eccentricity, as illustrated in Fig. 3, that is

$$\Delta Z = (Z_1 - Z_2)/2 \, .$$

Under the present experimental arrangement we have a relation between ΔZ and the magnetic induction B of the specimen,

$$(1) \qquad \Delta Z = \frac{eL}{mv} \int_0^l B \, \mathrm{d}l = \frac{eL\lambda}{h} \int_0^l B \, \mathrm{d}l \, ,$$

where e means the electron charge (1.6×10^{-20} emu), L means the camera length (495 mm), m means the electron mass, v means the velocity of the electrons, λ means the wavelength of the electrons, h means Planck's constant (6.6×10^{-27} erg s), and l means the distance travelled by the electrons in the magnetic field.

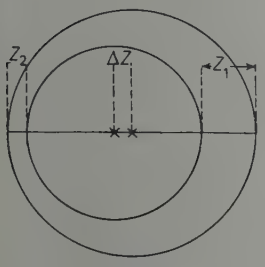

Fig. 3. – Illustration for measurement of the deflection of the incidence.

In Fig. 1 ($\lambda = 0.0292$ Å and $\Delta Z = 2.0$ mm) we can calculate the mean value of l according to Eq. (1), if we assume a mean uniform field for B whose intensity is equal to the remanence of the hard steel (10 000 G). Thus we obtain

$$(2) \qquad \bar{l} = 5.7 \cdot 10^4 \text{ Å} \, .$$

This value was applied for the analysis of the results obtained in the following experiments.

The same process as for the hard steel was carried out for a rolled plate of nickel. The edge of the blade ($10 \times 10 \times 0.5$ mm) was sharpened by mechanical polishing (minimum thickness: about 3 000 Å). An electron beam grazed this edge of the specimen. Fig. 4 is a double figure consisting of the diffraction pattern of nickel and that of gold ($\lambda = 0.0293$ Å and $\Delta Z = 0.66$ mm). From this figure we can calculate the magnetic induction B of the specimen

with the $\bar{l}$-value of (2). We obtain

$$B = 3300 \text{ G} .$$

This value coincides satisfactorily with the known remanence of nickel.

When a surface of austenitic 18-8 stainless steel is mechanically polished, a martensitic ferromagnetic Beilby layer is formed on the surface as the result

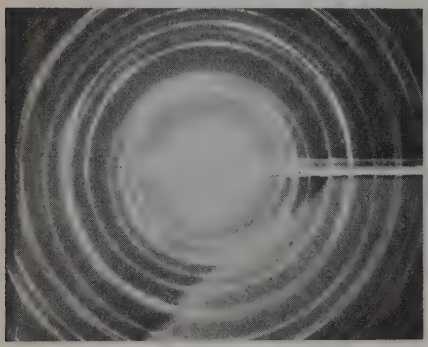

Fig. 4. – Nickel and gold. Wavelength, 0.0293 Å.

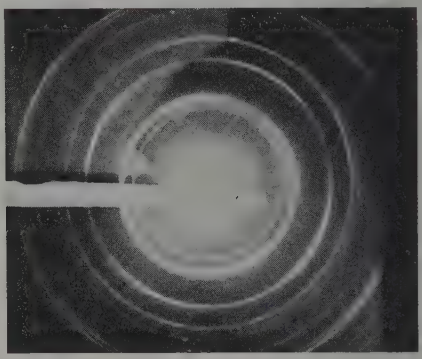

Fig. 5. – 18-8 steel mechanically polished and gold. Wavelength, 0.0294 Å.

of the strain-induced transformation (1). This magnetic state was studied by the present process. The edge of a test piece ($10 \times 10 \times 0.5$ mm) was sharpened by mechanical polishing. The minimum thickness of the wedge was about 3000 Å. This edge was observed by electron diffraction in the same way as for Figs. 1 and 4. Fig. 5 contains the diffraction pattern of the test piece and that of a gold foil. It is noticeable in Fig. 5 that the diffraction rings from the test piece and those of gold are not concentric ($\lambda = 0.0294$ Å and $\Delta Z = 0.43$ mm). It is also recognized in Fig. 5 that the series of the rings from the test piece is characteristic of the body-centred lattice (lattice constant = 2.86 Å).

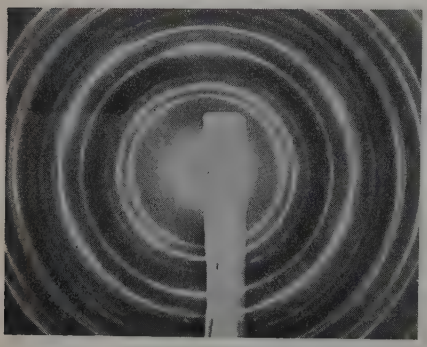

Fig. 6. - 18-8 steel electro-polished and gold. Wavelength, 0.0301 Å.

A test piece of 18-8 stainless steel, which contains a small quantity of molybden (about 2% by

(1) J. T. BURWELL and J. WULFF: *Trans. Am. Inst. Mining Met. Engrs.*, **135**, 486 (1939); S. YAMAGUCHI: *Journ. Chem. Phys.*, **27**, 1310 (1957).

weight) as retarder for the transformation, was examined by the present process. The ring eccentricity here measured ($\lambda=0.0288$ Å and $\Delta Z=0.33$ mm) was smaller than that in Fig. 5. The diffraction pattern of the test piece was characteristic of the body-centred lattice.

Fig. 6 was obtained from the test piece of stainless steel completely finished by electro-polish and from a gold foil. There is found a slight eccentricity of the diffraction rings here ($\lambda=0.0301$ Å and $\Delta Z=0.17$ mm). This magnetic effect is not due to the Beilby layer, but due to the ferromagnetic inclusions originally existing in the substrate.

TABLE I.

Material	Polish	Lattice	B (gauss)
Hard Steel	—	b.c.c.	10 000
Rolled Nickel	—	f.c.c.	3 300
18-8	Mechanical	b.c.	2 100
18-8-Mo	Mechanical	b.c.	1 700
18-8	Electrolytic	f.c.c.	800

b.c.c: body-centred cubic
f.c.c: face-centred cubic
b.c.: body-centred

According to Eq. (1) and to the $\bar{l}$-value in (2) we can estimate the magnetic inductions B of the test pieces. The results obtained are summarized in Table I. The B-values depend on the thickness of the Beilby layer, on the orientation of the magnetic domains, and on the nature of the ferromagnetic substance.

RIASSUNTO (*)

L'effetto Lorentz osservabile nella diffrazione degli elettroni è stato utilizzato per misurare la magnetizzazione di sostanze ferromagnetiche. Nel presente lavoro si sono studiati per mezzo della diffrazione degli elettroni i caratteri magnetici e cristallografici di uno strato di acciaio inossidabile austenitico che aveva subito una trasformazione martensitica.

(*) *Traduzione a cura della Redazione.*

LETTERE ALLA REDAZIONE

(La responsabilità scientifica degli scritti inseriti in questa rubrica è completamente lasciata dalla Direzione del periodico ai singoli autori)

Electrical Conductivity of Metals at Low Temperatures.

I. SUPEK

Institute « Rudjer Bošković » - University of Zagreb

(ricevuto il 10 Aprile 1959)

A previous paper [1] has shown that Bloch's integral-equation [2] for metal-electrons in an eletrical field can, at very low temperatures, be reduced to a differential equation on the energy surface $E(k_x, k_y, k_z) = \zeta$. The same can be done for Peierls' system [3], where the change of lattice quanta distribution is taken into account.

In an external electrical field there are two stationarity conditions for the electron and the lattice quanta distribution

$$(1) \qquad \left(\frac{\partial f}{\partial t}\right)_{\text{collisions}} + \left(\frac{\partial f}{\partial t}\right)_{\text{field}} = 0\,, \qquad \left(\frac{\partial N}{\partial t}\right)_{\text{collisions}} = 0\,.$$

We have applied the same functions for electrons and phonons as Peierls did:

$$(2) \qquad \begin{cases} f(\boldsymbol{k}) = f_0 - \dfrac{\mathrm{d}f_0}{\mathrm{d}E}\,\Phi(\boldsymbol{k})\,, \\ N(\boldsymbol{q}) = N_0 - \dfrac{\mathrm{d}N_0}{\mathrm{d}x}\,\dfrac{1}{KT}\,\Gamma(\boldsymbol{q})\,, \qquad x = \dfrac{\hbar\omega}{KT}\,, \qquad \varepsilon = \dfrac{E-\zeta}{KT}\,. \end{cases}$$

Hence the stationarity condition takes the form [4]

$$(3) \qquad \frac{2G^{-3}}{9M\hbar}\sum_{\boldsymbol{q}}\frac{q^2}{\omega_{\boldsymbol{q}}}\Big\{C^2\Omega(E_{\boldsymbol{k}+\boldsymbol{q}} - E_{\boldsymbol{k}} - \hbar\omega)\,\frac{1}{(e^{-\varepsilon-x}+1)(e^{\varepsilon}+1)(e^{x}-1)}\,[\Phi(\boldsymbol{k}+\boldsymbol{q}) - \Phi(\boldsymbol{k}) - \Gamma(\boldsymbol{q})] +$$

$$+ C^2\Omega(E_{\boldsymbol{k}-\boldsymbol{q}} - E_{\boldsymbol{k}} + \hbar\omega)\,\frac{1}{(e^{-\varepsilon}+1)(e^{\varepsilon-x}+1)(e^{x}-1)}\,[\Phi(\boldsymbol{k}-\boldsymbol{q}) - \Phi(\boldsymbol{k}) - \Gamma(\boldsymbol{q})]\Big\} =$$

$$= \frac{eF}{\hbar}\,\frac{\partial E}{\partial k_x}\,\frac{\mathrm{d}f_0}{\mathrm{d}E}\,,$$

---

(1) I. SUPEK: *Zeits. f. Phys.*, **149**, 324 (1957).

(2) F. BLOCH: *Zeits. f. Phys.*, **52**, 555 (1929).

(3) R. PEIERLS: *Ann. d. Phys.*, **12**, 154 (1932).

(4) Compare all the calculations with the article by SOMMERFELD – BETHE in *Handbuch der Phys.* Vol. 24/II or WILSON: *Theory of metals.*

$$\sum_{\boldsymbol{k}} C^2 \Omega (E_{\boldsymbol{k}+\boldsymbol{q}} - E_{\boldsymbol{k}} - \hbar\omega) \frac{1}{(e^{\varepsilon}+1)(e^{-\varepsilon-x}+1)(e^{\dot{x}}-1)} [\Phi(\boldsymbol{k}+\boldsymbol{q}) - \Phi(\boldsymbol{k}) - \Gamma(\boldsymbol{q})] = 0 .$$

It is useful to introduce polar-coordinates with the axis in the direction of grad E in the integral over $\boldsymbol{q}$-space. We can first integrate over ϑ taking into account only the factor Ω

$$\int \Omega \sin\vartheta \, \mathrm{d}\vartheta = -\frac{1}{q \operatorname{grad} E(\boldsymbol{k}+\boldsymbol{q})} \int \Omega \, \mathrm{d}E = \frac{1}{q \operatorname{grad} E(\boldsymbol{k}+\boldsymbol{q})} ht .$$

At very low temperature it is possible to develop the electron function in small quantities q_r, q_u and q_v, the projections of $\boldsymbol{q}$ in the direction of grad E and two perpendicular tangents on the surface.

$$(4) \qquad \Phi(\boldsymbol{k}+\boldsymbol{q}) - \Phi(\boldsymbol{k}) = \frac{\partial\Phi}{\partial r} q_r + \frac{\partial\Phi}{\partial u} q_u + \frac{\partial\Phi}{\partial v} q_v + \frac{1}{2}\frac{\partial^2\Phi}{\partial r^2} q_r^2 + \frac{1}{2}\frac{\partial^2\Phi}{\partial u^2} q_u^2 + \frac{1}{2}\frac{\partial^2\Phi}{\partial v^2} q_v^2 + \\ + \frac{\partial^2\Phi}{\partial r \partial u} q_r q_u + \frac{\partial^2\Phi}{\partial u \partial v} q_u q_v + \frac{\partial^2\Phi}{\partial v \partial r} q_v q_r + \dots .$$

In a similar way also $1/\operatorname{grad} E$ has to be expanded.

$$\frac{C^2}{\operatorname{grad} E(\boldsymbol{k}+\boldsymbol{q})} = \frac{C^2}{\operatorname{grad} E} + \frac{\partial}{\partial r}\left(\frac{C^2}{\operatorname{grad} E}\right) q_r + \frac{\partial}{\partial u}\left(\frac{C^2}{\operatorname{grad} E}\right) q_u + \frac{\partial}{\partial v}\left(\frac{C^2}{\operatorname{grad} E}\right) q_v + \dots .$$

The averages over Φ can be easily calculated [5].

$$(5) \qquad \overline{q_r} = -\frac{q^2}{2}\frac{1}{2}\left(\frac{1}{r_1} + \frac{1}{r_2}\right), \qquad \overline{q_u^2} = \overline{q_v^2} = \frac{1}{2} q^2 .$$

The average value in the equation (3) contains the powers in q^2, q^3, etc. We maintain only the part in q^2. The higher powers are negligible at low temperatures. By neglecting the change of lattice quanta distribution in the electric field and after the integration over E (the factors $\mathrm{d}f_0/\mathrm{d}E$ on the left and right side act as δ-function with the singularity on the $E=\zeta$) we obtain the differential equation, which can be transformed in ortogonal surface variables.

$$(6) \qquad \Delta\Phi + \frac{2 \operatorname{grad} E}{C^2}\left[\frac{1}{g_1^2}\frac{\partial}{\partial u}\left(\frac{C^2}{\operatorname{grad} E}\right)\frac{\partial\Phi}{\partial u} + \frac{1}{g_2^2}\frac{\partial}{\partial v}\left(\frac{C^2}{\operatorname{grad} E}\right)\frac{\partial\Phi}{\partial v}\right] = \\ = -\frac{18\Pi M u_0}{\hbar C^2 \Omega_0 I_5} (\operatorname{grad} E)^2 \cos\theta_1 \left(\frac{\theta}{T q_{0r}}\right)^5 eF .$$

Here Δ_r is the Laplace operator on the surface ($\Delta = \Delta_r + \Delta_r$). These equations can be also written in general surface variables [5]

$$(7) \qquad \left(\frac{\operatorname{grad} E}{C}\right)^2 \frac{1}{\sqrt{g}} \partial_\alpha \left(\frac{C}{\operatorname{grad} E}\right)^2 g^{\alpha\beta} \sqrt{g} \partial_\beta \Phi = -\frac{18\Pi M u_0}{\hbar C^2 \Omega_0 I_5} (\operatorname{grad} E)^2 \cos\theta_1 \left(\frac{\theta}{T q_{0r}}\right)^5 eF .$$

---

(5) I. Supek: *Zeits. f. Phys.*, **117**, 125 (1941).
(6) Glaser and Jakšić: *Glasnik mat. fiz.* **12**, 257 (1957).

This is just Bloch's stationarity condition translated into the differential form; it does not contain the change of lattice quanta distribution. We have in fact to solve the symultaneous system (3) for $f(\boldsymbol{k})$ and $N(\boldsymbol{q})$. Here we can first eliminate the phonon's function by integrating the second equation over the energy surface $E(\boldsymbol{k})$.

$$\int \frac{\mathrm{d}f}{\operatorname{grad} E}\,[\Phi(\boldsymbol{k}+\boldsymbol{q}) - \Phi(\boldsymbol{k}) - \Gamma(\boldsymbol{q})] = 0\,. \tag{8}$$

The phonon's function must therefore have the same expansion in q_r, q_u and q_v as the electron's functions

$$\Gamma(\boldsymbol{q}) = a_1 q_r + a_2 q_u + a_3 q_v + \frac{1}{2} a_{11} q_r^2 + \frac{1}{2} a_{22} q_u^2 + \frac{1}{2} a_{33} q_v^2 + a_{12} q_r q_u + q a_{23} q_u q_v + a_{31} q_v q_r + \dots\,. \tag{9}$$

By elimination of Γ we finally obtain the integro-differential equation, in which we have to expand the differential forms

$$\frac{\partial \Phi}{\partial k_i} \to \frac{\partial \Phi}{\partial k_i} - \alpha_i\,, \qquad \frac{\partial^2 \Phi}{\partial k_i \partial k_j} \to \frac{\partial \Phi}{\partial k_i \partial k_j} - \alpha_{ij}\,,$$

$$\alpha_i = \left(\int \frac{\mathrm{d}f}{\operatorname{grad} E}\right)^{-1} \int \frac{\partial \Phi}{\partial k_i} \frac{\mathrm{d}f}{\operatorname{grad} E}\,, \qquad \alpha_{ij} = \left(\int \frac{\mathrm{d}f}{\operatorname{grad} E}\right)^{-1} \int \frac{\partial^2 \Phi}{\partial k_i \partial k_j} \frac{\mathrm{d}f}{\operatorname{grad} E}\,.$$

The transformation in general surface variables is obvious.

Direttore responsabile: G. POLVANI Tipografia Compositori - Bologna

Questo fascicolo è stato licenziato dai torchi il 15-IV-1959